ADDIS ABABA UNIVERSITY SCHOOL OF GRADUATE STUDIES

LEGADEMBI GOLD
OPEN PIT MINE SLOPE STABILITY
&
UNDERGROUND MINE GEOTECHNICAL STUDY

A THESIS
SUBMITTED TO THE SCHOOL OF GRADUATE STUDIES
ADDIS ABABA UNIVERSITY

IN PARTIAL FULFILMENT OF THE REQUIRMENTS FOR THE
DEGREE OF MASTER OF SCIENCE IN GEOLOGY
(ENGINEERING GEOLOGY)

DEPARTMENT OF GEOLOGY & GEOPHYSICS

BY YONAS BEKELE
JUNE 2004

LEGADEMBI GOLD
OPEN PIT SLOPE STABILITY AND UNDERGROUND MINE GEOTECHNICAL STUDY

BY: YONAS BEKELE
FACULTY OF SCIENCE

Approved by: Board of Examiners

Dr. Dereje Ayalew _____.
Chairman

Dr. Tenalem Ayenew _____.
Advisor

Dr. Tarun Kumar Raghuvanshi Tarun Raghuvanshi.
Advisor

Dr. Adisalem Zeleke _____.
External Examiner

Ato. Kebede Tsehayu _____.
External Examiner

June 2004

AKNOWLEDGEMENT

I am greatly indebted to my advisor Dr. Tenalem Ayenew with out whose guidance and corrections the thesis may not have its present form.

I would like to acknowledge my advisor Dr. Tarun Kumar Raghuvanshi, who generously shared his knowledge, guided me during my fieldwork, supplied his personal resource, and sacrificed holidays in reading and correcting the thesis.

I would like to acknowledge my sponsor, Ministry of Mines for all the support provided to me for the success of this study. My special thanks go to Mr. Getachew Tesfaye, head Mineral Operations Department, and all the staffs for their consistent help.

I would like to thank Midroc Gold Private Limited Company for the cooperation provided during the fieldwork.

I would also acknowledge Construction Design Share Company for the financial discount for the strength tests.

I also extends my sincere thank to Dr. Derje Ayalew, head Department of Geology and Geophysics of Addis Ababa University, for his persistent help in administrative and academic maters.

I wish to express my gratitude to Dr. Worash Getaneh, Department of Geology and Geophysics, A.A.U., who supplied material and commented on the geological aspect of the present research work.

I would like to express my thanks to Dr.Tamiru Alemayehu, Dr. Tesfaye Korme, and Dr. Tesfaye Kidane for their support for different aspects of the study.

I would like to acknowledge Prof. Dr. Josyula Chinna Venkata Sastri, Geology and Geophysics Department of A.A.U, for his valuable advises in hydrogeological aspect of the study.

Last, but not the least, I would contribute all the success of my work to my lifelong partner and wife, Asnaku Abate. She has always motivated me in moments of depression and she extended all the support, through out this work. I would also acknowledge all my family, who contributed to the success of this work in one or other ways.

TABLE OF CONTENTS

LIST OF TABLES

LIST OF FIGURES

LIST OF PLATES

ANNEXES

ABSTRACT

In Southern Ethiopia in Adola Precambrian rocks, the Legadembi primary gold occurrence have been under exploration and feasibility study within a period of 1975-1990 G.C.. In 1990 G.C the Legadembi Gold Mine has been established and officially started mining. In 1997 the mine has been privatized to Midrock Gold Private Limited Company.

The Adola area Precambrian rocks are regionally grouped into Awata, Mormora (dominantly gneissic) and the Adola Group (metavolcano-sedimentary) rocks. These Precambrian rocks have been intruded by pre to post tectonic maifc to granitic intrusives. The gneissic terrains envelope the metavolcano-sedimentary rocks. The contact between the gneissic and the metavolcano-sedimentary units is marked by horizontal, N-S striking, transcurrent shear fault. In the region the metavolcano sedimentary rocks occur in two zones, namely, the Kenticha and Megado belts. The Legadembi Gold Mine occurs in northeastern flank of the Megado belt.

From east to west the main lithotypes are gneissic unit, talc/talc-actinolite-tremolit schists, quartz-biotite-actinolte talc schist, graphitic quartz mica schist, amphibolite and gabbro intrusives. The gold mineralization is localized mainly in quartz veins, which forms discontinuous lenses, stretched parallel with the regional foliation (N-S). The auriferous quartz veins are hosted mainly in quartz-biotite-actinolite talc schist and some in graphitic- quartz-mica-schist.

During privatization the mine gold resource has been estimated to be totally 83 tons, of which, 37 ton from the open pit, 23 ton from the underground mine, and 23 ton from Sacharo, deposit.

The open pit mining has been active since 1990 G.C. In the present work, the stability of the open pit has been studied using: structural data, collected in the present and previous works; Geomechanics (RMR) rock mass classification; laboratory physical property test results, on samples collected during this study and the previous work results; hydrogeological studies around the open pit slope. Accordingly the Eastern slope has been found to be stable for existing and possible worst conditions. Whereas the Western slopes (hanging wall) have been found to be unstable for possible worst condition represented by moderately saturated dynamic conditions. Based on the slope stability studies Safe slope design for FOS 1.3 and 1.2 has been evolved. The western slope will be stable in possible worst conditions, with general slope angle 35°- 40°, 20 m height and 6 m bench width at 50°- 60° slope angle.

The Legadembi Underground Mine geotechnical study has been started in 2000 G.C. In the period of 2000-2004 G.C., 1.3 km access tunnel, 250 m North exploration drive, 250 m ore drive, 35 m South exploration drive, with turning and transformer bays have been excavated. The upper Legadembi ore body has been crossed at 1770 m above sea level. The underground mining will be from the ore zone level to 1990 m above sea level towards the surface. In the present study the geotechnical study has been carried out manly on the ore zone rock mass, between 1770 m and 1990 m.

The geotechnical study has been conducted in steps involving; geotechnical database compilation; geological and geotechnical mapping; structural data analysis; hydrogeological study, laboratory physical property determination tests; computer based wedge failure stability analysis, and empirical calculations to determine the rock mass rating values, maximum excavation span, and deformation modulus.

The underground rock mass Q-rating average value result indicated that the ore zone rock mass quality is within Fair to Poor class (average Q is 5.8). At its present excavation dimension (6-9.5 m diameter and 6-8 m height), based on the Q-rating support system, it has been found that it does not require permanent support and it can be supported with spot bolting. The maximum excavation span, empirically calculated, from Q- rock mass rating is 15 m.

In the underground mine excavation there are two major and two random joint planes. The major joint strike is parallel with the main drive. These discontinuity planes are in unfavorable conditions with the excavation. The ore zone excavation roof is manly constituted by quartz vein with uniaxial compressive strength greater than 100 Mpa (grouped as strong rock). In places where the quartz vein is mined out the sidewalls are constituted by quartz-biotite-actinolite-talc schist rocks, with uniaxial compressive strength ranging 20-50 Mpa (grouped as weak rock).

With the Legadembi underground ore zone rock mass conditions, in permanent development excavations systematic bolting and shotcreeting will be required. The cut and fill mining method has been recommended as the safe mining system.

CHAPTER 1

INTRODUCTION

1.1 PREAMBLE

The Legadembi Gold Mine is located in Oromia National Regional State, Borena and Guji zone, Odo Shakiso District, 500 km southeast of Addis Ababa. Midroc Gold Private Limited Company owns the Legadembi Gold Mine.

A systematic search for economic gold deposit at Legadembi started in 1975 after the accidental discovery of gold in quartz veins. Between 1980-1987 G.C. intensive exploration work has been conducted and 30 ton of gold reserve has been proved (EMRDC, 1990).

The Legadembi Gold Mine was established in 1990 under the former Ethiopian Mineral Development Corporation (EMRDC, 1990), to mine the Northern part of the deposit, using open pit mining method and Carbon in Pulp Absorption (CIP) processing plant with a capacity of processing 3000 ton of ore per day.

The Legadembi Gold mine was privatized in June 1997. Midroc Gold Private Limited Company took the acquisition of the mine right. During the privatization process resource inventory has been made and the total minable reserve was estimated to be 83 ton, of which 37 ton from open pit, 23 ton from Sakaro, and 23 ton from Legadembi Underground deposit (unpublished report).

At the time of privatization totally there were 625 employees. Since then the number of employees increased to 1286 as of March 2003 (unpublished report) . The mining and exploration agreement was signed on March 1998 between the Ethiopian Government Ministry of Mines and the Midroc Gold Private Limited Company. As per

this agreement the production is scheduled for fourteen years. However, Midroc Gold Private Limited Company aims to optimize the benefit by increasing the annual gold production up to 15 ton envisaging the development of the Sakaro and the Legadembi underground mine.

1.2 LOCATION & ACCESSIBILITY

The area is bounded by geographic coordinates, latitude 5° 42' to 5°44' N and longitude 38°52' to 38°55' E, on the Southeastern slopes of the Ethiopian Highlands. The area falls within the topographic sheet 0538 B4 of the Ethiopian Mapping Authority.

The project site is accessible from Addis Ababa by 315 km asphalt road up to Abosto (Yirgalem) and there after through 185 km gravel road.

The nearest town to the Legadembi mine is Shakisso, which is 7 km northeast. It is a residential place and administrative head quarter of the Legadembi Mine. The nearest large town is Kibre Mengist, 27 km northeast from the project area. The location map of the study area is presented as Fig 1.1.

1.3 CLIMATE OF THE AREA

The climate of the area is subtropical with moderate temperatures (Fig.1.2). The precipitation and temperature data (1974-2003) of the area has been collected from National Meteorological Service Agency. The daily average temperature varies between 11°C-27°C. The average annual temperature ranges between 15°-20°C, with maximum daily temperature variation being during the rainy seasons, i.e. March to May and September to November.

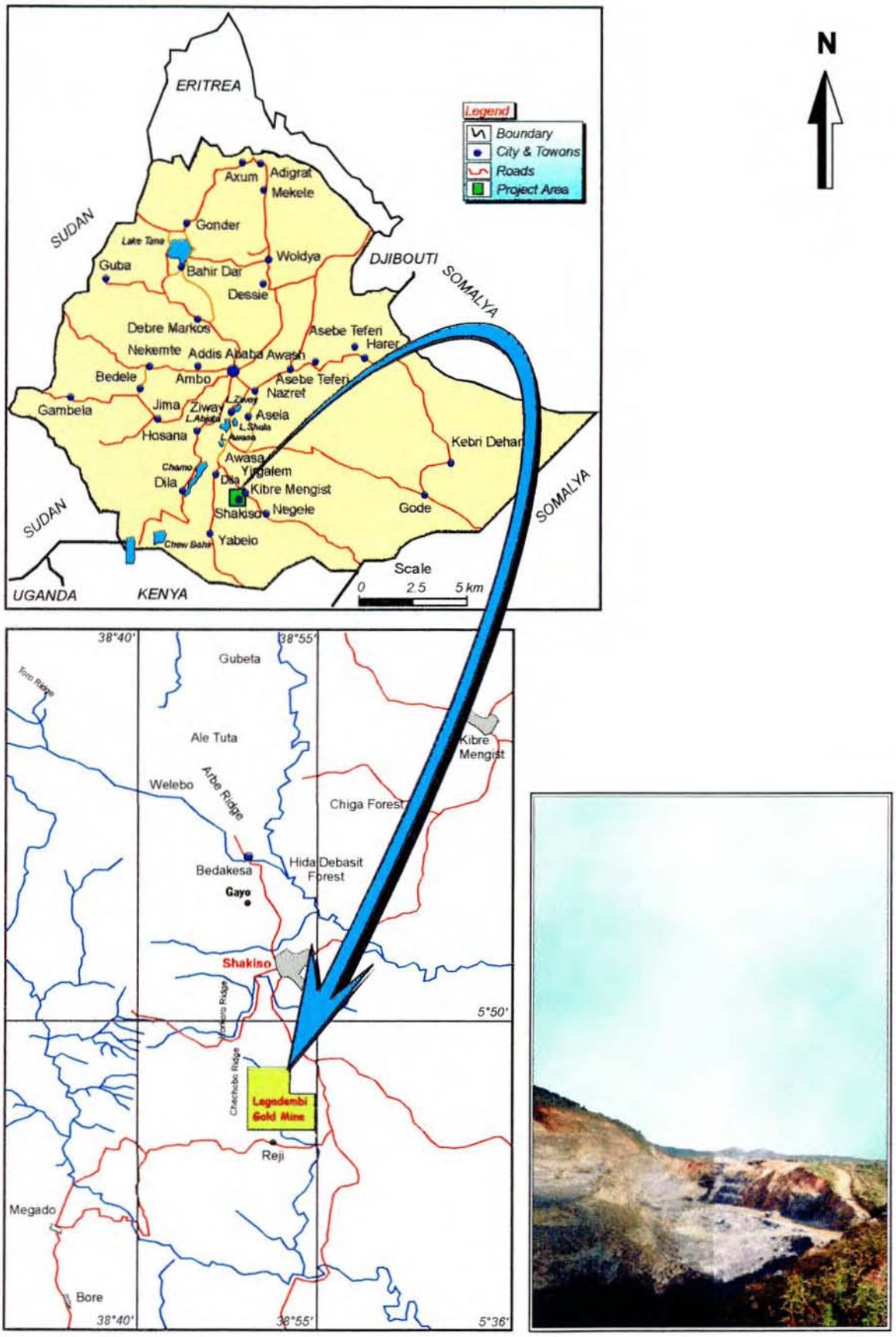

Fig.1.1 Location Map of the project area.

Based on the rainfall distribution the 12 months are categorized into four: (i) June to August, average rainfall of 30 mm; (ii) September to November, average rainfall 108 mm; (iii) December to February, average rainfall 26 mm; (iv) March to May, average rainfall 171 mm. The area has 1000 mm annual average precipitation. The highest monthly average precipitation was 415 mm in May 1987. The precipitation graph (Fig.1.2) shows that, there are two distinct rainy seasons from March to May and from September to November. The maximum daily rainfall of 83.6 mm was recorded in Shakisso in March 1980. Showers and thunderstorms are not uncommon during the dry season, and the Southern part of the area is characterized by low air humidity during the winter dry season.

The observed seasonal variations are best explained by reference to the position of the Inter Tropical Convergence Zone (ITCZ). Seasonal oscillation of the ITCZ causes variation in the wind pattern. Between June and September, the area comes under influence of westerly and southerly winds, whilst from October to May; the Easterly air currents dominate this part of the country (BRGM, 1991).

Mean annual evaporation recorded in the Adola area is 1,235 mm, ranging from 90 to 130 mm per month (BRGM, 1991).

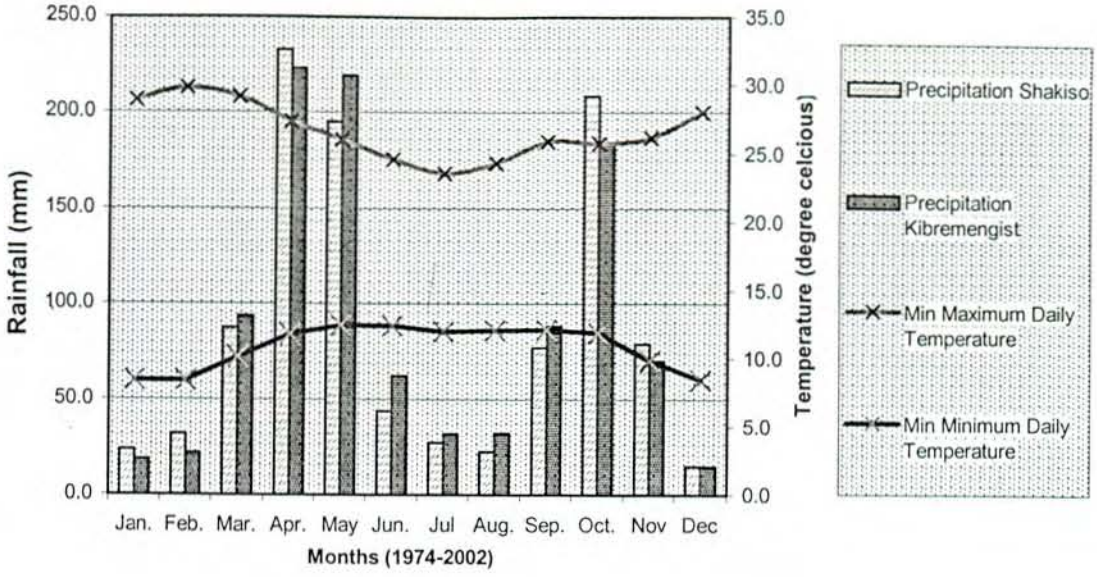

Fig 1.2. Precipitation and temperature at Kibremengist and Shakisso towns.

1.4 PHYSIOGRAPHY

The region is known as the Adola Gold belt. It is approximately 180 km long and has 10-12 km width. In the region the altitude ranges from 2250 m to 2300 m at the Awata-Mormora watershed and to 1600 m in Upper Bore Valleys. The watershed rise about 250-300 m above the adjacent valleys in the northern part where areas are covered by basalt flows and that have been deeply dissected by the erosive activity of the rivers. In the central and Southern parts, the local relief is 100-150 m.

The territory has an overall tilt from northwest to southeast, which has been a controlling factor in the formation of the drainage system, especially the main streams of the area, the Mormora and Awata rivers and their major tributaries (Wellebo-Bedakessa and its tributaries Alem Tshay and Donkoro, as well as left-bank tributaries of the Mormora River mid reaches). In contrast the young erosion valleys gulches and gullies developed on the planation surfaces (Upper Bore Valley, Kelecha, Legadembi, Sakaro and others) are controlled by the underlying geology. It

comprises undulating hills and valleys with a relief of some 300 m. Most of the valleys in the area are dry. The two perennial rivers, the Awata and Mormora, which are about 10km and 20km north and south, respectively from the project site, are the main sources of water.

The Awata and Mormora rivers and their tributaries (Bedakessa, Kojowa, Legadembi, Wollena) are characterized by long profiles. In the region the volume of water within the rivers is mainly controlled by annual precipitation. Throughout the year the run-off occurs only in the Awata and Mormora River beds and in Bedakessa creek, a right-bank tributary of the Awata River. In the vicinity of Shakisso the width of the Awata river is 20 m, with the average depth being 0.7m and the velocity 1.5 m/sec, the water discharge is 21 m^3/sec (BRGM, 1991). The Mormora River, near Megado village, is 18 m wide, 0.8 m deep, its velocity being 1.2 m/sec, and discharge being 17.3 m^3/sec (BRGM, 1991).

Springs are not uncommon in the valleys where ground and vadose water is being discharged onto the surface, and as a rule confined to tectonic fractures. The springs are important source of water supply for local inhabitants. There are marshy plains, known as Wellebo, Bedakessa, Wollena, and Lega Dembi representing groundwater discharge areas. Shakisso and Megado recives water from the Awata and Mormora rivers respectively.

The Legadembi deposit is situated 7 km Southwest of Shakisso on the eastern slopes of Wosho Mountain, which is 2200 m high above sea level. This mountain is the southern salient of the *Meleka Planation* surface, and forms the watershed between the Awata and Momora Rivers. Its width in the central part (at the latitude of Shakiso) is 7 km to 8 km. Before the open pit mining activity the eastern slope has been presented on the topographic sheet as having well defined erosion scarps. At

present the open pit mining activity has changed the Eastern flank of the Wosho Mountain. At the top where the soil cover thickness ranges 30-35 m, the topography is marked by gentle slopes with gradient upto 30°. Just below the soil cover at elevation level below 2150 m the working slopes are steep ranging between 50° and 70°. Being on the Southeastern flank of a massif, the local relief within the Legadembi drainage system varies from 350 to 400 m, within the upper reaches of the Legadembi River. The Legadembi river course at the eastern flank of the mountain is now serving as a tailing pond. The drainage map of the area is presented as Fig.1.3.

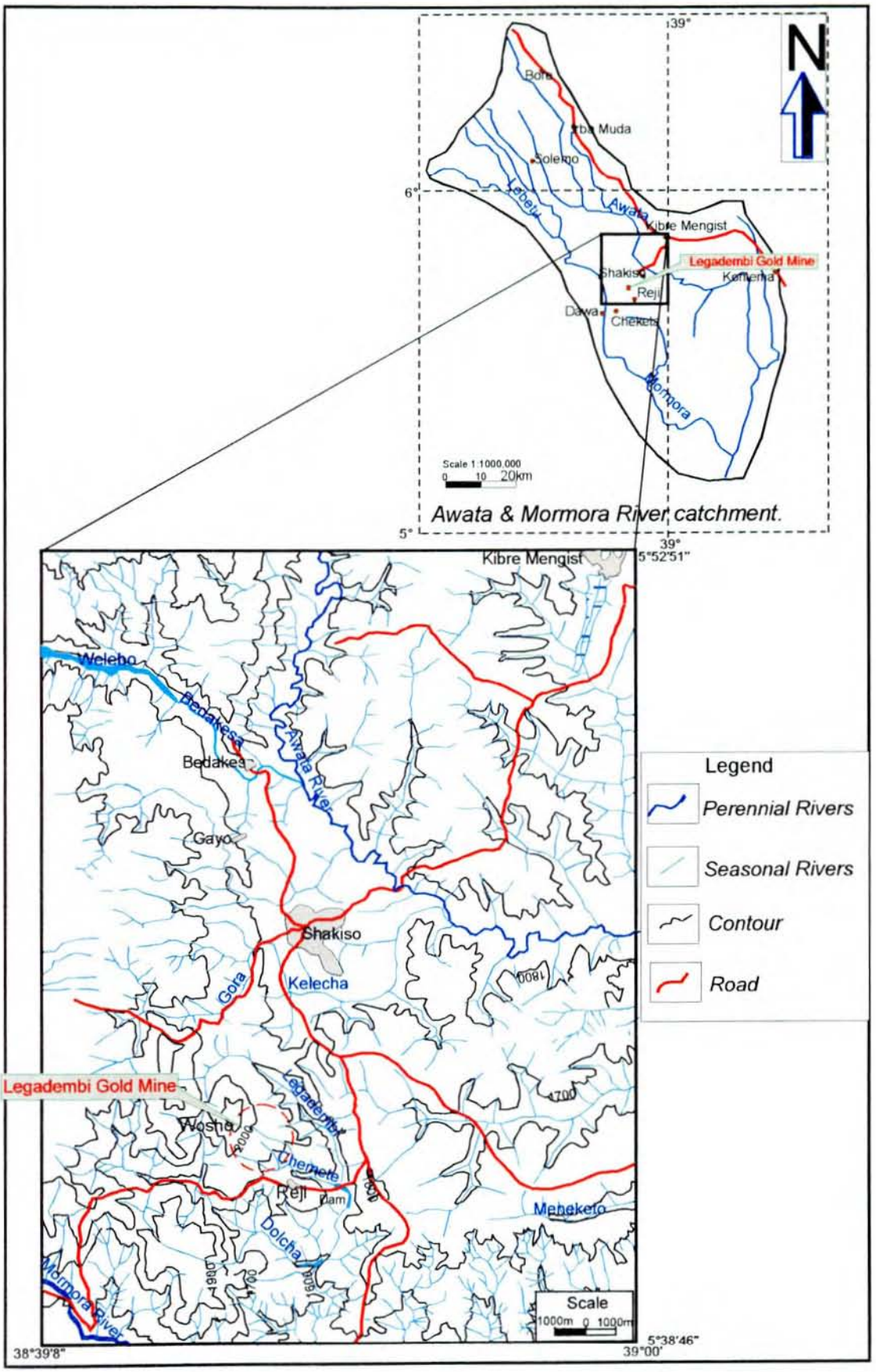

Fig. 1.3 Drainage map.

A slope 1 to 2.5 km long characterizes the western erosion scarp with a gradient ranging between 15° and 45°. The valleys, and gullies of the western slopes are rather developed and mature in aspect; they have gentle slopes and wide floors in sites where it is vividly pronounced.

The Legadembi (Wosho) mountain demonstrates a vivid examples of recent landforms strongly controlled by underlying geology. Being comb-shaped in plan it is cut into separate blocks by tectonic fractures. These faults break the whole ridge into Upper, Northern, Central, and Southern part. The faults bordering the blocks are sites of active erosion processes. Gulches and gullies of the Legadembi basin are developed along these fractures.

1.5 PREVIOUS WORKS

Gelogical investigation in the Adola area dates back to 1940 with the discovery of placer gold in various valleys. Astrup (1948), made the earlier attempt to prospect the placer gold potential of some of the valleys. As part of the search for economic mineral deposit in all parts of Ethiopia, Jellenc (1966) conducted systematic work in the region. After Jellenc, the Ethiopian Government in collaboration with international organizations and foreign Governments have conducted systematic regional mapping and detail mineral exploration and prospecting in the Adola belt and other parts of Ethiopia.

The geology of the Legadembi Gold Mine area, have been mapped in detail during the pre-feasibility, feasibility stages, and after the development, by different researchers under different objectives. The discussion in chapter II has well addressed the geological aspect of the previous works.

At the early stage of the mine, geotechnical studies have been conducted to design the open pit mine slope. Consultants from France (BRGM or Bureau de Recherches

Géologiues et Miniéres) conducted the geotechnical studies during the feasibility study to design the open pit. The study included collecting fracture data, sampling, and laboratory strength test on intact rocks and fractures. The fracture survey was conducted on data collected from surface outcrops, core samples, and former exploration adits. Analysis of the stability of the slope of the pits using charts and computer calculations have been made to design the open pit slope at Factor of safety 1.2. The result of the BRGM (1991), study is summarized below:

(i) In the top weathered surface (35 m thick), the slopes will be stable at an overall angles of 35°, these slopes will be arranged in benches, 10 to 20 m high, inclined at 40°, with berm widths varying from 2.5 to 5 m.

(ii) In unweathered rock mass and with the exception of the west side of the central Legadembi, the slopes will be arranged at an overall angles of 70°, with benches 10 to 20 m high inclined at 80° and berm widths; varying 2 to 4 m.

(iii) On the west side of the Central Legadembi open pit the overall slope angle will be reduced to 50°, and the slope will include benches inclined at 60°, with berms of 2.6 m (for 10 m high).

(iv) The consultants recommended additional investigation involving geotechnical boreholes and pizometric survey to obtain more details of the mechanical characteristics of the rock mass and the presence or absence of groundwater.

Since 2000 G.C the Legadembi Gold Mine has been conducting geotechnical feasibility study to develop the underground mine. During the filed work of the present study (January, 2004) it has been advanced to a level of opening the ore

body located at 1770 m above sea level. The conceptual development of the underground resource has been designed and being implemented in three phases:

(i) The first phase envisaged the excavation of the access tunnel with turning and transformer bays. The access tunnel portal is located at point 05° 43' 02" North and 38° 53' 47" East, within the footwall gneiss at elevation 1900 m. The excavation for the access tunnel started in the year 2000 G.C., from eastern flank of the upper Legadembi footwall, towards west at 5% gradient. The 1.35 km long excavation and the associated structures have been completed at the end of the year 2003. The access tunnel aimed to cross the upper Legadembi lower ore zone perpendicularly. The tunnel is Horseshoe shaped with average dimensions of 6 m diameters and 6 m heights. The ore zone is intersected almost perpendicularly after 1.2 km drive, at 1770 m above mean sea level. The layout of the underground mine is presented in Fig 6.2.

The geological and geotechnical mapping of the underground access tunnel work was conducted by Teshome Legesse and others of the Mine Geology division at 1:200 scale. This data has been used for the engineering geological rock mass characterization of the access tunnel and associated structures.

(ii) The second phase envisaged the excavation of exploration drives north and south parallel to the ore zone. The excavation has been within the footwall gneiss. The aim of the construction of these drives has been to acquire drill core samples from the ore zone and the host rocks for geological, geotechnical studies, and gold content assay. The excavations are Horseshoe shaped and has the same dimension as that of the access tunnel. The portal of these drives is located within the access tunnel.

The North drive has been excavated to explore the Upper Legadembi ore body. It consists 12 m long, 10 m wide and 6 m high four cubbies at 50 m intervals. Within each cubby, vertically fan shaped exploration drill holes of 54.7 mm diameter, have been drilled towards west to the ore zone. The drilling array is presented in Fig. 6.2 . The drilling holes have an average length of 80 m. The drilled core samples from the North exploration drive have been geotechnically and geologically logged. The geotechnical logging involves determination of geotechnical parameters, such as RQD, hardness, joint filling, joint set numbers, joint opening and joint roughness. For 9 boreholes geotechnical data have been supplied to this work from the Mine Geology Department. These borehole data has been used to evaluate the rock mass between the footwall gneiss and the ore zone in the underground geotechnical study (Chapter VI).

The South Exploration drive would have been the other major excavation, but the excavation has stopped at 39 m from the access tunnel towards south, parallel to the ore zone. The purpose of the excavation was to explore the Central Legadembi Underground ore body. The excavation has stopped within the footwall gneiss.

(iii) The third phase envisaged the development of the underground mine. This task involves the excavation of the ore zone drive. The drive is within the ore zone parallel to the regional foliation direction.

Currently, most of the geological and geotechnical work is concentrated on the Northern exploration drive. The ore zone drive is located about 1.2 km from the access tunnel portal at an elevation 1770 m above mean sea level. The major orientation of the drive is N330° and at places north south. It is Horseshoe shaped with width varying 6 to 9.5 m and height 6 to 8 m. As on January 2004 a total length of 242 m was completed.

The development of the underground mine will include installation of permanent dewatering system, raise boring to the surface for reliable ventilation system, ramps and drifts for different levels of future ore stops.

1.6. BACKGROUND

In mechanical or civil engineering practice it is customary to ensure the stability of a structure by designing it so that the stresses in each element of the structure are always less than the strength of that element, defined in some appropriate way. The criterion that the stress should always be less than the strength would certainly appear to be adequate to ensure the stability of a structure and to be applicable to those structures in the form of underground excavations. However the options available for underground mining excavations designer are fewer than the corresponding counter civil-work designer. These options even are often circumscribed by other considerations, especially in mining, where the major excavation results from the extractions of the ore body.

In mining it is not possible to keep the stresses everywhere in the rock less than its strength. The rock fails in parts surrounding many underground excavations, but only occasionally does this fact impair the stability or safety of the excavation. The criterion that the stresses must always be less than the strength may therefore be sufficient to ensure the stability of a structure, but in mining it may not be acceptable, as it would preclude mining in many situations where it is practiced with comparative safety.

According to the studies of potential mining companies (Ashanti, 1996), the current open pit mining method in Lega-Dembi will be practiced economically up to 1930 or 1920 m above sea level, below which the mining method should be underground.

In the previous works, during the exploration, pre-feasibility and at the feasibility stage it is indicated that the area consists different sets of fractures and lithological units, which imparts a highly heterogeneous mechanical properties to the rocks around the underground excavations. Hence the stability condition of each excavation in the underground mine development should be based on a clear picture of the mechanical properties of the rock mass. If the afore mentioned condition is not met, any failure within the underground mine structure may cost the lives of the people on duty, loss of expensive machineries and eventual failure of the underground mine. Even if the failure condition may not endanger the safety of humans and machineries, it can cause dilution of ore and waste making the mining activity uneconomical. In order to counter act these problems in the Legadembi underground mining development, it is necessary to understand the cause of instability and to design measures, which minimize these problems.

After the design life of the open pit mine the excavation has to be made stable for long time. The slope stability analysis will provide the safe slope angle with acceptable Factor of safety. The slope design is based on the shear strength property of the rock mass and its discontinuity plane orientation with respect to the excavation orientation.

1.7 OBJECTIVE

This research in general aimed to:

- Indicate the state of the stability of the underground excavations based on, sampling results, field measurements and observations;
- Stability studies of excavated slopes in the open pit, determination of factor of safety for static and dynamic conditions;
- Based on the stability studies to work out a safe cut slope design for open pit;

- Collecting the existing geological, hydrogeological and geomechanical information of the under ground mine;
- Recommend the best remedial measures for problems related with the geotechnics of the underground excavations.

Thus by achieving the above objectives the following may be produced:

i) Geological map of the open pit and underground mine.

ii) Engineering geological map of the underground mine.

iii) Assessment of the effect of the hydrological and hydrogeological conditions of the study area on the stability of the slopes of the open pit and underground mine excavations.

iv) Safe slope design for the open pit mine.

v) Identify potential problem areas and recommend possible remedial measures.

1.9 APPROACH AND METHODOLOGY

The following methods have been employed to achieve the above-mentioned objectives:

i) Literature review on geology, structure, geomorphology, hydrology, and engineering geology of the Legadembi gold mine from both published and unpublished reports, maps and journals.

ii) Prepare geological map of the study area with emphasis to surface and subsurface lithologies and structures available from previous work and refine the map by undertaking fieldwork.

iii) To acquire good understanding of the hydrological and hydrogeological conditions of the area, hydro-meteorological data of the area had been collected and compiled.

iv) After evaluating the compiled data, additional actual data has been collected to fill the gap between the available and the required data. The field investigations have been concentrated on geological, structural, and geotechnical mapping, sampling, on site measurements, and tests.

v) To determine the mineralogical and geotechnical properties of some of the rocks in the study area, laboratory analysis has been conducted on samples.

vi) After compilation of the actual field observations and the analysed results, the data has been systematically grouped and analysed using available techniques and computer programmes.

vii) Interpretation of the results has been made in-view of the objective of the research and a draft of the thesis has been prepared.

viii) Based on the result, conclusion and recommendations have been drawn and the thesis is finalized.

CHAPTER - II

GEOLOGICAL SETUP

2.1 REGIONAL GEOLOGY

The study of the Geology of Ethiopia goes back to 1860 by Blanford, and since then, major advances in the understanding of the geology of Ethiopia have been made from the works of various researchers, e.g. Danieli (1943); Mohr (1971); Kazmin (1972, 1974, 1978). The outcome of these studies outlined the lithostratigraphy of Ethiopia into three major categories:

1. The Precambrian Basement
2. The Late Palaeozoic to Early Tertiary sediments
3. The Cainozoic volcanic and associated sedimentary rocks.

The Precambrian rocks of Ethiopia contain a wide variety of metamorphosed sedimentary, volcanic and intrusive rocks. They are localized in four major regions: in the north, in Tigray ; in the west, along the Sudan border, in Gojam, Wollega, and Illubabour; in the south, in Kibre Mengist, Hagere Mariam, Moyale and Bale; and in the east, Harar highland areas.

The Ethiopian basement rocks, to the west, along the Ethio-Sudan border are mainly gneisses and migmatites known as Baro Group and to the East of the Baro Group it is dominantly the volcano-sedimentary succession known as Birbir, Tulu Dimtu, Tsaliet, Tambien Groups and Didikama and Shiraro Formations and associated plutonic rocks.

In the southern part of the country the volcano-sedimentary belt (Adola Group), with its attendant intrusives, occurs enclosed by the gneissic terrains (Mormora and Awata Group).

Recent works classify the Precambrian rocks of Ethiopia in to two major lithotectonic assemblages (Ayalew et al., 1990; Teklay et al., 1993; Hailu Worku ,1996):

- The Gneissic terrains (pre-Pan-African Crust) of upper to late Proterozoic age.
- Metamorphosed Volcano-Sedimentary Belts (the Pan-African juvenile crust) associated with minor ultramafic bodies and intrusives ranging from mafic to granitic in composition.

The blocks of gneissic terrains are considered to be older than the volcano-sedimentary belts, and the metamorphism ranges from the upper amphibolite to granulites facies. Metamorphic facies in the low-grade volcano-sedimentary succession typically ranges from green schist to lower amphibolite facies.

The general foliation trend is north south with exceptional deviation to the northeast and northwest. The boundaries between the gneissic and volcano-sedimentary sequences are of tectonic origin, represented by sheared mylonitized and tectonically highly deformed ultramafic rocks.

The Precambrian shield in Ethiopia occupies a unique position in this part of the African continent situated between the predominantly gneissic rocks of the Mozambique Belt, to the south, eastern and southern Africa, and the volcano sedimentary-plutonic complexes (the Arabian-Nubian Shield), along a strike to the north bordering the Red Sea. The Mozambique Belt has been recognized as a polycyclic complex, comprising units of highly varying lithology, metamorphic grade and augens (Almond, 1984; Chaen et al., 1984). It contains gneisses of at least Early Proterozoic and possibly Archaean age. Fig. 2.1 shows the distribution of the basement rocks of Ethiopia.

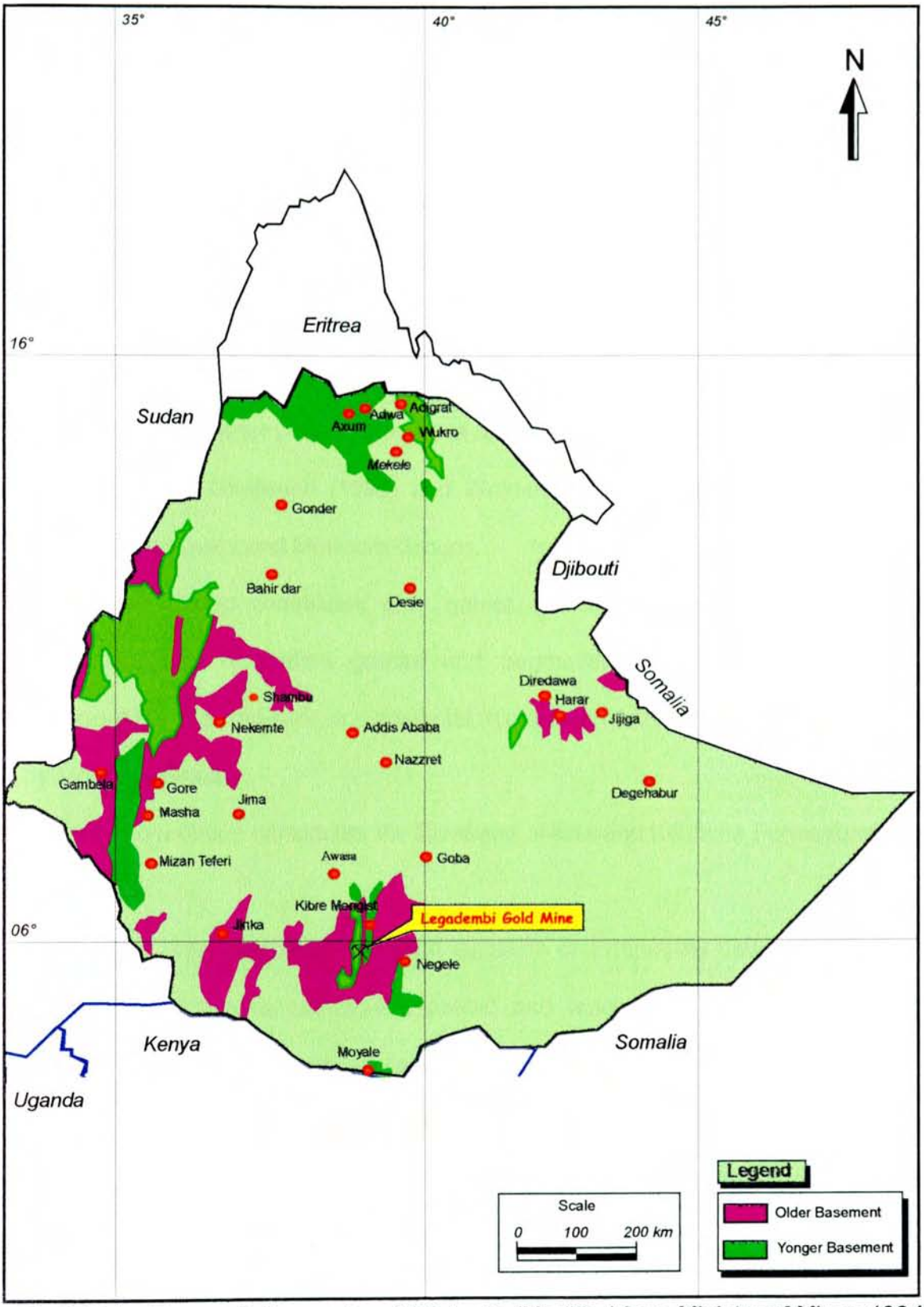

Fig.2.1 The Precambrian rocks of Ethiopia *(Modified from Ministry of Mines, 1994).*

Two major structural zones are identified in the Adola Belt:

i) A folded and refolded gneisses and schists with complex structural and lithologic relationship in the western and eastern part of the Adola Belt.

ii) A linear N-S trending belt made up of intercalated metavolcano-sedimentary, mafic-ultramafic and gneissic rocks that form the Megado, Shakisso, Kentcha and Zembaba Terrains.

The lithostratigraphic associations of the Adola Belt are outlined in different works of Gilboy (1970), Charter (1971), Kazmin et al., (1978), Kozyrev et al. (1985), Worku et al., (1992), Wolday Ghebreab (1992) and Woldehaimanot (1995). The high-grade rocks comprise the Awata and Mormora Groups.

The Awata Group constitutes gray gneiss, which contains syn-to post-tectonic concordant and discordant granite and pegmatite intrusions. It is considered to represent the pre-Pan-African continental microplate (Kozyrev et al., 1985) and overlain by Mormora Group.

The Mormora Group constitutes the Zembaba, Aflata and Kenticha Formations (Kozryev et al, 1985):

- The Zembaba Formation Consists of extensively developed and strongly schistose quartzo-feldspatihic and leucocratic biotite gneisses of both sedimentary and volcanic origins.
- The Kenticha Formation constitutes amphibolites, graphite-staurolite-kyanite and silimanite bearing mica shists, sulphide-bearing pelitic and psammo-pelitic metasediments and marble.
- The Aflata Formation constitutes interlayered biotite gneiss, biotite-hornblend gneiss, amphibolite, and mica schists. The rocks of this group

crop out to the east and west of Megado Graben that is filled with the Adola Group rocks which are the most important ore bearing formations. The interfaces between the Mormora and Adola Groups are straddled by the occurrence of ultramafic bodies.

Granitoid intrusive rocks occur both in the high-grade gneisses and schists as well as the metavolcano-sedimentary sequences of the Adola area. In general the intrusive rocks range in composition from mafic to granitic.

The lithostratigrahic association of the Adola Belt is summarized by Kozyrev et al. (1985) and modified by Worku Hailu (1996) is presented in Table 2.1.

Table 2.1 Lithostratigraphic association of the Adola Gold Belt.

Lithostratigraphy		Lithologies	Comments	Interpretation
			Post-and syn-deformational granitoids intrude all formations.	Post-and syn collision granitoids.
Low-grade meta-volcano-sedimentary terrain	Kajimiti Beds	**Kajimiti Beds**: Arkosic metasandstone and metaconglometerate	Contains clasts with predepositional schistocity, preserved primary sedimentary features.	Foreland basin association
	Adola Group	**Finkilcha Formation**: Phyllite, metasiltone and metasandstone.	No clear boundary between the two formations. Ultramafic rocks, tonalite and gabbros are integral part.	Inter-arc/back basin association and subduction related granitioids.
		Cheketa Formation: Amphibolite, plagioclase-chlorite-actinolite schist, phyllite, quartzite.		
High-grade gneiss and schist Terrain	Mormora Group	**Kenticha Formation**: Mica schists, garnet-staurolite-gneiss, amphibolite, graphitic schist and marble.	Mafic-ultramafic rocks are associated with Kenticha formation. Most of those rocks which are found to be Aflata formations are found to be	Passive continental margin and ocean floor rocks, Associated-subduction related granitoids.
		Aflata Formation: Biotite gneiss, biotite hornblende-gneiss with inter-bedded amphibolites, mica-schists, quartz-kyanite-muscovite schists.		

		Zembaba Formation: Quartzofeldspathic gneiss and leucocratic biotite gneiss.	subduction related intrusives. Zembaba formation constitutes clastic shelf sediments and an orogenic granities	
	Awata Group	**Buluka Formation**: Migmatitic biotite gneiss **Bore Formation**: banded hornblende or biotite-hornblende migmatitic gneiss.	Both formations are gray gneisses and are considered as the same formation (Buluka or Bore Formation).	May represent pre-Pan-African continental-microplate

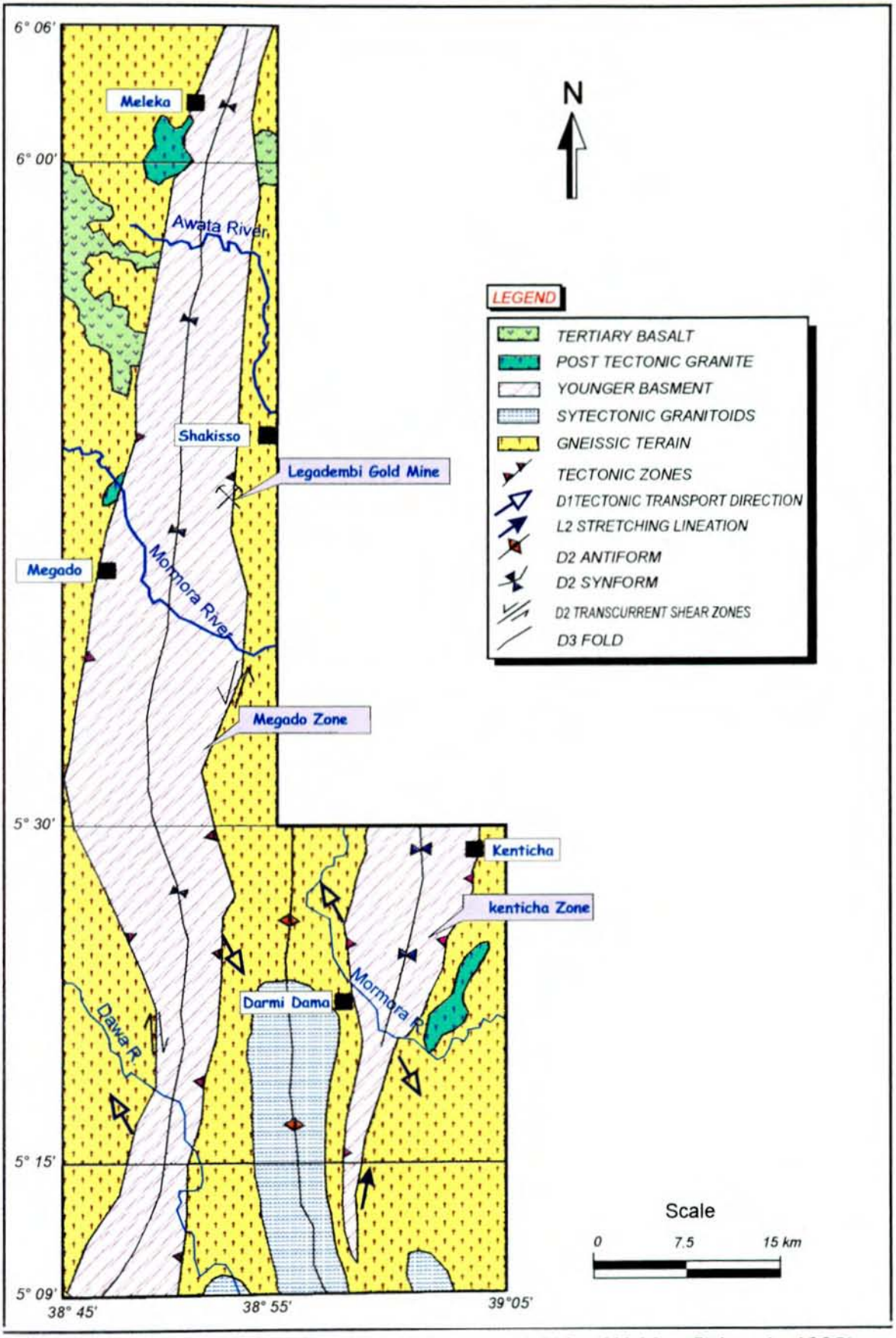

Fig.2.2 The regional geology of Adola Gold Belt (After Welday Gebreab, 1992).

2.2 GEOLOGY OF THE LEGADEMBI DEPOSIT

The regional and structural setting of the Legadembi deposit is confined to a deep fault separating the rock units of the Mormora Group from those of the Adola Group. The auriferous quartz veins occur in the zone of a tectonic suture in the eastern limb of the Megado graben-syncline. This ore-controlling structure has a N-S strike and represented by mylonitized and brecciated rocks.

The ore field is chiefly composed of volcano-sedimentary sequence of the Adola Group (Late Proterozoic- Early Palaeozoic) and underlying gneisses of the Mormora Group (Late Proterozoic).

Within the deposit area, the stratified rocks form four successive lithostratigraphic members which are (from the base upward):

1. Biotite gneiss member;
2. Biotite-Quartz-Feldspar Schist member;
3. Graphitic quartz mica- schist member;
4. Amphibolite .

The *biotite gneiss member* crops out in the eastern part of the deposit. Its colour ranges from light gray to pinkish, some times dark green, medium grained, commonly very quartzose and with schistocity well developed at places. It contains quartz (40-60%), plagioclase (albite to oligoclase 1-5%), feldspar (microcline 20-30%), and biotite (1-5%) (Worash Getaneh, 1994). It is commonly associated with amphibolite, and hornblend-biotite-feldspar schists. All members elongate parallel to the regional foliation direction (N-S). It's contact with the volcano sedimentary series is marked by ultramafic rocks and quartz sericite schist. The following rock unit are observed in the gneiss:

- Quartzo-Feldspathic-Gneiss: Its colour varies from light gray, to pinkish, and dark gray, partly varigated, highly silicified and at places, altered to quartzite. Near the ore bearing low-grade rocks, it is intercalated with minor biotite-actinolite-schists and talcouse crushed soft rocks. At places affected by fault zones manifested by brecciation and features of polished surfaces. Discontinuities are normally filled with alteration products like, chlorite, biotite, and carbonates or impregnated by pyrites.
- Amphibole/Biotite/Hornblende schist: Greenish dark coloured, slightly to moderately silicified; locally alternating with light to pinkish coloured quartzo-feldspathic gneiss; characterized by porphyroblastic texture and giving the unit light to pinkish coloured bands in the greenish dark schist. Quartz veins (glassy), veinlets and stringers are observed in places. Sample from this rock have been petrographically analysed, in Ethioipian Geological Survey Mineralogy and Petrography Laboratory and it consists Quartz 39%, Biotite 20%, Plagioclase 25 %, Epidot 7%, and calcite 3%.
- Amphibole Gneiss: light to dark grey, sometimes greenish; medium grained and poor schistocity; the gneissosity is formed by bands of feldspars and quartz along the gneissocity plane. Needle like hornblende occur as a massive body and coarse grained. At places there are spots of quartz stringers.

The *biotite-quartz-feldspar schist member* consists talc biotite-actinolite schist, quartz sericite schist, and quartz biotite actinolite talc schist. The talc tremolite actinolite schist and quartz sericite schists marks the transition zone between the high grade rocks and the low grade rocks.

- Talc-Biotite-Tremolite Actinolite Schist: represent the shear zone marked by the highly mylonitized unit forming an impermeable zone for the gold mineralization. It is light to dark greyish green with pinkish spots, medium to fine grained and at places intercalated with amphibolite. Samples from this unit have been petrographically analysed and they have Tremolite 50%, Talc 40 %, and Biotite 7 %.
- Quartz-Sercite schist: also this unit represents the shear contact between the high grade and lowgrade rocks at Upper Legadembi. It is white gray, medium grained, silicified with intercalation of mica schist. Sulphide mineralaization such as pyrite, chalcopyrite and pyrhotite are impregnated. At places it consists mineralized quartz veins.
- Quartz Biotite Actinolite Talc schist: commonly mineralized with sulfides as points and impregnations. It is light to dark greenish, highly silicified consisting 30% to 70% quartz veins, stringers and networks. The schistocity dips at 50 to 70° towards WNW. Intercalated with this unit quartz graphitic/carbonaceous micaschist occurs with scattered mineralization.

Graphitic Quartz Mica schist members: these units constitute the western part of the volcano-sedimentary series. In places it is replaced or intercalated with carbonaceous-mica schist but the graphitic material is dominantly observed. It is black to dark gray, fine grained, slightly silicified consisting of quartz veins, veinlets and stock works. At some places it is mineralised with spots and impregnations of sulphides. Locally intercalations of quartz-feldspar-mica schist and talcous-biotite/actinolite schists are observed. During this work three rock samples have been

petrographically analysed and it has Quartz 27- 35%, Graphite 10-25 %, Biotite 20-25 %, chlorite1-8 %, Plagioclase 5%, and calcite trace to 3%.

The intrusive rocks of the ore field and its vicinity consist of metamorphosed ultrabasic rocks, amphibolite and gabbros. Bodies of fine-grained gabbros discordantly intersecting the schistose series outcrop on the west side.

A major part in the geological and tectonic evolution of the deposit area was played by faults, which are extensively developed in both space and time. They considerably modified the folded structure of the ore field. Three systems of faults are recognized: one N-S-trending system comprises deep faults initiated in the Late Proterozoic. At the surface these faults are represented as linear bodies of quartz-sercite schist, talc and talc-tremolite-actinolite rocks. The other two trends are the WNW-ESE, and ENE-WSW faults. All the fracture types intersect one another at different angles and form fault blocks with various relative displacements.

Apart from the above fault sets, individual near E-W-trending fractures are also observed. They extend from the major fault systems and complicate the overall structural pattern of the study area. The geological map of the area is presented as Fig 2.3.

Alteration

The rocks in the area evidence different alteration products among these silification, feldspathization, sulfidization, sericitization, actinolization, argillization, chloritization, biotitization, carbonization and talcization are identified and addressed in Worash Getaneh (1994). Due to alteration the permeability and strength of rocks considerably change. The intensity and dominance of the alteration type, in the area, shows variation from the centre to the periphery of the ore zone. Silicification, feldspatization, sulfidization, actinolization, sericitization and biotitization overlap with

the richest gold and sulphide-bearing zone. Argilization sercitization and biotitization are bounding alteration products dominant at the periphery of the reach ore-bearing zone. Chloritzation, amphibolization, and carbonization are alterations dominant at the outskirts of the shear zone, near the contact with high-grade rocks.

Mineralization

The Legadembi ore body occurs in the N-S trending shear zone and consists numerous tabular and lens shaped bodies parallel to the shear zone, regional foliation and lithologic contact. The gold mineralization is concentrated within quartz veins, vein lets, intervening silicified rocks with quartz stockworks mainly within Quartz Biotite-Actinolite-Talc schist members and the lower part of the Graphitic-Quartz-Mica-schist members.

The rocks in the area experienced progressive deformation (D_1-D_3) and various degree of metamorphism (Gebreab, 1992). The first original lithological layering (S_o) is deformed by F_1 folds whose, axial surfaces (S_1) are regionally dominant. During the D_2 deformation event, F_1 folds have been folded about tight close, upright to steeply inclined, subhorizontal F_2 folds. In D_3 deformation event generally E-W open upright to steeply inclined, subhorizontal moderately westerly and easterly plunging F_3 cross folds were produced. Through out the ore zone and the non-mineralised rocks, quartz veins occur in discontinuous asymmetric arrays parallel to the shear zone. They represent boudnaged quartz veins, which are the product of successive regional tensile, ductile and brittle-ductile deformation of the country rocks.

The vertical and longitudinal dimensions of the veins ranges from few to hundreds of meters, and their width varies from few centimetres to 7 m. The ore-bearing zone is about 1.3 km long and 200 m wide (EMRDC, 1995). Gold mineralization is associated with sulphidization, generally in pyrhotite and chalcopyrite-rich quartz

veins, with minor amounts of pyrite galena and arsenopyrite and traces of sphalerite. Wall rock schists between veins have a considerable amount of fine disseminated gold (Hailu Worku, 1996).

During the exploration stage the deposit has been grouped into three ore bodies, namely, the 'north', 'central' and upper Legadembi zones (NLD, CLD and ULD), separated by late, en-echelon brittle faults trending ENE-WSW, which displace earlier north-south sets parallel to the shear zone. With an overall north plunge they comprise relatively linear steeply dipping bodies. Currently the mine geologists had regrouped the three deposits to two deposits, after grouping the North and Upper Legadembi ore as Upper Legadembi.

The ore body is open at depth (with the deepest drill intersection at around 1500 m above sea level, 700 m below surface), particularly in the North and Upper sections of the mine, extends to depth at grades and width that could support an underground mining operations (Ashanti, 1996).

Different Mining companies evaluated the mine (in their tender document) and estimated that the ore can be extracted by open pit method up to 1930 m or 1920 m above mean sea level. Ore below this level should be mined by underground mining. Based on seven deep drillings, below the Northern and Upper sections of the mine, the underground resource has been estimated to posses some 20 ton of gold from 2.9 million tonnes of ore at 6.84 g/t grade (Ashanti, 1996).

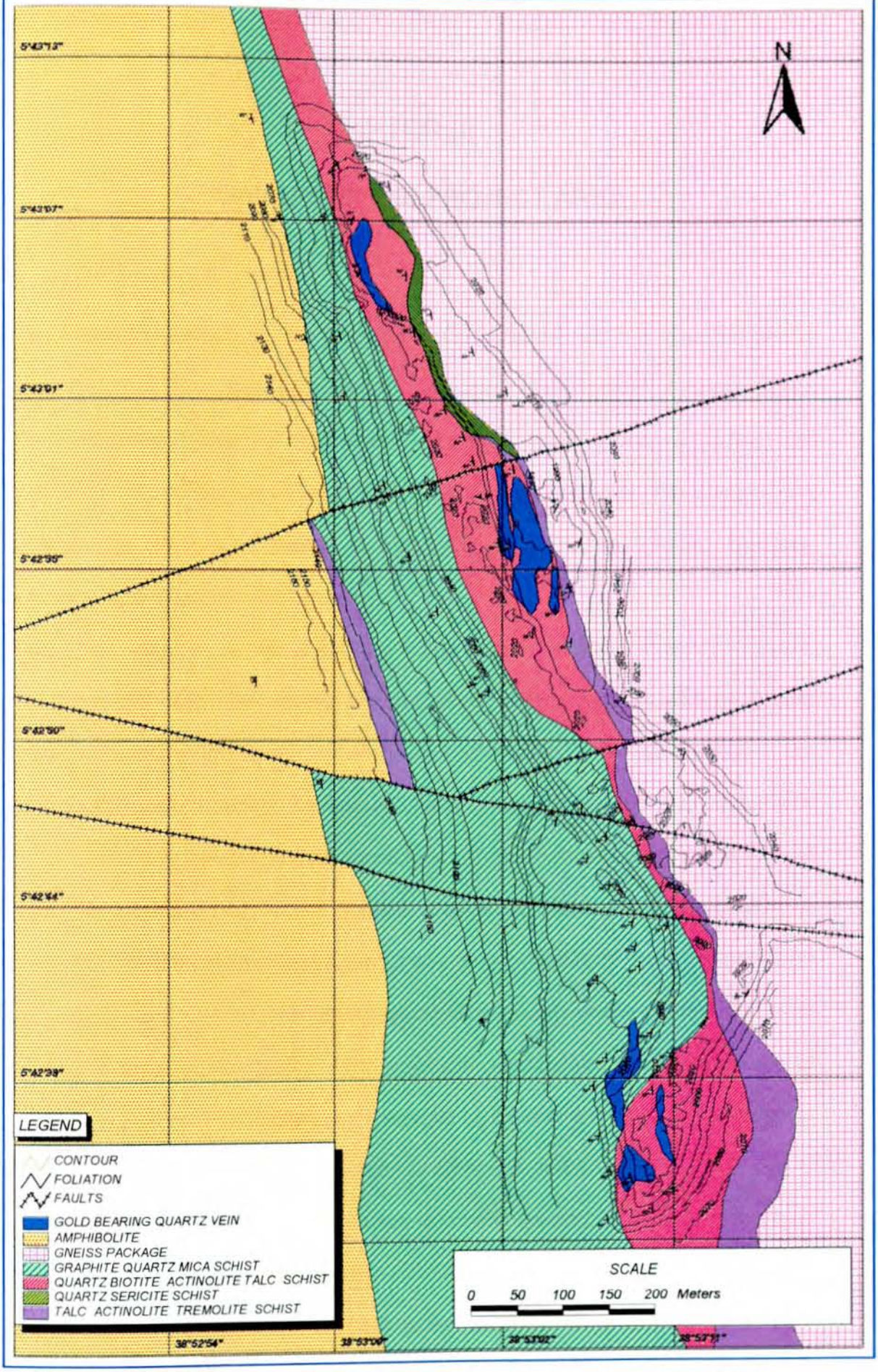

Fig. 2.3 Geological Map of the Legadembi Gold Mine *(Map modified after Project Authorities)*

CHPTER III

SEISMICITY OF THE PROJECT AREA

.1 INTRODUCTION

atural Hazard is defined as "the probability of occurrence within a specified period f time, within a given area of potentially damaging phenomena" (Johnson et al., 988). Earthquake is a natural hazard resulting seismic waves (dynamic loading) that ıay damage natural and man made structure around the epicenter. The damage can e manifested as ground failure in the form of landslides, ground cracking, ubsidence, and differential settlement.

latural hazard analysis is part of engineering geological feasibility study of a project. 's objective is to determine weather the natural risk is at acceptable level or not and ɔ consider the risk in the design parameter of the structure. The determination of the sk involves, measurement of the risk, and judging weather the risk is acceptable or ot. The engineering geologist is responsible in defining natural hazard in the area of ıterest. The definition of natural hazard requires a statement of probability of ccurrence. This prediction of future events of a given magnitude usually depends on asic geologic and seismic studies. These studies usually relate present and past onditions in an effort to identify some empirical relationship, which may serve to redict future events. The engineering geologist typically is forced to make the most f existing information to predict expected risk (Johnson et al., 1988).

/hen important engineering structures are to be constructed, in seismic risk areas, ıe peak earthquake ground acceleration will be a variable useful in the evaluation of ıe response of the structure to earthquake motions. The magnitude of past

arthquakes along with generalized curves on attenuation of generated motion for ifferent regions can be combined to provide estimates of expected peak ground cceleration (Johnson et al., 1988).

.2 SEISMICITY OF THE PROJECT AREA

he Seismic zone of Ethiopia have been delineated by Gouin (1979) and later pdated by Laike Mariam Asfaw (1986). In the later work previously omitted arthquake parameters measurements of Southern Ethiopia were included; strain elease and seismic risk maps has been produced for earthquake from year 1400 to 985 and 1900 to 1985; the probable return period of destructive earthquakes has een considered and a discussion of some unique features of earthquake hazard in he Afar Depression has been presented.

n the same study, a graph for attenuation of intensity with distance, based on the urves for North America (Fig.3.1) has been formulated.

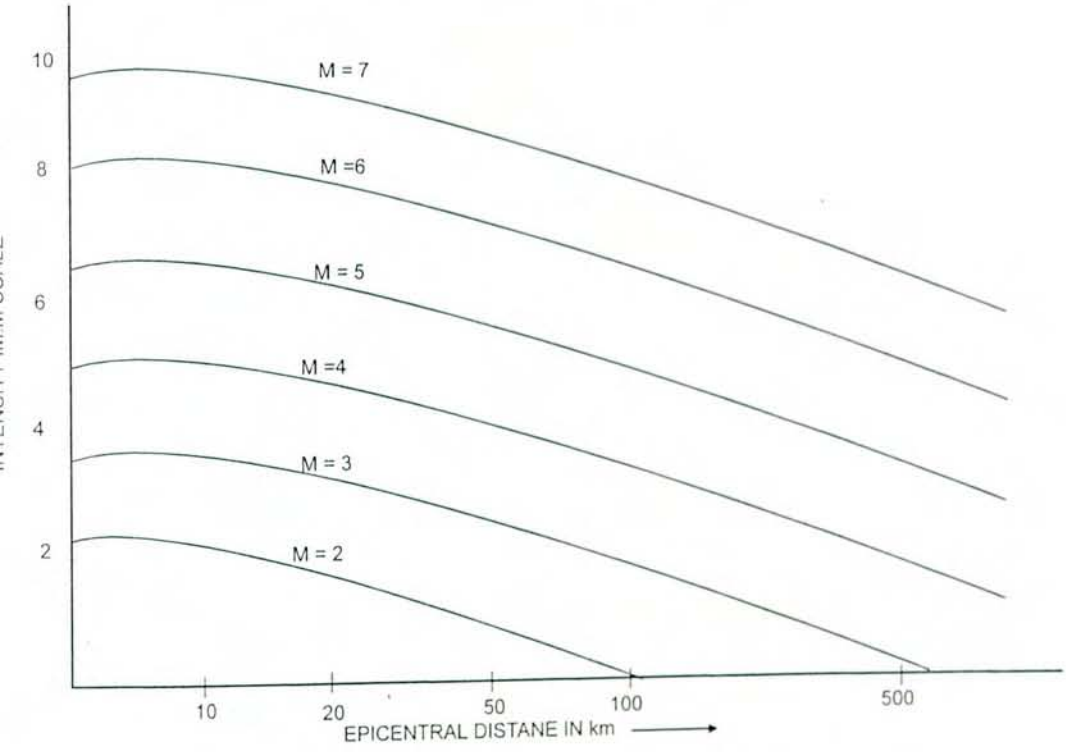

Fig 3.1 Intensity Attenuation curve. (After Laike Mariam Asfaw, 1986).

the curve M.M is the intensity in Modified Meracali and M is the magnitude. The ttenuation curve indicates the intensity attenuation from the earthquake epicenter.

he Legadembi area regionally flanks the southern extension of the Ethiopian Main ift. In the works of Fekadu et al. (1996) the Southern main Ethiopian Rift (SER) (Fig. 2) has been characterized as a region of large and intermediate size earthquakes. he stated notable earthquake occurrences were the 1906 Langano earthquake Maximum 6.8), the 1928 earthquakes (6.0) and the 1987 southernmost rift arthquake (6.2).

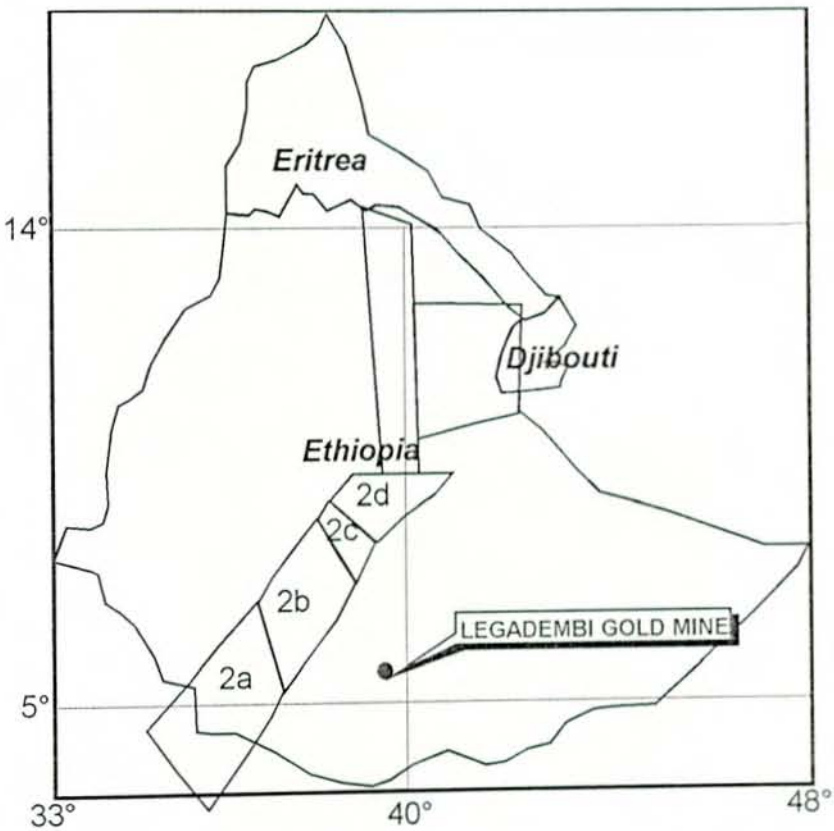

Fig.3.2 The main Ethiopian and southernmost rifts earthquake sources.
Fekadu et al., 1996).

The project area is within the influence area of the SER earthquake sources (Based n the attenuation relation) hence, the effect of dynamic loading on the stability of the ite has been considered in this study.

The 'Seismic Risk Map' produced by Laike Mariam for a hundred year return period and 0.99 probability shows that the study area falls within 7 to 6 M.M scale. The map showing the Seismic Risk zones of Ethiopia and the location of the Project area is presented in Fig. 3.3.

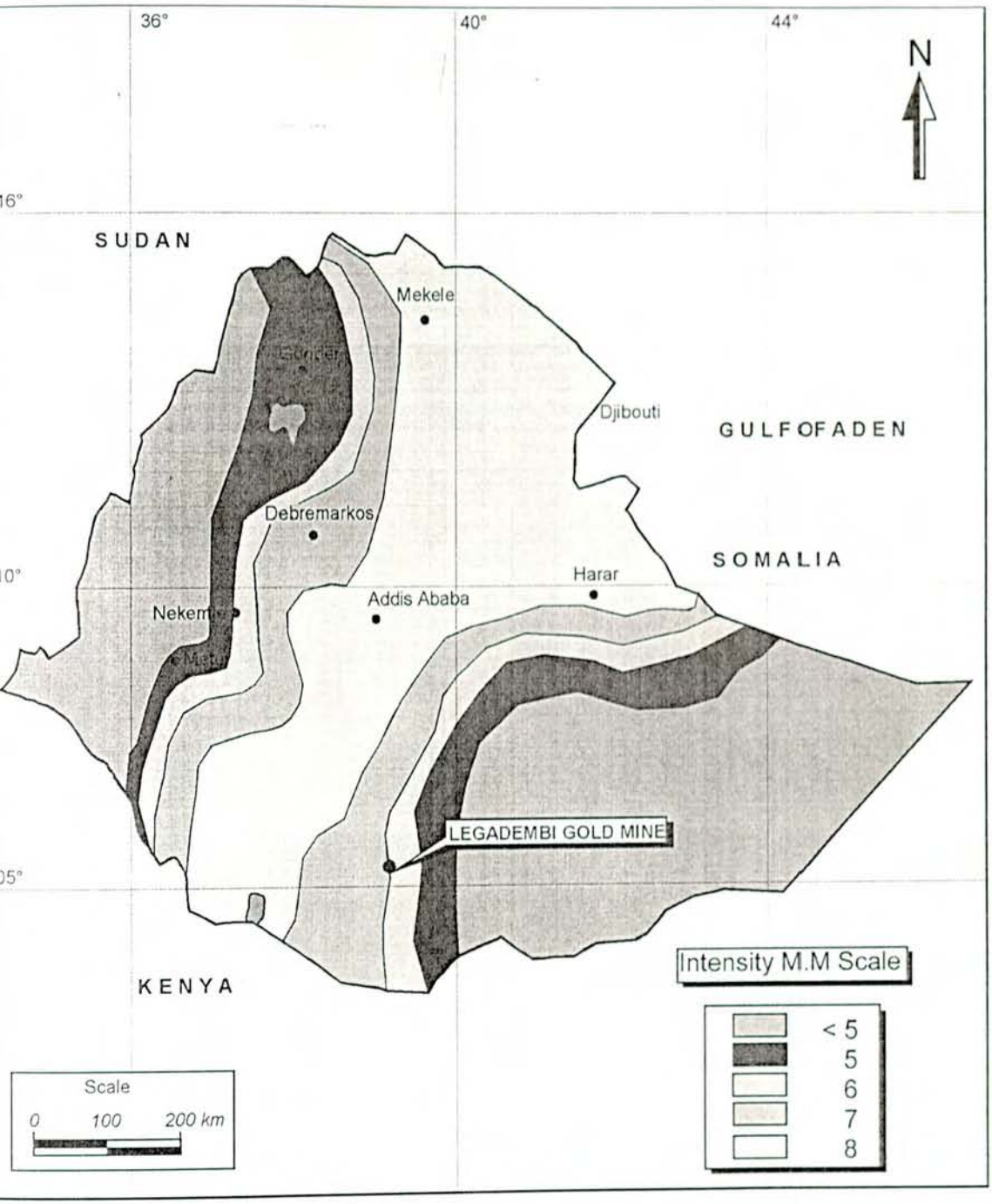

Fig. 3.3 Seismic risk map of Ethiopia 100 year return period, 0.99 probability. (After Laike Mariam Asfaw, 1986).

ased on the chart presented in the book of Johnson et al. (1988), for proposed elations of intensity to ground acceleration, for intensity level 7 M.M., the ground cceleration range from 0.07 to 0.1g.

or the slope stability and underground excavation stability analysis, dynamic ondition, to be on the conservative side the ground horizontal acceleration has been onsidered as 0.08g.

CHAPTER 4

HYDROGEOLOGY

4.1 INTRODUCTION

Water is the most essential natural resource for mankind. It is needed for irrigation, drinking, industry and other domestic purposes. In order to meet the daily needs of life, water is taped by various engineering techniques. For engineering structure groundwater is considered to have a negative impact. The scale of the effect has to be determined and accounted in the design of the structure. For this purpose hydrogeological study has been considered as a part of the site investigation in the present study. Groundwater can affect the stability of a rock mass in five ways (Abramson et.al, 1995):

I. It reduces the strength of the rock mass;

II. It may change the mineral constituents through chemical alteration and solution;

III. It may change the bulk density of the rock;

IV. It may generate pore water pressure;

V. It may cause erosion.

Groundwater is derived from many sources but primarily originates from rainfall. Groundwater level is rarely static and it varies with the rate of recharge or discharge of the groundwater. Rainfall in a given area rarely have uniform distribution, hence fluctuation in groundwater level may vary with geology, topography, and proximity to local centres of discharge, such as springs, rivers, and dams that store water or pump water from the ground.

The infiltrated water can move with ease in soils, rocks and typical fractures of rocks. These are called aquifers. Aquifers are either confined, by two impermeable strata, or unconfined, if exposed or not overlain by an impermeable layer.

The extent to which infiltration from rainfall, reduces the stability of slopes is dependent on a number of factors, such as the original position of groundwater table, the intensity and duration of the rain fall, the antecedent rainfall within the groundwater catchments, the recharge potential of the area, the geology, the degree of saturation, and the topography. In the book of Selby, (1993), the groundwater flow in 10 m^2 rock mass has been classified as slight < 25 l/min, moderate 25-125 l/min; and great > 125 l/min.

There are two possible approaches to obtaining data on water pressure distribution within a rock mass:

a) Deduction of the overall groundwater flow pattern from consideration of the permeability of the rock mass and sources of groundwater.
b) Direct measurement of water levels in boreholes or wells or of water pressure by means of pizometers installed in boreholes.

During the feasibility and development stage of the mine, the hydrogeology of the area has been studied. The study included an observation and investigation of springs, measurement of groundwater in mine workings, fractures, and shears zones. During the prospecting and exploration work it was found that none of the workings contained significant amounts of water throughout the year, including the rainy season. This along the reported frequent encountered loss of drilling fluid during the dip drilling exploration phase, indicated high degree of fracturing in the rocks of the Legadembi deposit (BRGM, 1991).

No springs occur at, or in the vicinity of, the Legadembi deposit apart from one area situated 600 m east of the southern flank of the deposit, where swampy area occurs in the Chameti valley (right-bank tributary of Legadembi creek). The swamp lies at an altitude lower than the southern section of the Legadembi deposit, and is active throughout the year, apparently fed by groundwater seepage from a deep fault zone developed in the fractured gneisses and variable schistes underlying the locality.

Water appears in the Legadembi River channel only locally during the rainy seasons.

4.2 THE OPEN PIT MINE HYDROGEOLOGY

The existence of groundwater around the open pit and underground mine is manifested by wetting bands on the western slope of the open pit, at the Upper and Central Legadembi. This fact can indicate that in the open pit, the groundwater depth is located almost entirely above the local erosion base. The groundwater is mainly unconfined and is associated with fissured zones in all the lithological rock varieties. The depth varies from 10 m to 50 m. It is fed by atmospheric water infiltration, and discharge is via springs and drainage through the underground workings.

The former underground exploration adits are now open both at the western and eastern flanks of the open pit mine. The discharge is mainly observed in the openings located in the western flank. The discharge rates measured in the former exploration Adit No1 and No2, of the central Lega-Dembi area , ranges 0.37 l/s (22.2 l/min) and 0.066 l/s (3.96 l/min) in March and 0.49 l/s (29.4 l/min) and 0.11 l/s (6.6 l/min) in November, respectively (BRGM, 1991).

The groundwater dripping from the western wall accumulated and formed a pond of few centimetre depths. There is also groundwater flow from the walls and roofs of older and recent underground workings, into the open pit excavation floor. This discharge has made ponds at central Legadembi.

Plate 1. Groundwater occurrence in open pit and underground mine.

In the Upper Legadembi western pit wall there are vivid wet bands almost at the same elevation, within weak highly fractured rock mass. At the bottom of these rock mass slopes, the groundwater have been dripping from fractures and wetting the wall surface. This dripping flow have been accumulated on the pit floor and made a pond of very shallow depth.

4.3 THE UNDERGROUND MINE HYDROGEOLOGY

In the underground mine workings groundwater effects have been observed in the access tunnel, the exploration drive, and the ore zone excavation. The groundwater is transmitted through major fault fractures, boreholes, and rock boltholes.

The groundwater surface within the underground mine could have been correctly defined if pizometers were installed at different part of the excavation. With the absence of the groundwater and pressure level measuring device it is very difficult to measure the effect of groundwater on the stability of the excavation. However the effect of groundwater is indirectly accounted in the rock mass classification. In general in the excavation high groundwater inflow has not been observed.

In the permanent excavation the groundwater chemistry may have effect on the support strength. In the underground mining, the main support system is rock bolting and around the portal area it is shotcreeting. To determine the effect of the groundwater chemistry and inflow, observations at different groundwater occurring locations, has been made and two representative samples have been taken for chemical analysis. In 9 locations groundwater occurrences have been observed (Fig.4.1), and the details of each location is presented below:

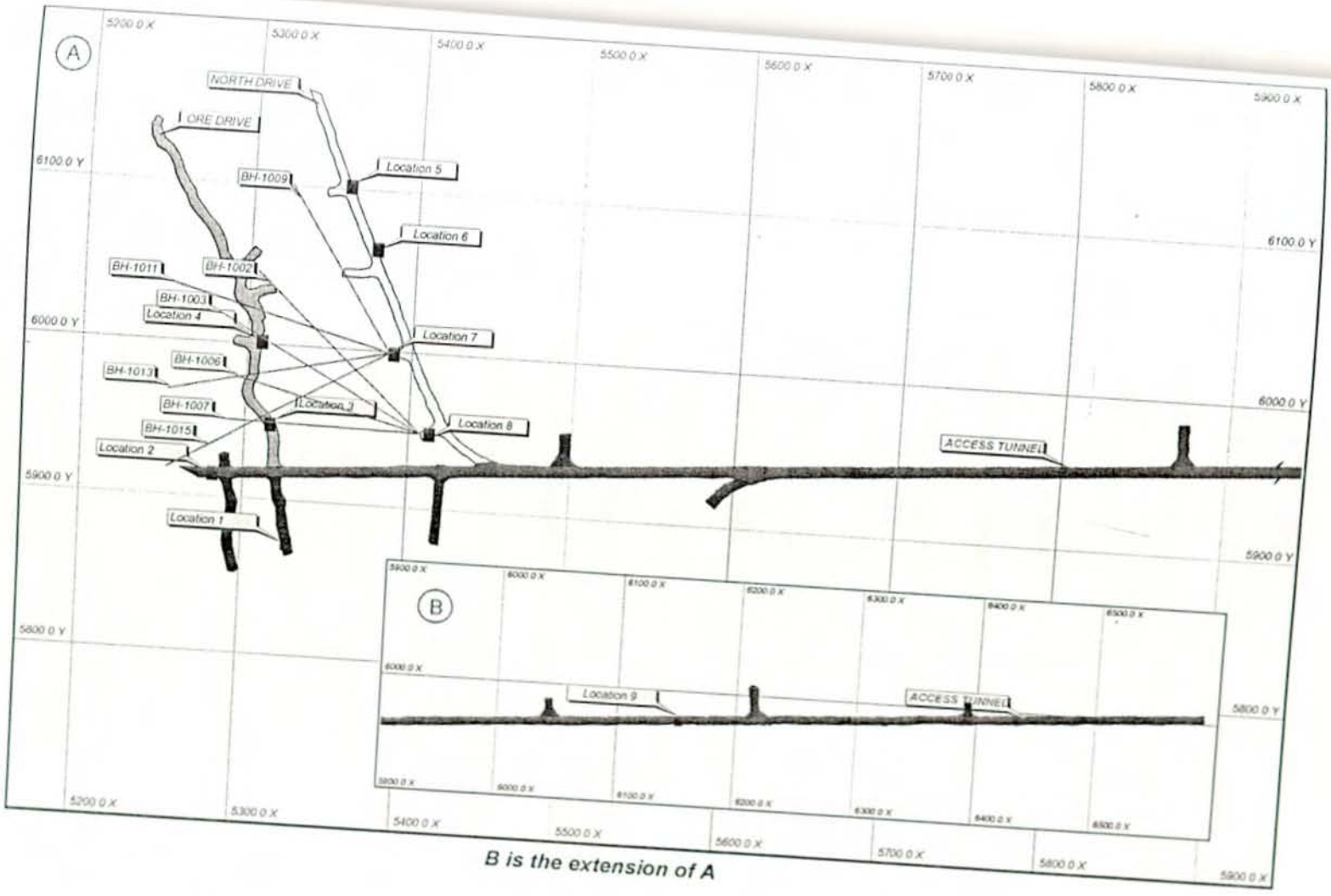

B is the extension of A

Fig 4.1 Underground excavation groundwater occurring location.

- Location 1 is at the southern most part of the ore zone. The water flow has been estimated by measuring the time elapsed to fill1 liter bucket. The flow has been estimated to be 1.0 l/m. It flows from a weak faulted folded and sheared quartz vein of the roof. The fracture dips in N250°/ 80°.
- Location 2 is at the Western extreme of the access tunnel. It has been observed that the groundwater is not in amount of flow but it has made the roof wet. It is coming through a shear zone filled with quartz vein. The shear zone dips in N270°/ 70°.
- Location 3 is in ore zone excavation, on the eastern wall. The groundwater has been observed in the form of droplets falling from a fault fracture.
- Location 4, is in the ore zone excavation at around 80 m from the opening. The water has been dripping from a down ward plunging exploration drill hole, drilled from the north exploration drive and crossing the ore drive eastern wall. The flow amount is consistent and approximately 2 lit/sec.
- Location 5 is located in the northern extreme of the North exploration drive. The water has been dripping from a bolthole and through fractures. The rock is highly fractured and brecciated. The dip direction and dip of the fracture is N270°/60°. The flow is in droplets and approximately a liter per second.
- Location 6 is located within the North Exploration drive on the eastern Wall. The water has been wetting the rock mass around a joint sets dipping towards N270°/ 70°. The groundwater is not flowing but wetting the wall.
- Location 7 is located within the North Exploration drive in cubby 2. In the cubby the water has been flowing mainly through exploration drill holes, number BH 1009, and BH 1011. These drill holes plunge upward crossing the

regional foliation. There is also a wider fracture parallel with the regional foliation direction. The rate of flow from the boreholes has been approximately 1 l/m. For chemical analysis about 1 liter water sample has been collected from this site and submitted to Laboratory (S7).

- Location 8 is located in the North exploration drive cubby 1. In this cubby water flows from the drill holes 1002, 1003, 1006 at a rate of 1 lit/minute. These boreholes are plunging upward with 60° to 70°.
- Location 9 is located in the access tunnel. The area is a shear zone with fault plane crossing perpendicularly the tunnel roof. The groundwater flows from fractures on the north wall and the roof. The rate of flow was approximately 1.0 l/m. On the wall the watercourse has made red and yellowish stains with color gradation red on the top and yellow on the lower part. On the other hand there was a rock bolt near the roof and groundwater is also flowing into the excavation from the rock bolthole. The groundwater from the bolthole has also made red stain on the wall. For chemical analysis Water sample has been taken from this location (S8).

4.4 THE CHEMICAL PROPERTY OF THE GROUNDWATER

The corrosiveness of groundwater affects the weathering intensity of rocks, buried pipes and structures. Total sulphate content of 300 ppm (75 milligram/litre) in groundwater has been classified as potentially aggressive in Abramson et.al (1995). Sulfate when present in large amount, is aggressive to concrete/metallic structure, like rock bolts. Sulfide mineral contained in rocks will be oxidized into hydrogen sulfide. Hydrogen sulfide may result sulfuric acids by the action of oxygen and water. The sulphuric acid will facilitate the weathering process of the native rock causing decrease in strength.

Chemical analysis of the underground water has been made during the environmental impact assessment in the feasibility stage (BRGM 1991). The report indicated that the groundwater from the old adits has been found to be salt free (up to 0.3 g/l); in exceptional cases, when the groundwater has been stagnant, the mineralization was found to be as high as 3-4g/l. The chemical composition of the water was found to vary from sulphate-hydrocarbonate potassium-magnesium to hydrocarbonate-sulphate magnesium-potassium; total hardness of the water varies from 3.1 to 44.8 mmol/l; the carbonate hardness is 1.1 - 4.9 mmol/l.

During the present study two groundwater samples have been collected from the underground mine north drive (S7) and the access tunnels (S8). The samples have been tested at the Ethiopian Geological Survey laboratory. The results are presented in Table 4.1.

Table 4.1 Underground mine groundwater chemical analysis result.

(Concentration in ppm)

Field No.	S7	S8
Sample Location	North exploration drive, Cubby 2	Access tunnel
Lab. No.	1100	1101
Carbonate (CO_3)	-	-
Bicarbonate (HCO_3)	139	328
Chlroide (Cl)	17	99
Sulphate (SO_4)	1146	717
Flouride (F)	0.24	0.18
Nitrate (NO_3)	22.2	15.51
Sodium (Na)	25	60
Potassium (K)	32	13.5
Calcium (Ca)	330	295
Magnesium (Mg)	110	75
Silica (SiO_2)	13	32
Bromide (Br)	0.28	3
Iodide (I)	0.01	0.23
Carbon dioxide (CO_2)	13	23
pH	7.4	7.52

4.4.1 *Corrosivity of the underground mine groundwater*

The coexistence of sulphate and chloride ions in groundwater causes deterioration of reinforcement (concrete or rock bolt). The corrosivity of the groundwater can be determined from the corrosivity ratio coefficient, CR (Mahadevaswamy, 2002). If the CR value is > 1 the groundwater is corrosive. In corrosive groundwater conditions, while doing excavation, a proper precaution has to be taken to reduce the effect of corrosion, especially in permanent excavations. According to Mahadevaswamy (2002), the value of the corrosivity coefficient can be determined from:

$$CR = \frac{0.028Cl + 0.021SO_4}{0.02(HCO_3 + CO_3)}$$

Thus by applying this relation, CR value for samples S7 and S8 are 8.8 and 2.71 respectively.

The groundwater analysis data shows that both in the North exploration drive and the access tunnel the groundwater has high content of sulphate (> 700 ppm) and chloride (> 17 ppm) with corrossivity coefficient, CR > 1 . According to Abrahamson et.al 1995, if total sulphate content of the groundwater is greater than 300 ppm the groundwater can be classified as aggressive to concrete/metallic material. Thus the groundwater leaking in the underground structure is corrosive with respect to concrete/metal materials. The same conclusion has been drawn from samples taken during the feasibility stage, also.

Thus while suggesting the support measures care has been taken to account for the corrosiveness of the groundwater for concrete and metallic materials.

In general the groundwater flow observations indicated that the flow is through the regional foliation of the rock mass. This conclusion is based on the fact that groundwater flow has been mainly through structures, drill holes and boltholes

crossing perpendicularly the regional foliations. The regional foliation has been regionally continuous and intersected by different fracture sets; hence it can be suitable for groundwater movement.

CHAPTER V

SLOPE STABILITY STUDIES OF THE OPEN PIT

5.1 INTRODUCTION

Open excavation for mining or other purposes involves the removal of earth material to a greater depth. In order to accomplish this economically the character of the rocks and soils involved, their geological setting must be investigated.

One of the main characteristics of open pit mining economy is the stripping ratio, which is relatively numerical volume of barren rock per ton or m^3 of mineral excavated. Generally when the slope is cut steep the amount of overburden to be removed will be reduced. However, the economic benefits gained in this way can be negated by a major slope failure. Hard rock masses are liable to sudden and violent failure when the excavated slope is very steep or high and exceeds their peak strength. On the other hand soft materials tend to fail by gradual sliding. Evaluating the stability of the ultimate slopes is an important part of open pit design.

The design of slope excavation in rock must be based on understanding of geological set up of the site and spatial relationship between contained discontinuity planes. These input data will help to identify the basic dominant mode of failure in the area and shear strength along failure planes, which are important for the stability analysis. Besides making the over all slope steep the stability of individual bench slopes should be considered. The benches have to be stable and wide enough to accommodate heavy mining machineries. The stability of individual benches is controlled by local geological condition, the shape of the overall slope in that area, local groundwater conditions and also by excavation condition (Hoek et al., 1977).

While the overall slopes are clearly important in terms of the economics of the entire mining operations, the stability of individual benches is usually a matter of more immediate concern to the engineers and for the day-to-day mining operations.

Identification of potential unstable slopes in the initial stage helps the designers and engineers to plan further excavation of the mine in such a manner that the risk to human and machineries is minimized. Based on the stability results, a safe slope design can be generated, which not only maintains the economy of the mine but fulfilling the safety considerations for man and machinery.

In the present study the stability of excavated slopes in open pit mine has been carried out by limit equilibrium method. The stability study for slopes has been carried out for static and dynamic conditions, of dry, moderately saturated and saturated water conditions. Safe slope design has been evolved for a possible worst conditions i.e. a slope in a moderately saturated dynamic (earthquake loading) condition.

5.2 SURFACE GEOLOGY OF THE OPEN PIT

The Legadembi gold mine lies in the eastern flank of the Megado Graben syncline within Adola gold belt. The open pit lies at the western slope of the Wosho Mountain, partly forming the Legadembi valley. The contact between the different units is a N-S stretching horizontal shear zone. The main rock types exposed in the open pit mine, from east to west, are gneiss, talc tremolite-actinolite schist (quartz sercite schist), quarz biotite actinolite talc schist, graphite quartz mica schist, amphibolite, and gabbro. The detail of the geology of the Legadembi gold deposit has been addressed in chapter II.

In general from top to bottom the pit consists:

-a few meters of red reworked clay, lateritic on the surface:

-a clay-silt weathering mantle, resulting from the insitu decomposition of the parent rock varying from 10 meters to 30 meters thick.

-a zone of weathered and fractured rocks, 10 m to 15 m thick.

-the fresh rock.

5.3 TOPOGRAPHY OF THE OPEN PIT

The Legadembi open pit mine is located at the western flank of the Wosho Mountain. The Wosho Mountain lies at 2200 m above sea level and it is a N-S stretching mountain. The mining activity started roughly at the level of 2200 m above sea level (BRGM, 1991). The ore body is aligned with the regional foliation direction, which has a N-S strike with 10° to 15° deviations from North. The pit layout follows the strike direction of the ore body. For work convenience locally the pit has been divided into two parts namely, the northern pit, known as Upper and the southern part, known as Central Legadembi. During this study the bottom level at Upper Legadembi was at 1999 m, and at Central Legadembi it was 2020 m above sea level. The topography of the pit is presented as triangulated network 3D view map, Fig. 5.1.

5.4 GEOMETRY OF THE SLOPE SECTIONS

In order to carry out the stability studies in the open pit area, totally 7 slope sections have been selected. The selection has been based on the topography and the geometry of the slopes. Section line 2, 4, and 5 were further divided into subsections based on the lithologic and topographic difference. Fig. 5.2 shows RMR data observation locations and the distribution of section lines in the open pit. Cross sections along the section line were prepared, which indicates the overall geometry of the slope (Fig.5.3 to Fig. 5.5) sections. Table 5.1 presents the slope geometry (collected from slope sections) data.

Table 5.1. Details of slope geometry and lithology at various section Lines.

Slope section	Slope face angle	Upper slope angle	Height of the slope (mt)	Lithology
SL1	50°	25°	40	Graphitic quartz mica schist
SL2A	50°	5°	40	Graphitic quartz mica schist
SL2B	35°	20°	40	Graphitic quartz mica schist
SL2C	30°	0°	35	Soil
SL3	45°	20°	115	Graphitic quartz mica schist
SL4A	50°	25°	90	Graphitic quartz mica schist
SL4B	30°	0°	60	Amphibolite
SL5A	53°	20°	45	Graphitic quartz mica schist
SL5B	50°	25°	58	Amphibolite
SL6	40°	0°	40	Gneiss
SL7	40°	0°	55	Qtz.Biotite.Actinolite.Talc. Schist.

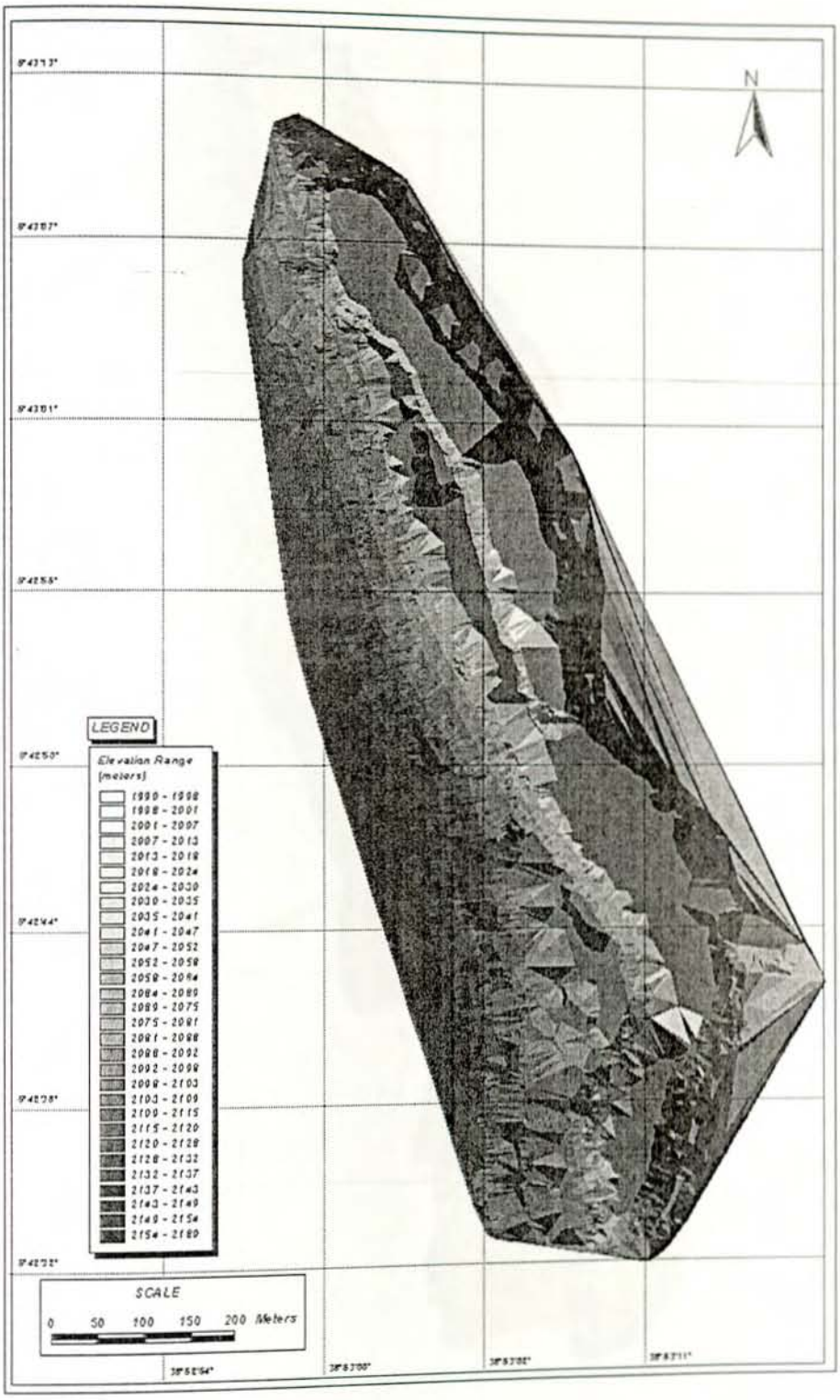

Fig. 5.1 Triangulated network (TIN) model-a 3D view representation of the open pit. (Source data from the Mine)

Fig.5.2 Open pit layout, slope sectionlines, and RMR data locations.

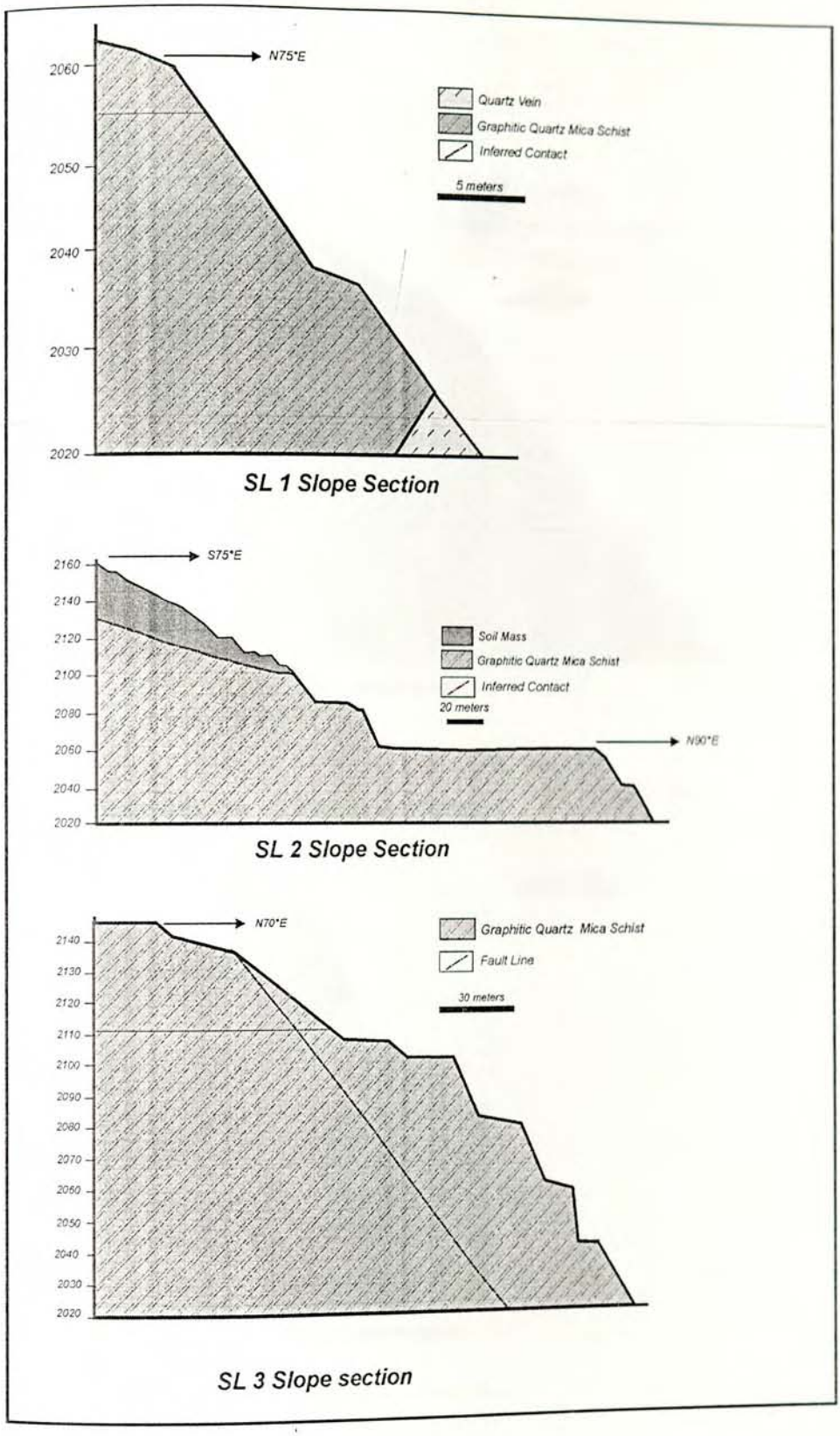

Fig 5.3 Geological cross sections along section lines SL1, SL2 and SL 3.

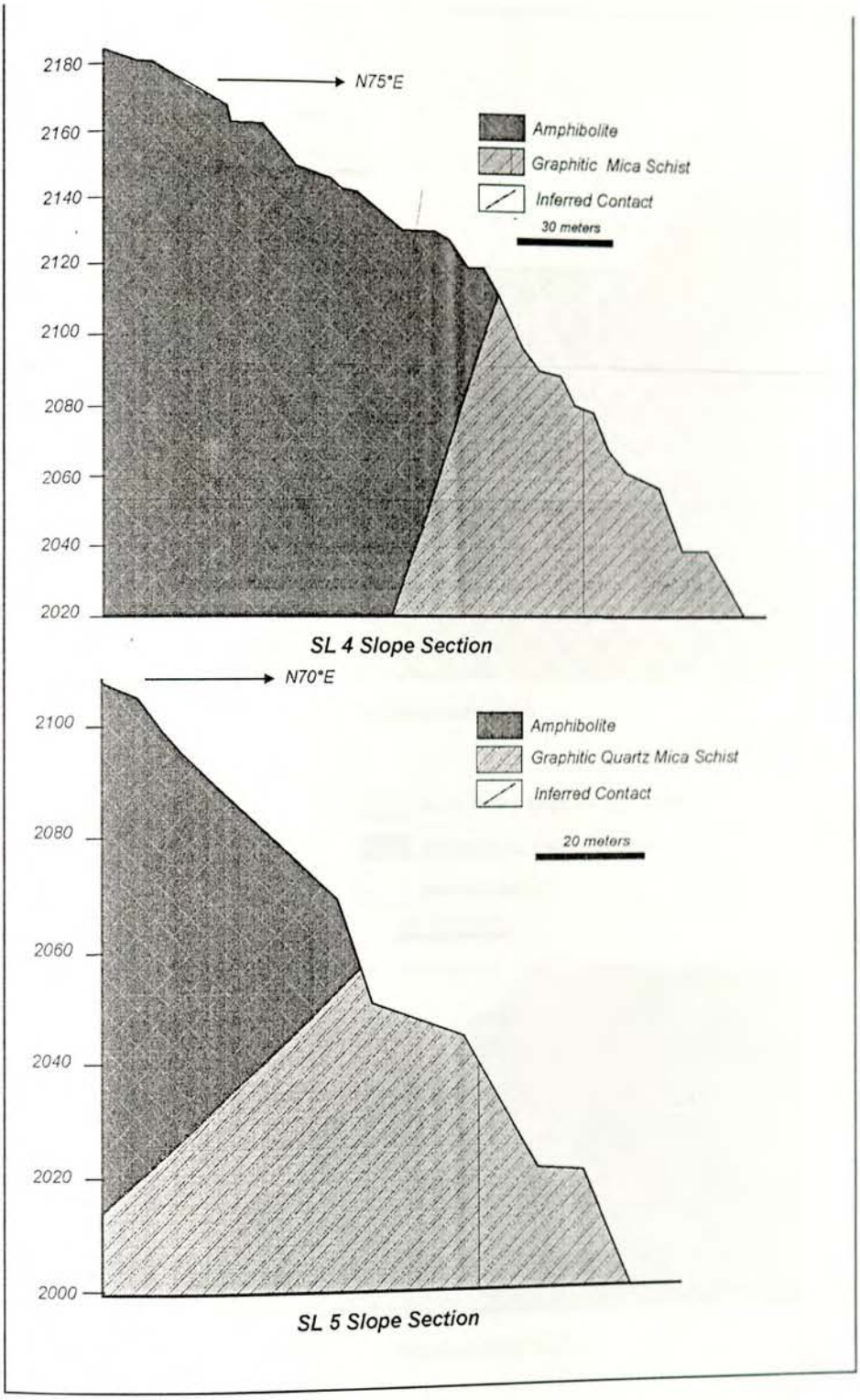

Fig. 5.4 Geological cross sections along section line SL4 and SL 5.

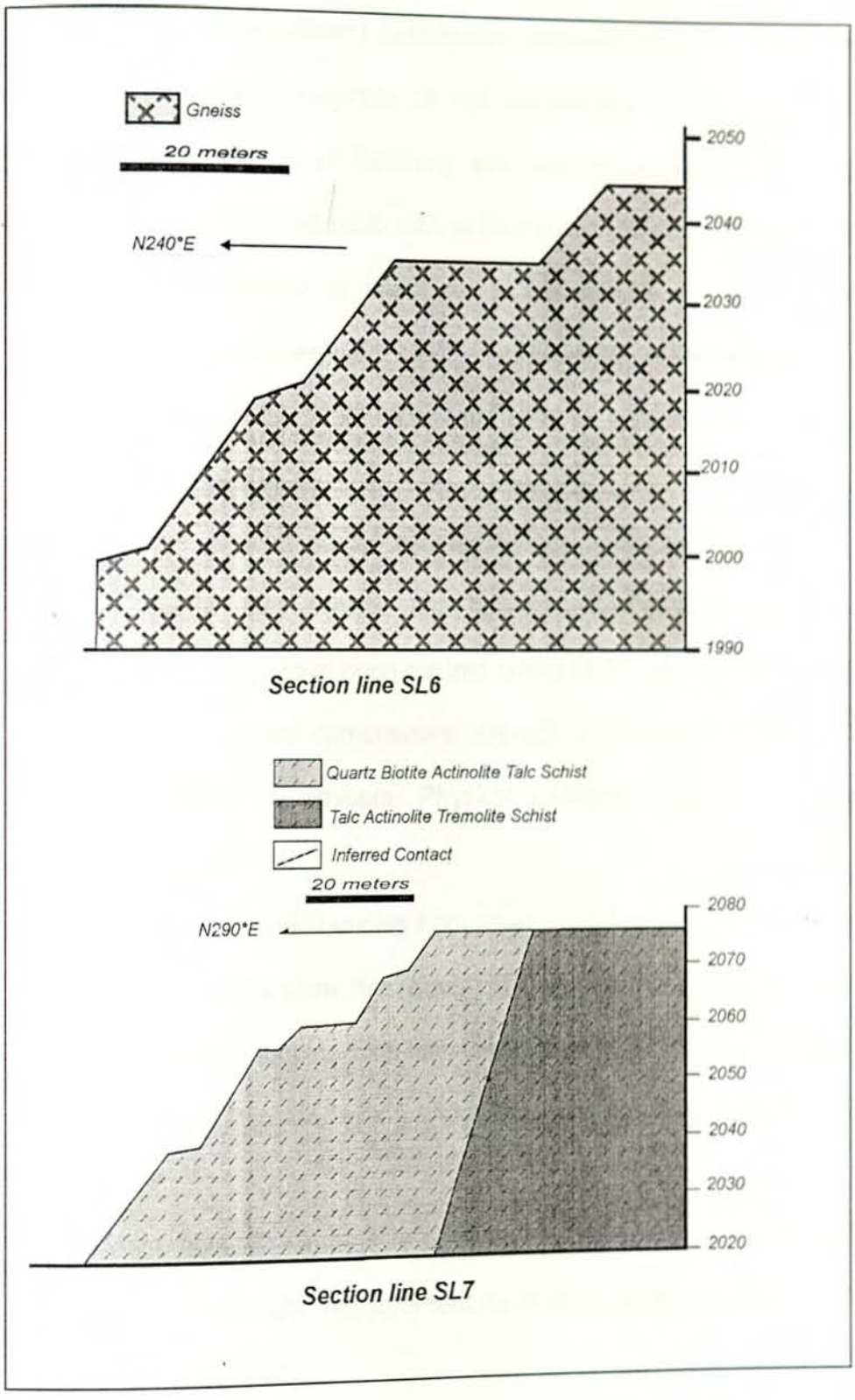

Fig.5.5 Geological cross sections of section lines SL 6 and SL 7.

5.5 ENGINEERING PROPERTY OF ROCKS

Rock mass generally show different deformation behavior based on the rheological (stress-strain relation ship) properties of the constituting rock forming minerals, degree of weathering, degree of fracturing and orientation of discontinuities. The intrinsic physical property of the intact rock is an input in the slope stability analysis. The main physical properties of intact rocks are specific gravity, unit weight, compressive strength, tensile strength, modulus of elasticity, and poisons ratio.

The physical properties of the intact rock of the open pit mine has been determined from:

a) During the present study, boulder sample, collected from the gneiss, Graphitic quartz mica schists, and talc-actinolite-tremolite schists. These boulder rock samples have been cut into cubes of 38 mm^3 and measurements of unit weight, uniaxial compressive strength tests were conducted in the Geological Survey of Ethiopia, Physical Laboratory and the results are presented in Table 5. 2.

b) During this study core samples from abandoned borehole have been taken. The diameter of the core has been 54.7mm. Compressive strength, unit weight, and elastic modulus tests have been conducted in Construction Design Share Company, Material Testing Laboratory. The result is presented in Table 5.2.

c) During the feasibility study core samples have been taken and compressive strength and unit weight measurement have been done. The test results are presented in Table 5.2.

Table 5.2 Physical properties of rocks.

Rock Type	Density (T/m^3)	Compressive Strength (Mpa)	Source
Gneiss	2.64	356	Cube test (this work)
Biotite Gneiss	2.65-2.75	237	EMRDC*
Biotite Plagioclase schist	2.67	263.4	Cube test
Hornblede Schist	2.66-2.8	108.6-172	EMRDC
Quartz Sercite Schist	2.6	95.86	Core sample (this work)
Biotie Talc Tremolite Schist	2.85	38.83	Cube test
Talc/Talc Tremolite Schist	2.82-2.92	13.2-59	EMRDC
Quartz Biotite Actinolite Talc Schist	2.86	31.5	Core sample
Quartz Biotite Actinolite Talc Schist with Quartz vein	3.0	101.11	Core sample
Quartz Biotite Actinolite Schist	2.7-3.03	81.3-216	EMRDC
Quartz Vein	2.64-2.79	88.5-119.9	EMRDC
Graphitic Quartz Mica schist	2.97	143.97	Cube test
Carbonaceous Quartz Mica Schist	2.72-2.87	88.5-119.9	EMRDC

* *Ethiopian Mineral Resource Development Corporation, (1995).*

5.6 SHEAR STRENGTH OF DISCONTINUITY PLANES

At shallow depth the deformation property of rock mass is controlled by the density of discontinuity planes and their spatial relation. In order to analyze the stability of a rock mass one has to understand the available shear strength between adjacent discontinuity planes. The factors that control the magnitude of the shear strength are the degree of cohesion (c) and angle of internal friction (ϕ). The shear strength of discontinuity planes is represented by the equation:

$$\tau = c + \sigma_n \tan\phi$$

Where c is the cohesive strength of the surface, σ_n the normal stress and ϕ is the angle of internal friction. Both these parameters can be determined by laboratory shear tests on a rock containing discontinuity planes.

The natural discontinuity surface in hard rock is never been smooth. The undulation and asperities on a natural joint surface have significant influence on its shear behavior. Generally the surface roughness increases the shear strength of the surface, and this strength is extremely important in the stability analysis. Barton et al. (1973, 1976,1977,1990) have studied the behavior of natural rock joints in great details and have proposed the shear strength of discontinuity planes by a relation (Hoek, et.al. 1995):

$$\tau = \sigma_n \tan [\phi_b + JRC \log_{10} (JCS/\sigma_n)]$$

Where JRC is the joint roughness coefficient; JCS is the joint wall compressive strength; τ is peak shear strength; σ_n is effective normal stress and ϕ_b is basic friction angle.

To estimate the shear strength of the discontinuity planes the above empirical relation has been used. For this relation the joint roughness coefficient has been determined on site, by comparing the surface roughness profile with the table presented in Hoek et al (1995) and giving the corresponding JRC rating. The data is presented in Table 5.3. During the feasibility study of the open pit, laboratory shear tests have been conducted on discontinuity planes contained in core samples (BRGM 1991) the result is presented in Table 5.4.

Table 5.3 Joint roughness data from field visual observation

Site	Fracture Orientation Dir/Dip	Joint Roughness Coefficient (JRC)
Foot Wall	N270°/60°	4-6
	N040°/75°	10-12
	N260°/65°	6-8
	N100°/20°	12-14
	N80°/ 20°	4-6
	N280°/65°	4-6

Site	Fracture Orientation Dir/Dip	Joint Roughness Coefficient (JRC)
	N70°/20°	4-6
	N270°/60°	2-4
	N100°/30°	6-8
	N100°/30°	0-2
Hanging Wall	N260°/70°	4-6
	N100°/35°	10-12
	N260°/70°	4-6
	N100°/30°	10-12
	N260°/70°	6-8
	N100°/30°	4-6
	N260°/70°	2-4
	N090°/30°	8-10
	N260°/70°	2-4
	N100°/35°	10-12
	N110°/30°	6-8
	N260°/70°	4-6
	N260°/70°	6-8
	N100°/35°	12-14
	N260°/70°	6-8
	N090°/35°	4-6
	N100°/30°	16-18
	N270°/65°	6-8

Table 5.4. Shear strength characteristics of sets of structural discontinuities.

Site	Wall side	sets of structural discontinuities Dir/Dip	Shear Strength	
			Residual cohesion (kPa)	Angle of friction
Central Legadembi	West face	N160°-N210°/ 15°-30°	200	40°
		N300°-N325°/ 50°-90°	200	40°
		N45°-N85°/ 50°-70°	200	40°
	South Face	N230°-N265°/ 50°-90°	200	40°
		N20°-N90°/ 10°-65°	200	40°
		N155°-N200°/ 65°-90°	200	40°
	East Face	N135°-N155°/ 60°-90°	200	40°
		N230°-N265°/ 50°-90°	200	40°
		N260°-N270°/ 35°-65°	200	40°
		N20°-N90°/ 10°-65°	200	40°

	Northeast Face	N155°-N200°/ 65°-90° N135°-N155°/ 60°-90° N260°-N270°/ 35°-65°	200 200 10,000	40° 40° 40°
Upper Legadembi	West Face	N260°-N270°/ 35°-65° N230°-N265°/ 50°-65°	11,000 200	50° 40°
	North Face	N230°-N265°/ 50°-65° N20°-N90°/ 10°-65° N155°-N200°/ 65°-90°	200 200 200	40° 40° 40°
	East Face	N20°-N90°/ 10°-65°	200	40°

5.7 GEOMECHANICAL (RMR) CLASSIFICATION OF THE ROCK MASS

Rock mass classification schemes are in application as an engineering structure design input for more than 125 years. When little or no information is available to estimate the strength and characteristics of a rock mass, rock mass classification systems are ideal means. Among the various classification systems, Bieniawski's RMR (rock mass rating) and the Norwegian Geotechnical Institute Q-systems are widely used.

To characterize the rock mass and for stability analysis, Bieniawski's Rock Mass Rating system known as the Geomechnics Classification (1989) has been adopted. The data pertaining to RMR has been collected at 53 locations. The RMR data locations are presented in Fig. 5.2. Bieniawski's 1989, RMR is modified for mining purpose giving more weight on factors that control the stability. The five main parameters of the RMR, and the reduction are discussed below.

1. The strength of the intact rock mass was considered from laboratory uniaxial tests performed on samples collected during this work and during the feasibility stage.

2. RQD or Rock Quality designation was determined using the Palmeström's, Volumetric count method. This method gives three-dimensional picture of the joint spacing. In this system RQD is related with Joint count number (J_v) by the relation:

$$RQD = 115-3.3J_v$$

$$RQD = 100\% \text{ when } J_v \leq 4.5.$$

In areal mapping this system has the advantage of averaging out some of the anisotropy of the RQD term and gives representative value.

3. Joint spacing: joint spacing were measured in each cubic (1 m X 1 m x 1 m) volume of rock mass. The measurement was taken using a steel meter tape. Based on the different ranges in the classification system as threshold, ratings were adopted for each joint set within the location. The rating ranges from 5 to 20.
4. Conditions of discontinuities: in this parameter the roughness of discontinuity surfaces, the continuity of discontinuity planes, separation of discontinuity openings, the weathering conditions of the walls of discontinuity planes were considered.
5. Groundwater conditions were also considered in the rating. Most of the pit slopes are dry and the rating values were mainly for completely dry (15) and at few places for damp condition (10).
6. Rating adjustment was considered according to the influence of the discontinuity orientation with respect to the excavation slope face. The adjustment rating ranges from 0 to 50 % of the RMR calculated value.

7. The two shear strength parameters Cohesion (C) and angle of internal friction value (ϕ), for each RMR locations, are empirically calculated from the relation developed by Bieniawski (1989), Geomechanic classification:

$$\phi = 0.5\,RMR + 5; \quad C = 0.05RMR$$

Based on their proximity to the section line the 53 RMR locations have been grouped into 7 section lines. The average RMR, cohesion and angle of internal friction value for the rock mass around each section lines are presented in Table 5.5.

Table 5.5. Average values of RMR and shear strength parameters of section lines.

Section Line	Average RMR (%)	Cohesion (kg/cm^2)	Angle of internal friction (ϕ) (degree)
SL1	57	2.83	33
SL2	49	2.45	30
SL3	46	2.28	28
SL4	43	2.15	27
SL5	48	2.41	29
SL6	50	2.47	30
SL7	51	2.54	30

According to the Geomechanics classification (Bieniawski, 1989) result, the rock mass around the open pit , is rated as class III (Fair Rock) with average cohesion value ranging 200-300 kPa and friction angle 25°-35°.

5.8 FRACTURE ANALYSIS

The presence or absence of discontinuities has a very important influence upon the stability of rock slopes and the detection of these geological features are most critical parts of the stability investigation (Hoek et al, 1977).

When the rock mass contains discontinuity surfaces dipping towards the slope face at angles between 30° and 70°, simple sliding can occur and the stability of the slope is significantly lower than those in which only horizontal and vertical discontinuities are present.

The rock mass forming the Legadembi open pit mine consists discontinuity planes mainly, joints, faults, and schistocity planes. To determine the main discontinuity sets, around the open pit, 954 dip and dip direction measurements of joints have been taken and analyzed using Spheristat 2. and Dips computer programs. The convention used to measure the fractures has been, the azimuth of the 'Dip-Direction' clockwise in relation to magnetic north from 0° to 360° and amount of dip.

For data analysis the data were feed in Spheristat 2., data table as Dir/Dip, then the poles of the measurements have been plotted on a circular diagram (Schmidt projection, lower hemisphere). Using the density analysis facility of the program the poles were contoured on Schmidt counting net. The major planes dip directions and dips are plotted in Dips computer program. The fracture analysis has been used for the Kinematic check of each slope section.

The contour density analysis of all the fracture data resulted four major clusters. The dip direction and dip measurement of these planes, on decreasing percentage are:

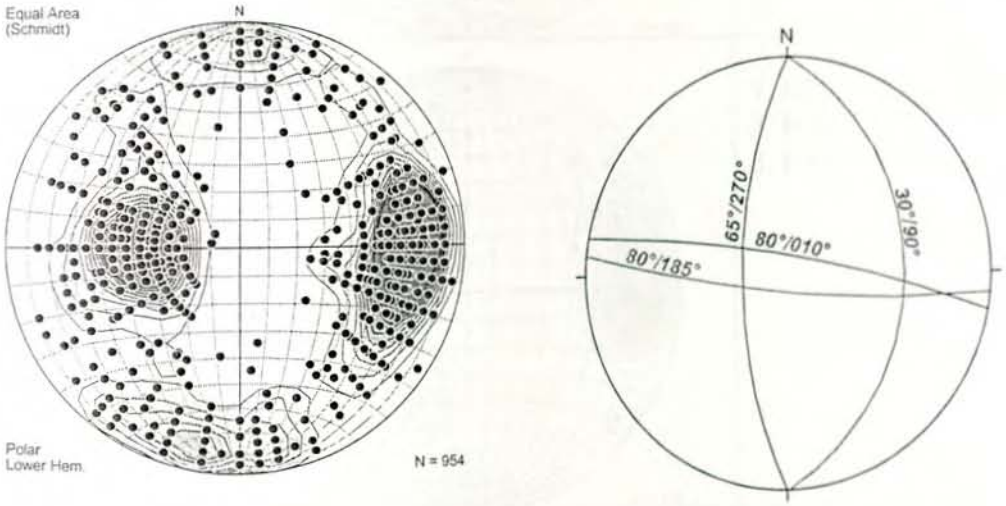

Fig. 5.6 Plots of poles of discontinuity planes measured around the open pit mine.

Table 5.6 Fracture analysis result around each section line.

Section Line	Contour Analysis	Major Plane (Dir/Dip)
Section Line 1	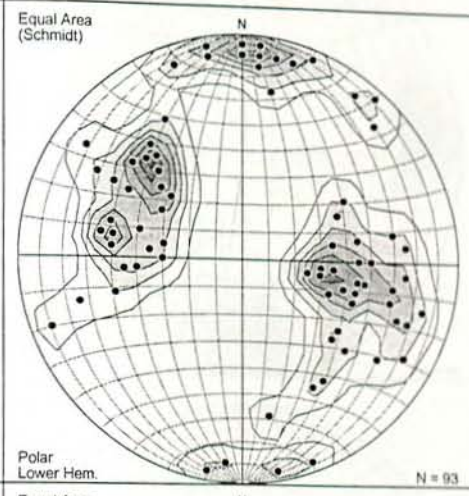	1. N135°/52° 12.98% 2. N185°/80° 10.84% 3. N100°/55° 9.67% 4. N275°/35° 9.36%
Section line 2A	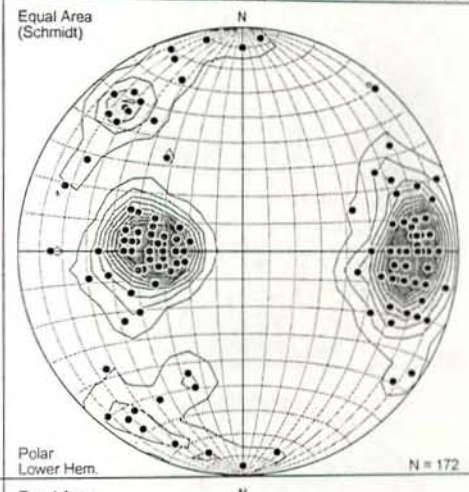	1.N270°/70° 31.30% 2.N090°/30° 30.19% 3.N140°/80° 6.29%
Section line 2B	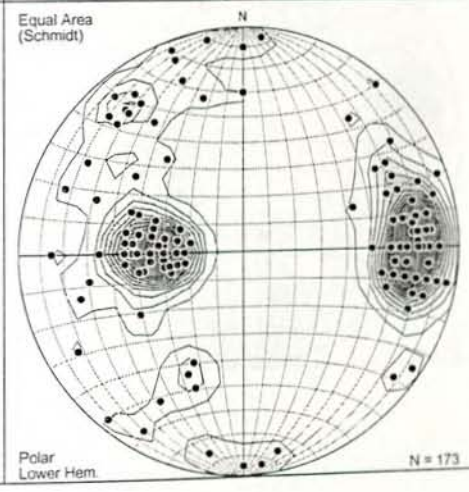	1. N270°/70° 35.22% 2. N090°/30° 30.24% 3. N145°/80° 6.26%

Section line 2C	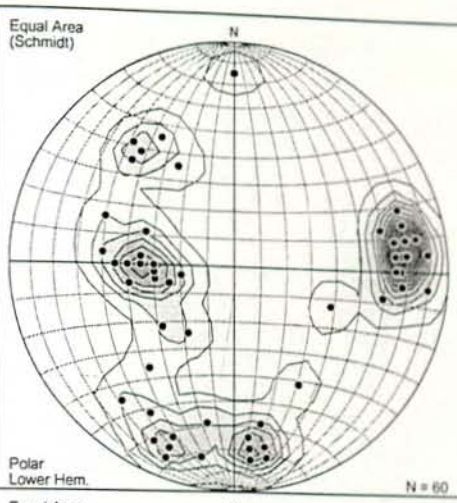	1. N265°/70° 23.51% 2. N090°/35° 12.84% 3. N355°/70° 11.21% 4. N140°/55° 6.58% 5. N020°/75° 6.54%
Section line 3	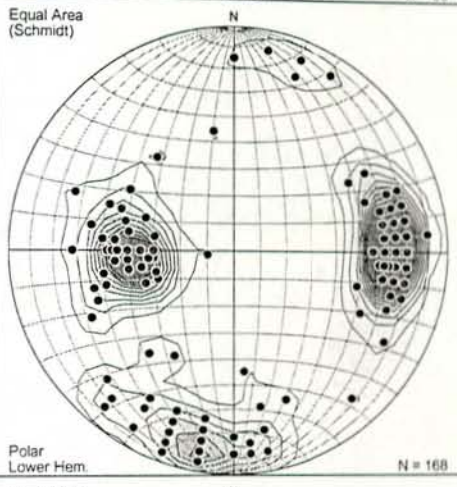	1. N270°/65° 48.19% 2. N090°/40° 24.43% 3. N010°/80° 11.46% 4. N356°/75° 6.59% 5.N082°/10° Fault 1 6. N290°/65° Fault 2
Section line 4	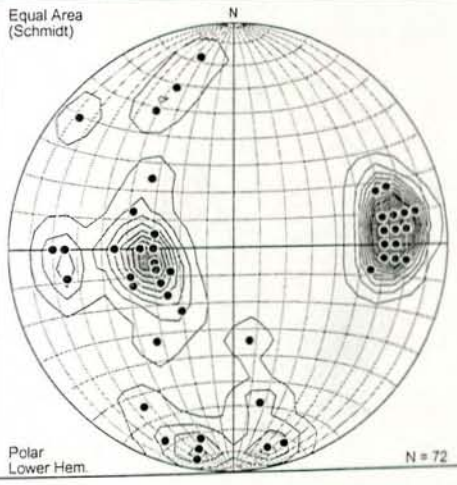	1. N266°/65° 30.70% 2. N090°/30° 15.21% 3. N010°/80° 7.17% 4. N350°/80° 7.17%

Section line 5	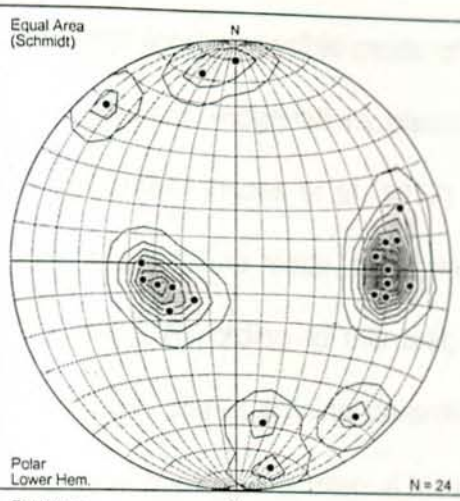	1. N280°/60° 19.3% 2. N075°/30° 14.3% 3. N178°/73° 4.15% 4. N350°/80° 3.26%
Section line 6	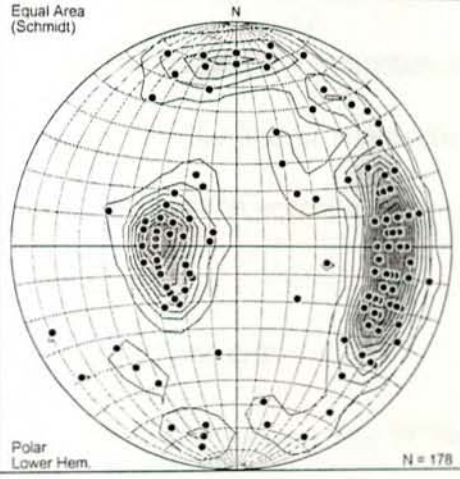	1. N270°/65° 24.33% 2. N100°/30° 19.05% 3. N180°/70° 6.81%
Section line 7	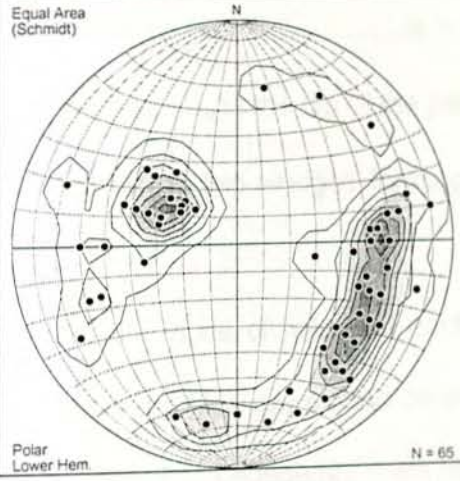	1. N270°/60° 12.7% 2. N125°/25° 12.33% 3. N310°/55° 11.92% 4. N010°/70° 5.85%

5.9 KINEMATIC CHECK

Rock mass can rarely be homogeneous, it contains different sets of discontinuity plane along which a wedge of rock mass can slide from open slope face. Discontinuity plane, slope face, and angle of internal friction along sliding planes can be plotted on circular projections for Kinematic analysis. The spatial relation of these

planes can be interpreted for the possible mode of failure. On hard rock mass slope the main modes of failures are wedge failure, plane failure, or toppling failure.

Markland developed a criteria (Hoek et al, 1977) to decide the dominant mode of failure from wedge or plane failure mode, along the intersection of two or more than two planar discontinuities. According to this test, wedge failure can prevail if the contact of two discontinuity planes dipping towards each other daylight on the slope face at angle greater than the angle of internal friction (ϕ) of the intersection plane. In other words, the plunge of the line of intersection must be less than the slope angle, measured in the direction of the line of intersection (Hoek et al, 1977). Similarly, a plane failure may take place if the potential failure plane dips towards the slope and is less than the slope angle.

In general Markland's conditions are:

- Plane failure..... $\alpha_f > \alpha_p > \phi$
- Wedge failure ..... $\alpha_f > \alpha_i > \phi$

Where α_f is the slope angle; α_p is the dip of the potential failure plane; α_i is plunge of the line of intersection of the two wedges forming plane; ϕ is the angle of internal friction.

To determine the possible mode of failure at each section line of the open pit, the structural data and the slope face are plotted on equal area projection 'Schmidt Net' in Dips computer program. The Legadembi open pit rock mass has been rated as fair rock (Table 5.5) and according to the RMR classification table (Bieniawski, 1989), for this type of rock the minimum angle of internal friction (ϕ) value is 25°. This value has been used as angle of internal friction in plane failure analysis.

The kinematic test indicated 6 possible plane mode of failure, 8 wedge mode of failure, and one circular mode of failure cases. The Kinematic check plot for each

section lines are presented as Fig. 5.7 and Fig.5.8. The Kinematic Check results are represented on Table 5.7.

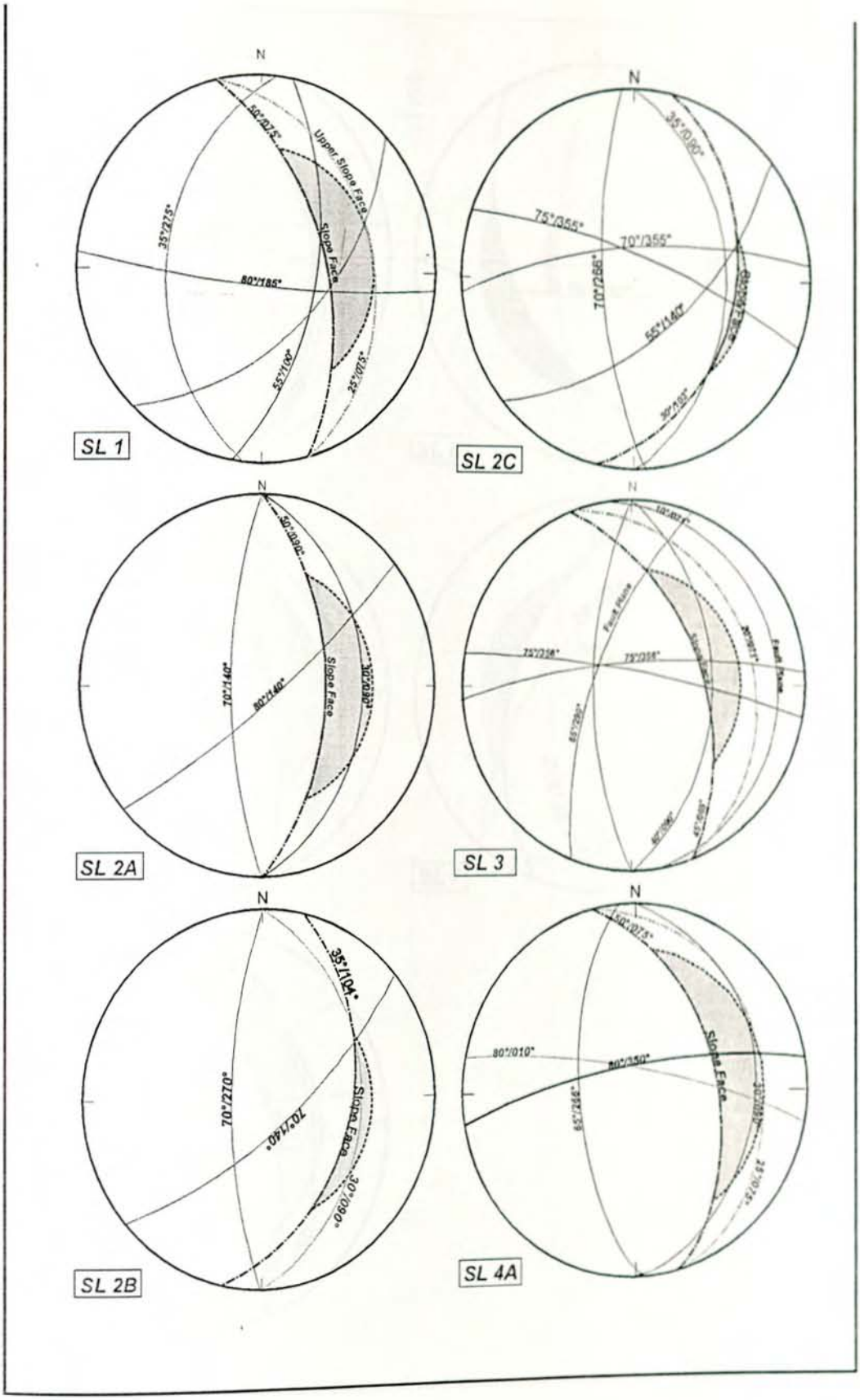

Fig.5.7 Kinematic check plot of SL1, SL2A, SL 2B, SL 2C, SL3, and SL 4A.

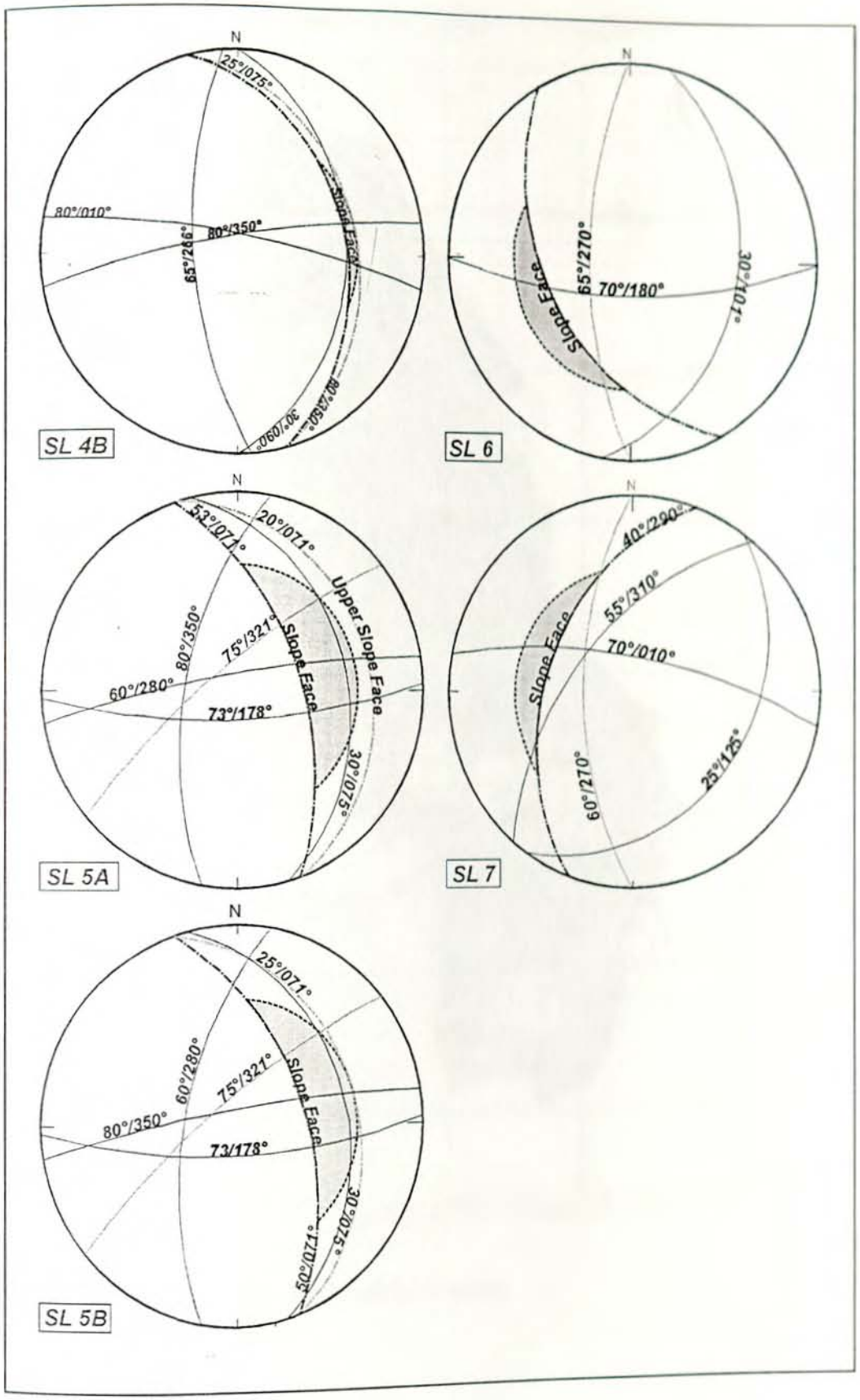

Fig.5.8 Kinematic check plot of SL 4B, SL 5A, SL 5B, SL 6 and SL7.

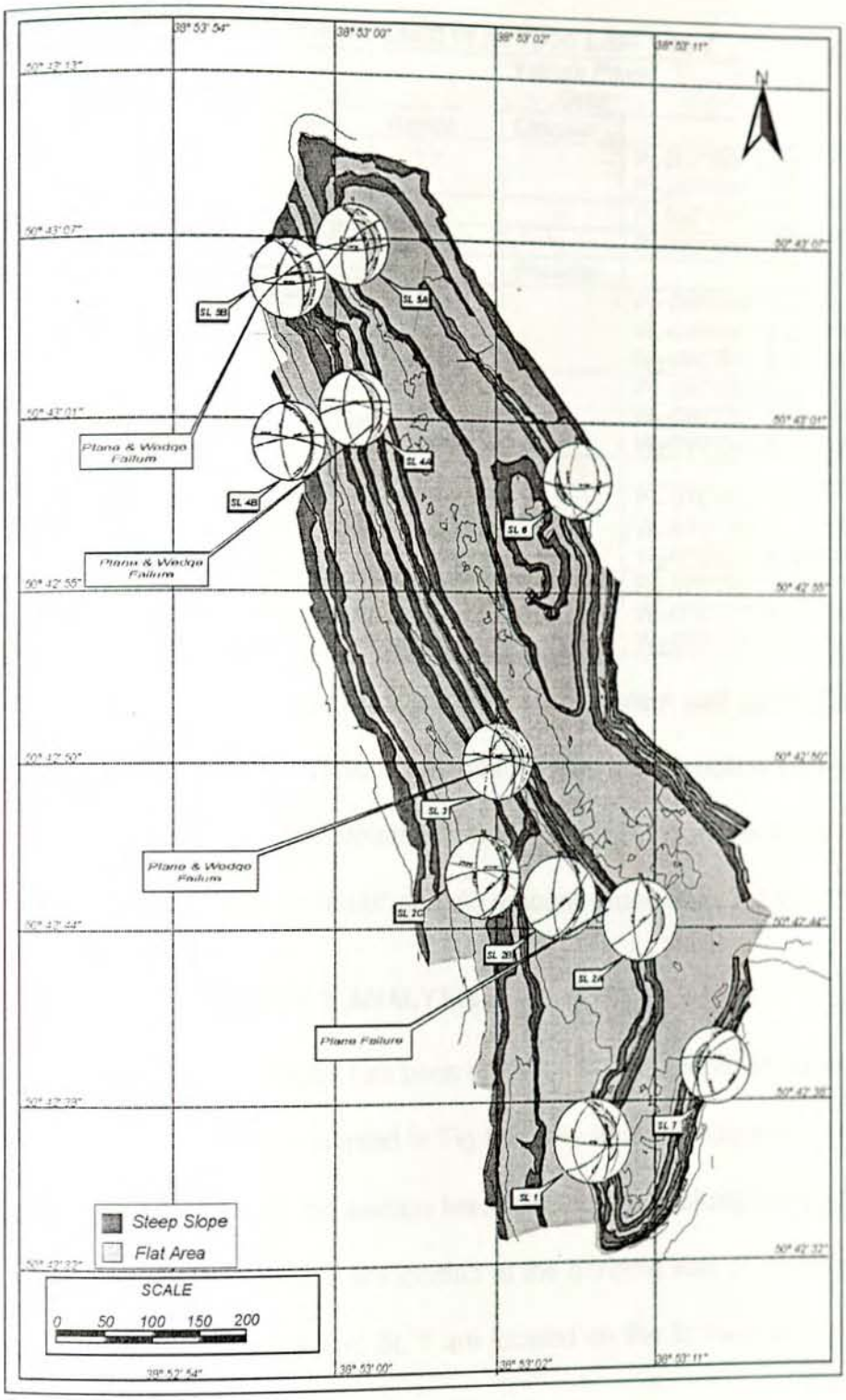

Fig. 5.9 Pit layout, and main failure modes.

Table 5.7. Kinematic check result of section Line 1 to 7

Slope Section	Failure Plane Data			
	Plane	Wedge	Circular	
SL 1	-	-	-	P_2-282°/65° P_7-280°/45°
SL 2A	P_1	-	-	P_1-090°/30°
SL 2B	P_1	-	-	P_1-090°/30°
SL 2C	-	-	Possible	
SL 3	P_2	W_1, W_2	-	P_2- 090°/40° W_1-090°/40° & 356°/75° W_2-090°/40° & 010°/80°
SL4 A	P_2	W_1, W_2	-	P_2- 090°/30° W_1-090°/30° & 350°/80° W_2-090°/30° & 010°/80°
SL4 B	-	-	-	
SL5 A	P_1	W_1, W_2	-	P_1- 075°/30° W_1-075°/30° & 350°/80° W_2-075°/30° & 078°/73°
SL 5B	P_1	W_1, W_2	-	P_1- 075°/30° W_1-075°/30° & 350°/80° W_2-075°/30° & 078°/73°

The Kinematic check result indicate that in the western wall section lines, the release joint sets are the sub vertical joint planes, the dip direction of which varies from N280° to N356° and dip amount 65° to 80°. The sliding plane is gently dipping plane which dips from N90° to N100° and dip amount varies from 30° to 40°.

5.10 SLOPE STABILITY ANALYSIS

The slope stability analysis has been done for the existing open pit feature. The slope layout of the mine is presented in Fig.5.2. The analysis has been carried out for the slopes represented by the section lines, distributed all along the periphery of the pit. Section lines SL 1 to SL 5 are located at the hanging wall or Western part of the pit, while section lines SL 6 and SL 7 are located on the footwall or the Eastern side of the pit.

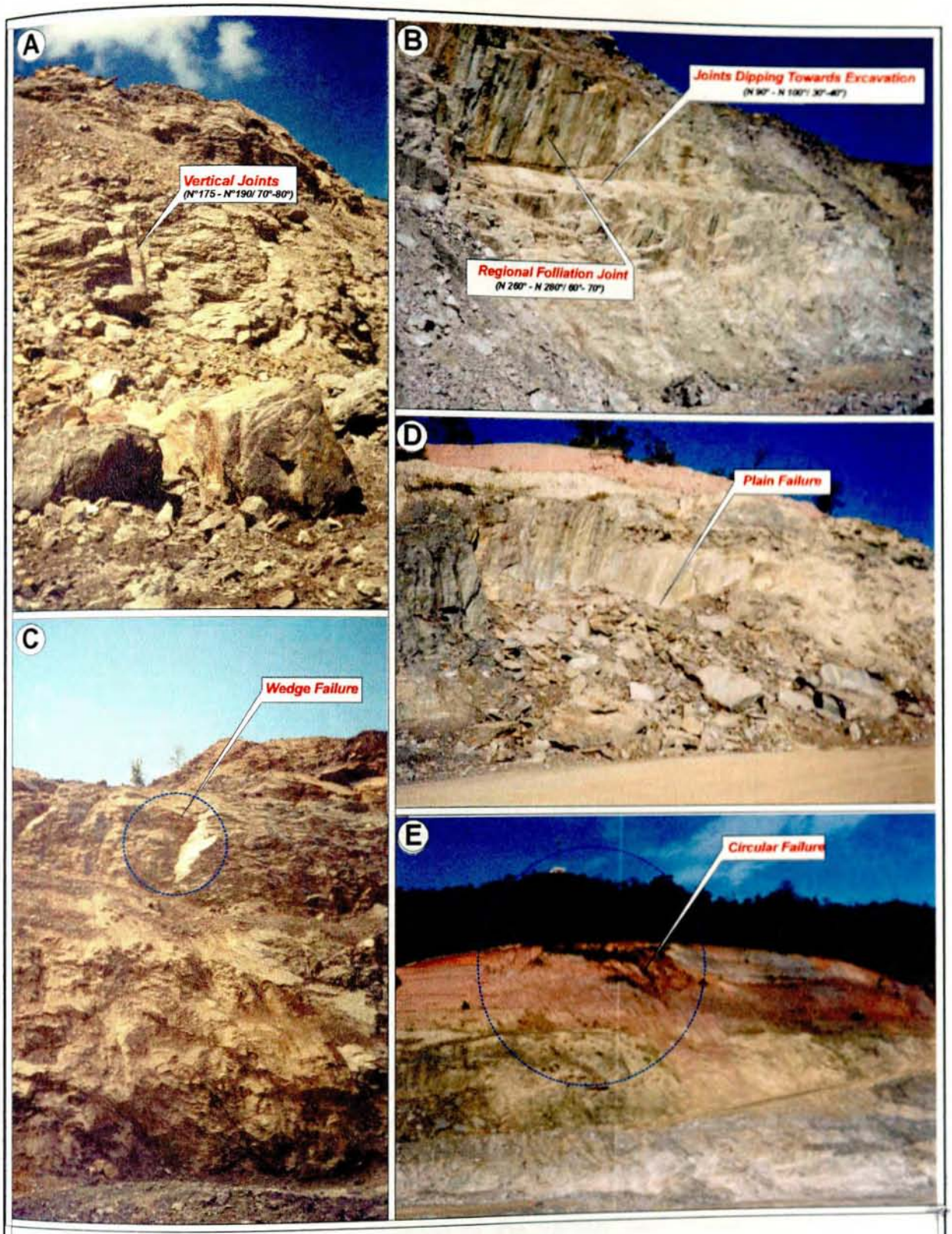

A - Vertical Joints.

B - Regional Foliation and gentle subhorizontal Joints.

C - Wedge Failure.

D - Plain Failure.

E - Soil slope, Circular Failure

Plate 2. Open pit structures and failure modes.

The unit weight for each rock unit has been taken from the laboratory analysis result during the feasibility study and from the laboratory analysis of the samples collected during the present study.

The cohesion of the failure plane is back calculated from one of the failed slope (Plate 2. D), for which the observations were made during the fieldwork. For the present study condition, where there is limitation to measure the shear strength of failure planes directly, back analysis provides a valuable information for design purposes. The observation data for back analysis of 'C' value are presented in Table 5.8:

Table 5.8. Field observation data of failed slope.

Parameter	*Value*
Height-	20 m
Failure plane angle (α_p)	40°
Slope face angle(α_f)	50°
Upper slope face (α_s)	10°
Tension Crack (α_t)	60°
Unit Weight of the rock(γ)	26.6kN/m^3
Unit Weight of Water(γ_w)	10 kN/m^3
Horizontal earthquake acceleration (α)	0.08
Basic Friction Angle (ϕ_b)	30°
FOS	1
Cohesion (c)	?

The back analysis calculation has been based on the factor of safety for critical condition, i.e FOS= 1. Other parameters needed for the factor of safety calculations are calculated by the modified technique of plain failure analysis (Sharma, et.al, 1995), which has been presented in detail in the latter parts of this chapter.

The Geometry and the annotation of the various parameters of the slope are presented in Fig. 5.12. The back analysis result of cohesion (c) value is 36.84 kN/m^2.

To estimate the shear strength of joints, the empirical low of friction (Barton 1973) has been used. The input data have been: Basic friction angle (ϕ_b) = 30° (from Table of Hoek et al., 1977); Joint roughness coefficient (JRC) = 5 (from field observation

based on Hoek et al., 1995); Compressive strength of weathered joint surfaces (JCS) = $\sigma_c/4$ (based on note of Hoek et.al, 1977 , Rock Slope Engineering); σ_c compressive strength of unweathered rock surface (Laboratory test results); σ_n effective normal stress acting on the joint surface.

$$\sigma_n = \frac{1}{2}\gamma H(\cot\alpha_p - \cot\alpha_s)\sin\alpha_p \cos\alpha_p$$

Thus substituting these values gives :

$$\tau = \sigma_n \tan[\phi_b + JRC\log_{10}\frac{(JCS)}{\sigma_n}]$$

$$\frac{\tau}{\sigma_n} = \tan[\phi_b + JRC\log_{10}(\frac{JCS}{\sigma_n})]$$

$$\tan^{-1}(\frac{\tau}{\sigma_n}) = \phi = [\phi_b + JRC\log_{10}(\frac{JCS}{\sigma_n})]$$

The failed slope mobilized cohesion (c) value has been back calculated from:

$$C = \frac{F[W(\sin\alpha_p + \alpha\cos\alpha_p) + V\cos\alpha_p] - [(W(\cos\alpha_p - \alpha\sin\alpha_p) - U - V\sin\alpha_p)\tan\phi]}{A}$$

Where *C* is the cohesion; *F* is the Factor of safety; *W* is the weight of the sliding block; *V* is the horizontal water force; *U* is the uplift water force; α_p is the failure plane angle, and *A* is the area of the sliding block.

5.10.1 Plane Mode of Failure Analysis

Plain failure occurs when the strike of the discontinuity plane nearly parallels the strike of the excavation and daylight on the excavation face.

In the Legadembi open pit some of the upper slopes are inclined and the tension cracks dips at 50° to 70°. Hoek et al (1977), in their analytical technique for plane failure analysis, made an assumption that the upper slope is horizontal and tension crack is vertical. The modified technique for plane failure analysis proposed by Sharma et.al, (1995) considers the effect of the inclined upper slope and non-vertical

tension crack. Thus, the modified technique of Sharma et.al, 1995 has been utilized to carry out the plane failure analysis.

The factor of safety, for slopes having plane mode of failure, has been carried out for static and for dynamic conditions, under varied saturated conditions. While calculating the Factor of safety (FOS) the saturation conditions has been represented as; dry slope; tension crack half filled; and tension crack completely filled with water.

Plane failure analysis input parameters

- Slope face inclination, (α_f), (°).
- Upper slope face inclination, (α_s), (°).
  Failure plane inclination,(α_p), (°).
- Release plane inclination,(α_t), (°).
  Cohesion, (c), (kN/m^2).
- Angle of internal friction, ϕ, (°).
- Unit weight of the rock, (γ), (kN/m^3).
- Unit weight of water, (γ_w).
- Height of the slope, H (m).
- Horizontal earthquake accelerations, (α), (g).

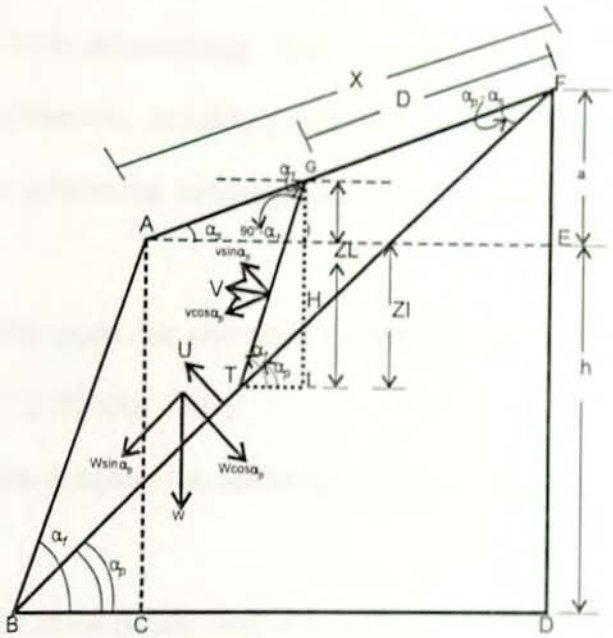

Fig. 5.10 Geometry of the slope for modified technique (after Sharma et.al, 1995).

For the slope stability analysis the input data (Table 5.9) has been derived from the slope topography, physical property, and structural analysis.

Table 5.9 Input data for plane mode of failure FOS calculation.

Section Line	α_f	α_s	α_p	α_t	c (kN/m^2)	ϕ	γ (kN/m^3)	γ_w (kN/m^3)	H (m)
SL 2A	50°	5°	30°	60°	36.84	40.43°	29.8	10	40
SL 2B	35°	20°	30°	70°	36.84	42.77°	29.8	10	40
SL 3	45°	20°	40°	65°	36.84	41.22°	29.8	10	115
SL 4A	50°	20°	30°	65°	36.84	38.66°	29.8	10	90
SL 5A	53°	20°	30°	60°	36.84	39.76°	29.8	10	45
SL 5B	50°	25°	30°	60°	36.84	39.64	29.5	10	58

The factor of safety for the 6 slope sections has been carried out for static as well as dynamic conditions under varied saturation conditions, based on the modified technique of Sharma et al, 1995. The modified technique applies the limit equilibrium method in calculating the factor of safety (FOS).

The FOS is the deciding factor for one to say the slope is stable or not. When the FOS is 1 the slope is critically stable and in a very sensitive condition that, if some parameters of the rock changes failure is an eminent thing. Thus in slope design the FOS required can be increased to more than one, depending on the degree of safety required for the structure. In mines for economical consideration FOS for open pit mines is usually 1.3 (Hoek et al, 1977).

During the Legadembi open pit feasibility study, for economic benefit the open pit layout design has been based on FOS=1.2 (BRGM, 1991).

In the modified technique of plain failure analysis, the following main assumptions have been made;

1. For saturated condition the tension crack is fully filled with water. The water in the tension crack seeps along the failure surface and escapes out on the slope face through the sliding plane, where it day lights on the slope face.
2. There is no resistance to sliding on the lateral boundaries of the sliding rock mass.
3. For moderately saturated condition the tension crack (Z_L) is half filled and the water level in the crack $Z_w = 0.5Z_L$. The water in the tension crack seeps along the failure surface and escapes out on the slope face via the sliding plane, day lighting on the slope face.
4. For dry condition the rock mass is completely dry and $Z_w=0$.

5. The slope geometry and the allocation of various parameters involved in the calculation is presented in Fig 5.10.

As per the modified technique of plain failure analysis (Sharma et.al, 1995) the area, weight, horizontal and uplift water force are calculated by the following equations;

1. Area of sliding mass:

$$A = (h - Z_1)\cos ec\alpha_p$$

Where: $Z_L = \dfrac{Z\sin\alpha_t}{(\sin\alpha_t - \tan\alpha_p \cos\alpha_t)}$

$$Z_1 = Z_L - IG$$

$$Z = h[(1 - \frac{\cot\alpha_f}{\cot\alpha_s}) + \sqrt{\frac{\cot\alpha_f}{\cot\alpha_p}} \times (\frac{\cot\alpha_p \cot\alpha_p}{\cot\alpha_s - 1})]$$

$$IG = \frac{h[\sqrt{\cot\alpha_f \cot\alpha_p} - \cot\alpha_f]}{\cot\alpha_s}$$

2. Weight (W) of the sliding mass is calculated from:

$$W = \frac{1}{2}\gamma[(h+a)X - DZ_L)$$

Where γ is the unit weight of the rock, X and D are the slope distance AF and GF respectively and a is the height EF as shown in Fig. 5.10.

$$X = h(\frac{\cot\alpha_f}{\cos\alpha_s}) \times (\frac{\tan\alpha_p - \tan\alpha_f}{\tan\alpha_s - \tan\alpha_p})$$

$$D = \frac{Z}{\tan\alpha_p \cos\alpha_s - \sin\alpha_s}$$

$$a = h(\frac{\tan\alpha_s}{\tan\alpha_f}) \times (\frac{\tan\alpha_p - \tan\alpha_f}{\tan\alpha_s - \tan\alpha_p})$$

3.Horizontal water force, V

$$V = \frac{1}{2}\gamma_w Z_w^{\ 2} \sin^2\alpha_t$$

Where, γ_w is the unit weight of water and Z_w is the water level in the tension crack.

4.Uplift water force, U

$$U = \frac{1}{2}\gamma_w Z_w \sin\alpha_t (h - Z_t)\cos ec\alpha_p$$

The Factor of safety, FOS, is determined as:

For static condition:

$$F = \frac{cA + (W\cos\alpha_p - U - V\sin\alpha_p)\tan\phi}{W\sin\alpha_p + V\cos\alpha_p}$$

For dynamic condition:

$$F = \frac{cA + [W(\cos\alpha_p - \alpha\sin\alpha_p) - U - V\sin\alpha_p]\tan\phi}{W(\sin\alpha_p + \alpha\cos\alpha_p) + V\cos\alpha_p}$$

Where, c is the cohesion and α is the horizontal earthquake accelerations.

The factor of safety has been determined for existing conditions and possible worst conditions, which may occur. These conditions are; static and dry conditions; static and moderately saturated; static and fully saturated; dynamic and dry; dynamic and moderately saturated; dynamic and fully saturated.

The results obtained for existing and possible worst conditions for plane mode of failure are presented in Table 5.10.

Table 5.10 Results of FOS for Plane Failure Analysis.

Section Line	FOS Static Condition			FOS Dynamic Condition		
	Water Saturation			Water Saturation		
	Sd*	MSd**	Dry	Sd*	MSd**	Dry
SL 2A	1.09	1.40	1.63	0.92	1.18	1.37
SL 2B	1.59	1.73	1.8	1.33	1.46	1.56
SL 3	0.81	1.00	1.17	0.68	0.85	1.00
SL 4A	1.17	1.32	1.40	0.99	1.11	1.17
SL 5A	1.29	1.40	1.48	1.08	1.19	1.24
SL 5B	1.39	1.42	1.43	1.16	1.19	1.20

**saturated; **moderately saturated*

The results of the FOS calculation indicate that for the existing condition (static and dry) all the 6 slope sections are stable. However under static conditions if the slope is

fully saturated, slope SL3 would be unstable as the FOS is 0.81. Even for moderately saturated conditions this slope would be critically stable as FOS is 1.00

5.10.2 *Wedge Mode of Failure Analysis*

In wedge failure mode the slope slides on structural planes striking across the slope face and dipping towards each other. The sliding is on the intersection of the two planes.

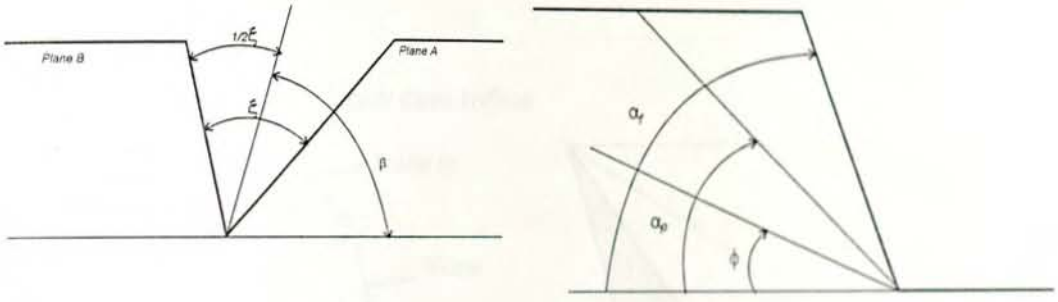

a) View along line of intersection

b) View at right angles to line of intersection

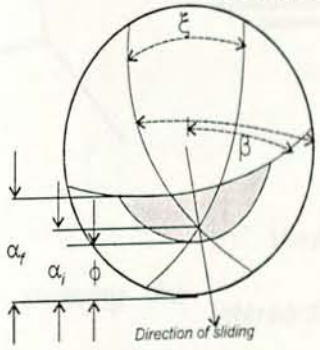

c) Stereo plot of wedge failure geometry

Fig 5.11 Geometry of wedge

The geometry of the wedge, is defined in the above Fig 5.11 a, b and c. The slope will slide when $\alpha_f > \alpha_i > \phi$, where α_f is the inclination of the slope face, α_i is the dip of the line of intersection.

In wedge failure analysis the simple case is when assuming the sliding is resisted only by friction angle, and that the friction angle ϕ is the same for both planes. In this case using Hoek et al (1977), analytical method the FOS can be calculated from:

$$F = \frac{(R_A + R_B)Tan\phi}{W \sin\alpha_i}$$

Where R_A and R_B are the normal reactions provided by planes A and B; "W" is weight of the wedge, and α_i is the dip of the intersection plane.

The slope stability analysis will be complicated further when cohesion and water pressure are included.

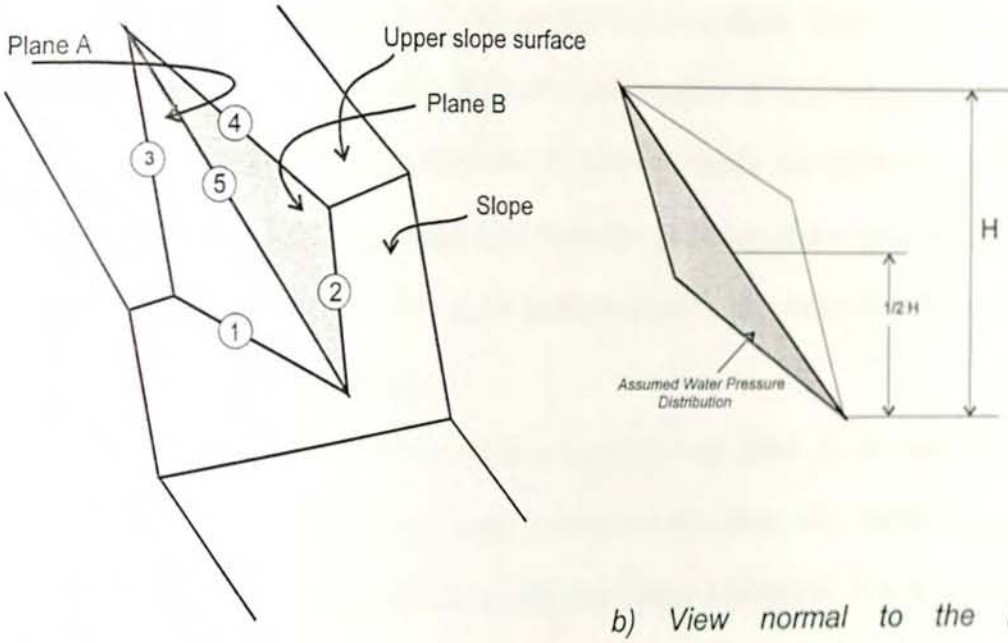

a) Pictorial view of wedge showing the number of intersection lines and planes

b) View normal to the line of intersection 5 showing the total wedge height and the water pressure distribution.

Fig. 5.12 Geometry of wedges including influence of cohesion and water pressure (Hoek et al., 1977).

Hoek et al (1977), assumed that the sliding will occur only along the line of intersection number 5. The factor of safety of this slope is derived from complicated mathematical manipulation and the final equation is:

$$F = \frac{3}{\gamma H}(c_A.X + c_B.Y) + (A - \frac{\gamma_w.X}{2\gamma})\tan\phi_A + (B - \frac{\gamma_w.\gamma}{2\gamma})\tan\phi_B$$

Where C_A and C_B are the cohesive strength of planes A and B; ϕ_A and ϕ_B are the angles of internal friction on planes A and B; γ is the unit weight of the rock; γ_w is the unit weight of water; H is the total height of the wedge; x, y, A, and B are dimensionless factors which depend upon the geometry of the wedge.

Since the base areas of both failure planes as well as the normal forces on these planes must be known, the manual calculation of the factor of safety is more complicated than of plain failure. There are softwares, which are created to handle the mathematical manipulation of the wedge failure analysis. One of these softwares is SASW, developed by Bhawani Sing of Indian Institute of Technology, Roorkee.

In the kinematic check 8 possible wedge failures cases are identified. The wedge failure stability analysis input data has been derived from slope section topography, physical property data, and structural analysis data. The input data for each slope sections is tabulated in Table 5.11.

In this study, the wedge failure FOS calculation has been done with the help of SASW software. The FOS has been calculated for static and dynamic conditions under dry, moderately saturated and saturated slope conditions. The results obtained are presented in Table 5.12.

The SASW Software input parameters are: number of slope; number of joint sets; number of cases; dip of the I^{th} joint plane (deg); c (I) cohesion of I^{th} joint plane (Ton/m^2); friction angle (ϕ) of I^{th} joint plane (deg); angle of slope of upper surface; dip direction of the upper surface; angle of rock slope; dip direction of the rock slope; height of the crest of the slope above toe of intersection; unit weight of the rock (γ_r); unit weight of water (γ_w); coefficient of horizontal acceleration near the crest of the slope (α); corresponding earth quake magnitude; water level above toe of

intersection; pore water pressure factor (0, for dry; 1, for wet slope).The SASW Software out put is the FOS value.

The results of the FOS calculation indicated that slope SL 3 is unstable for moderately saturated static conditions. The FOS further decreases when it is fully saturated. For dynamic conditions SL 3 slope remains stable when it is dry but becomes unstable when it is saturated.

Slope SL 2A and SL 4A are unstable when it is fully saturated under static and dynamic conditions. The rest of the slopes are stable for the existing and possible worst conditions.

Table 5.11 Slope stability wedge failure analysis input data.

Slope Section	Wedge	Joint 1		Joint 2 Dip		Slope face		H (m)	γ (t/cm³)	c (t/cm²)		ϕ (deg.)		Eq.acce. (α)	Eq. Mag.
		Dip	Dire.	Dip	Dire.	Dip	Dire.			c_{J1}	c_{J2}	ϕ_1	ϕ_2		
SL 3	$W_{2,4}$	40°	90°	75°	356°	45°	69°	115	2.98	3.68	20	40.08°	40°	0.08	7
SL 3	$W_{2,3}$	40°	90°	80°	10°	45°	69°	115	2.98	3.68	20	40.08°	40°	0.08	7
SL 4A	$W_{2,4}$	30°	90°	80°	10°	50°	75°	90	2.98	3.68	20	40.08°	40°	0.08	7
SL 5A	$W_{1,3}$	30°	75°	80°	350°	53°	71°	45	2.98	3.68	20	40.08°	40°	0.08	7
SL 5A	$W_{1,4}$	30°	75°	73°	178°	53°	71°	45	2.98	3.68	20	40.08°	40°	0.08	7
SL 5B	$W_{1,3}$	30°	75°	80°	350°	50°	70°	58	2.95	3.68	20	40.08°	40°	0.08	7
SL 5B	$W_{1,4}$	30°	75°	73°	178°	50°	70°	58	2.95	3.68	20	40.08°	40°	0.08	7

Table 5.12 Results of wedge failure analysis.

Section Line	Wedge	FOS Static Condition			FOS Dynamic Condition		
		Water saturation			Water saturation		
		Sd*	MSd**	Dry	Sd	MSd.	Dry
SL3	$W_{2,4}$	0.0	1.06	1.95	0.00	0.88	1.69
SL3	$W_{2,3}$	0.0	0	1.67	0.00	0.00	1.46
SL4A	$W_{2,3}$	0.96	1.3	1.64	0.78	1.08	1.38
SL4A	$W_{2,4}$	1.3	1.65	1.99	1.04	1.35	1.66
SL5A	$W_{1,3}$	1.27	1.65	1.97	1.05	1.37	1.65
SL5A	$W_{1,4}$	1.26	1.58	1.91	1.04	1.33	1.61
SL5B	$W_{1,3}$	1.16	1.5	1.93	0.95	1.25	1.61
SL5B	$W_{1,4}$	1.07	9.66	1.76	0.88	1.18	1.48

*saturated; **moderately saturated

5.10.3 *Circular Mode of Failure Analysis*

Wedge or plain modes of failures are the result of sliding of the rock mass along one or more discontinuity planes. In soil mass the above consideration does not work, the failure surface is generally circular. Circular failure mode is the result of loss of contact between individual soil particles.

According to Hoek et al (1977), for circular failure analysis the following assumptions should be made:

a) The material forming the slope is assumed to be homogeneous, i.e its mechanical properties do not vary with direction of loading.

b) The shear strength of the material is characterized by a cohesion (c) and friction angle (ϕ) which are related by the equation:

$$\tau = c + \sigma.\text{Tan}\,\phi$$

c) Failure is assumed to occur on a circular surface, which passes through the toe of the slope.

d) A vertical tension crack is assumed to occur in the upper surface or in the face of the slope.

e) The location of the tension crack and of the failure surface are such that the factor of safety is minimum for the slope geometry and the ground-water conditions considered.

f) A range of groundwater conditions, varying from a dry slope to heavy recharge, are considered in the analysis.

In the Legadembi open pit the top most portion of the slope (35 m) is highly weathered and its behavior is like a soil mass. During the feasibility geotechnical study, samples from the weathered surface have been taken and identification (Atterberg Limit), unit weight, and shear tests have been conducted. As a result, the

soil has been reported as silty clay with dry unit weight 12.9 kN/m^3, and natural water content of 38%. It has also been classified as highly plastic clay (LL=83%, LP=37%, IP=46%) and with slight swelling property (BRGM, 1991).

The result of the shear strength test on fifteen samples showed that the soil has very low cohesion (5 kPa), and angle of internal friction of 30°. In this study section line 2C passes on the soil overburden of the open pit mine. In the stability analysis of this homogeneous soil mass the main failure mode is considered to be as circular. During the field visit there has been a failed soil slope close to the section line.

The factor of safety for circular failure analysis has been calculated with the help of a SARC, Computer Program Package developed by Bhawani Singh of Indian Institute of Technology, Roorkee. This program has been developed to calculate the FOS on circular failure planes emerging at the toe of the slope. The input parameters are the coordinate of the slope profile line; pore water pressure; depth of tension crack at the top of the slope; depth of water in tension crack and earth quake force. The input data is presented in Table 5.13.

The factor of safety calculation is based on the Bishop's equation for various slip surfaces, until a minimum factor of safety of less than unity has been found. The calculation was for both dynamic and static conditions. The result of the factor of safety analysis is presented in Table 5.14.

Table 5.13 Circular mode of failure stability analysis SARC program input parameters.

Parameter	INPUT DATA	
	Value	
N	10	N=Number of profile coordinates (<50).
ROCK	0.0	ROCK= Reduced level of hard strata W.r.t river bed level (m).
XS	0.0	RWL= Reduced level of GWT (m) XS= X-coordinate of point from where surcharge starts (m).
WI	0.0	WI= Uniform surcharge intensity (T)
ZC	0.0	ZC= Depth of tension crack (m)
ZWR	0.0	ZWR= Depth of water in tension crack (m).
C	0.5	C= cohesion of soil (T/m^2)
PHI	30	PHI= Angle of internal friction (deg)
GAMA	1.26	GAMA= Unit weight of rock (T/m^3)
GAMAW	1.00	

BBAR	0 - 0.2 0 (dry); 0.1(for moderately saturated); and 0.2 (Saturated)	GAMAW= Unit weight of water (T/m^3) AH= Horizontal component of earthquake acceleration. AVR= Vertical component of earthquake acceleration. EQM= Corresponding earthquake magnitude on Richter scale. NENP= Number of entrey points of slip circles. ENTX= X-coordinate of entry point of slip circles (<10). ENTY=Y-coordinates of entry point of slip circle. NOPT=0, when minimum factor of safety is required = 1 when factor of safety of all slip circles is required. NEP=0 when no individual point is given. XEXITI= X-coordinate of first exit point of slip circle (m).
AH	0.08	
AVR	0.5	
EQM	7	
NENP	0	
XEXITI	70	
XEZITL	100	
GAP	30	

Table 5.14 ***SARC circular failure analysis FOS calculation result .***

Slope	Static Condition			Dynamic Condition		
	Water Saturation condition (BBAR)			Water Saturation condition (BBAR)		
SL2C	Dry	Wet (BBAR)		Dry	Wet (BBAR)	
	0.00	0.10	0.20		0.10	0.20
	0.09	0.00	0.00	0.07	0.00	0.00

The result of the SARC, analysis showed that the slope is not stable at static and dynamic conditions. This is further evident with the field observation of a failed slope in close vicinity of this section (Plate 2.E).

5.11 SLOPE DESIGN

Whenever a slope stability analysis is done the two important issues that must be addressed for safe slope excavation are how high and how steep the slope face should be. The answer to these quests is presented in the slope design. After identifying the main mode of failures in the excavation area and condition, the safe slope design parameters under the prevailing field condition can be derived from the plot of slope height and corresponding slope face. The resulting FOS values will be contoured for particular safety factor. The contouring work results a curve, which indicate the safe slope face angle at particular slope height.

From the kinematic check and factor of safety analysis, for Legadembi open pit , the two dominant mode of failures are plain failure and wedge failures. To design the safe slope, based on the present slope conditions, the slope section SL 3 and SL 4A parameters have been selected. The design was on FOS value of 1.3 and 1.2 based on the recommendation of Hoek et al (1977). Based on the stability analysis the safe slope design curve has been produced for section 3 and 4A rock mass condition at FOS= 1.3 and 1.2.

The design curve indicated the safe slope angle at the respective slope height, (Table 5.15 and Table 5.16) fro slope condition of SL 3 and SL 4A.

For moderately saturated dynamic conditions, the western slope hard rock sections will be stable at FOS 1.3, with 35° to 40° overall slope angle and 50°-60° bench slope face, 20 m bench height and 6 m berm width. The Eastern slope has been found to be stable for existing and possible worst conditions.

Table 5.15 Slope design for section 3 slope profile.

FOS 1.3 Suggested Slope design		**FOS 1.2 suggested Slope Design**	
Height (m)	Slope Angle	Height (m)	Slope Angle
0 - 35	85°	0 - 45	85°
35 - 55	54°	45-65	54°
55 - 75	44°	65-80	44°
75 - 115	40°	80-115	40°

Table 5.16 Slope design for section 4A slope profile.

FOS 1.3 Suggested Slope design		**FOS 1.2 suggested Slope Design**	
Height (m)	Slope Angle	Height (m)	Slope Angle
0 - 20	56°	0 - 40	70°
20 - 40	44°	40-60	46°
40 - 60	36°	60-90	43°
60 - 80	35°		
80 - 90	34°		

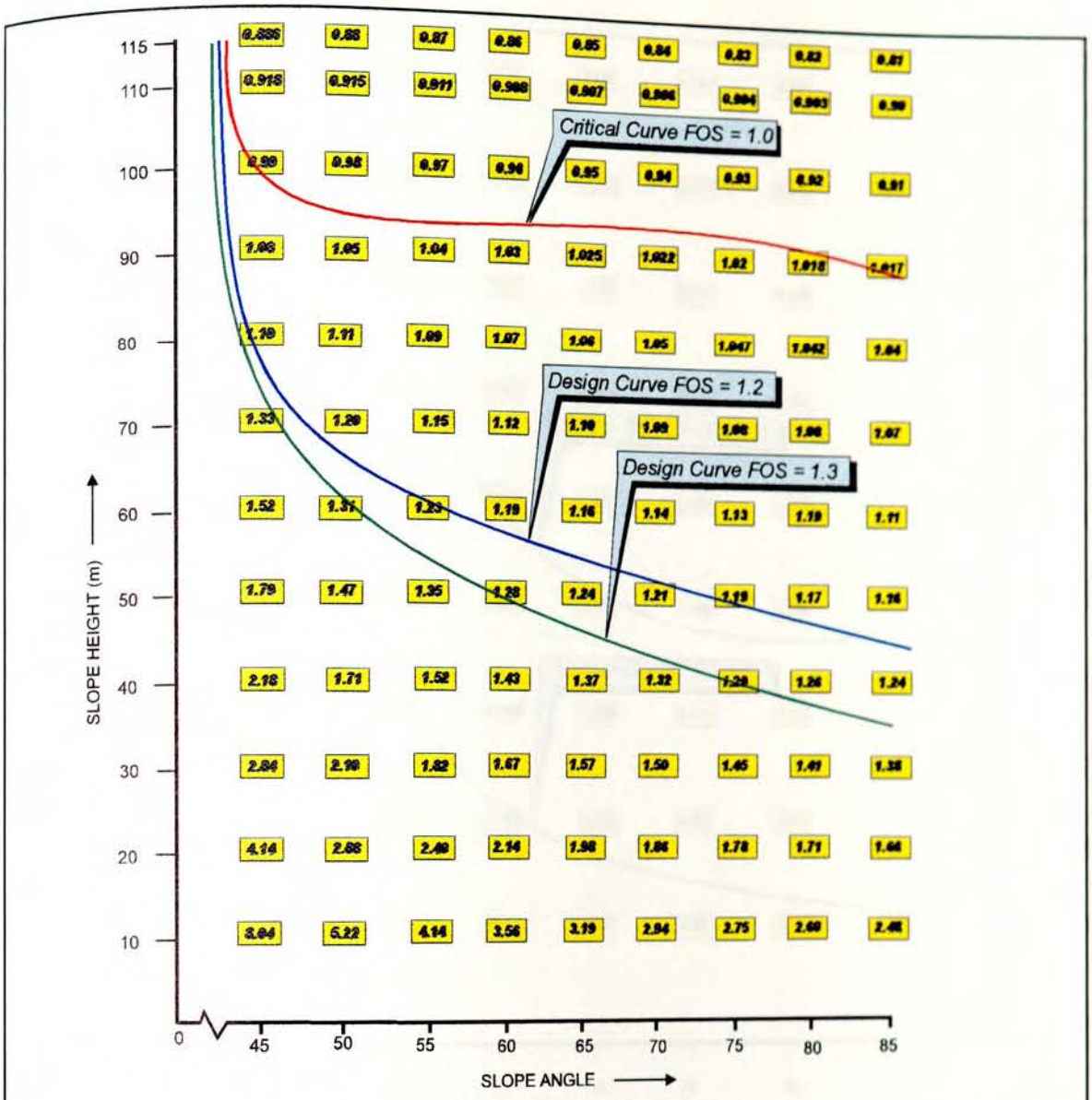

Determination of Safe Slope Angle

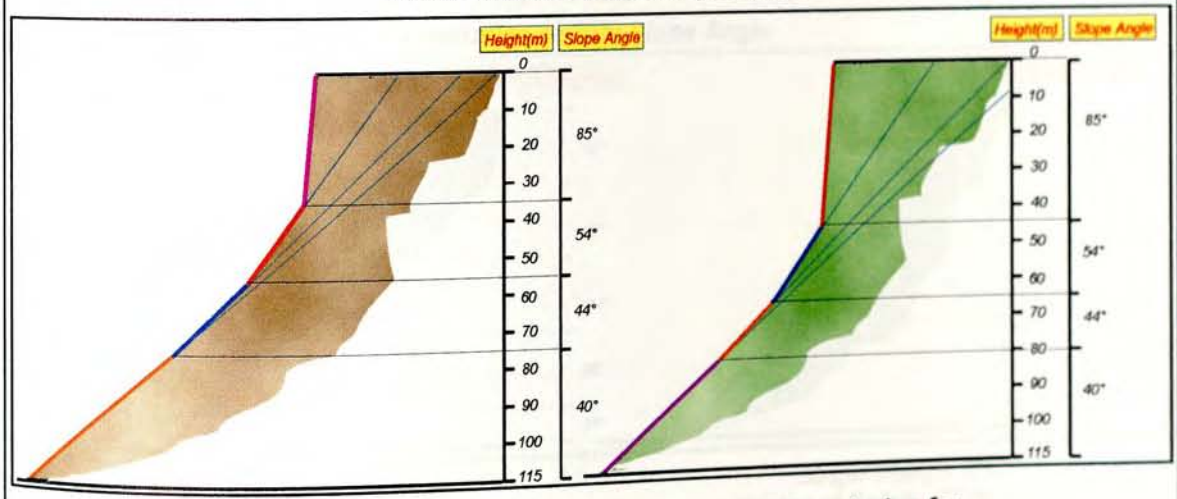

Slope design for Factor of Safety (FOS) = 1.3

Slope design for Factor of Safety (FOS) = 1.2

Fig.5.13 Section Line SL3 slope design based on wedge failure mode.

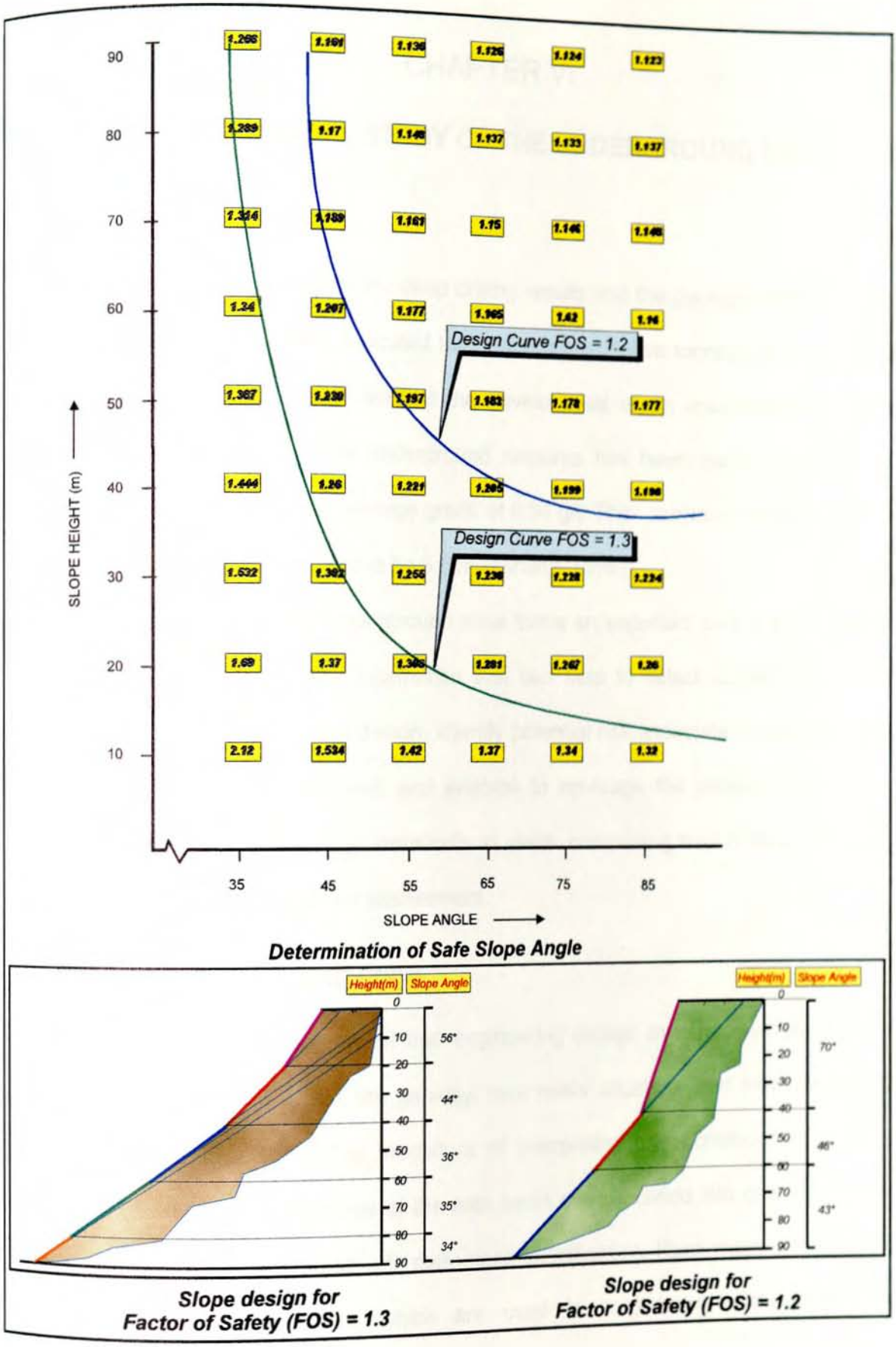

Fig. 5.14 Section Line SL 4A slope design based on plane failure mode.

CHAPTER VI

GEOTECHNICAL STUDY OF THE UNDERGROUND MINE

6.1 INTRODUCTION

A preliminary assessment of the deep drilling results and the geological data relating to the open pit ore bodies indicated that there is a sufficient tonnage of mineralised body at grades suitable to warrant the development of an underground mine at Legadembi Gold Mine. The underground resource has been estimated to be 2.9 million tonnes of ore at an average grade of 6.84 g/t. The minimum thickness of the ore body has been estimated to be 5.5 m (Ashanti, 1996).

Geotechnical study of an underground mine forms an important part of the feasibility study. The study provides information that can help to select appropriate mining method, input data for mine design, identify potential risk associated with the mining methods, support requirement, and enables to envisage the project finance. The study must be carried out systematically in steps, comprising mainly data collection, site characterization, and risk assessment.

6.2 SITE CHARACTERIZATION

There is unanimous agreement that engineering design must always start with a good understanding of the site geology, rock mass structure, and interpretation of possible failure modes. The procedure of interpreting site conditions and giving values to the various features of the rock mass can be called site characterization and should not be confused with rock mass classification. Rock mass classification systems are design tools, which are used in conjunction with engineering assessment and other design approaches.

Rock mass characterization consists of quantifying the parameters governing rock mass behaviour. These properties can be expressed as intact rock characteristics, discontinuity (joint) characteristics and the density and pattern of discontinuities.

The approach can be in phases of data collection, site characterization, modelling, analysis and design. The main elements of the site characterization are summarized in Fig 6.1.

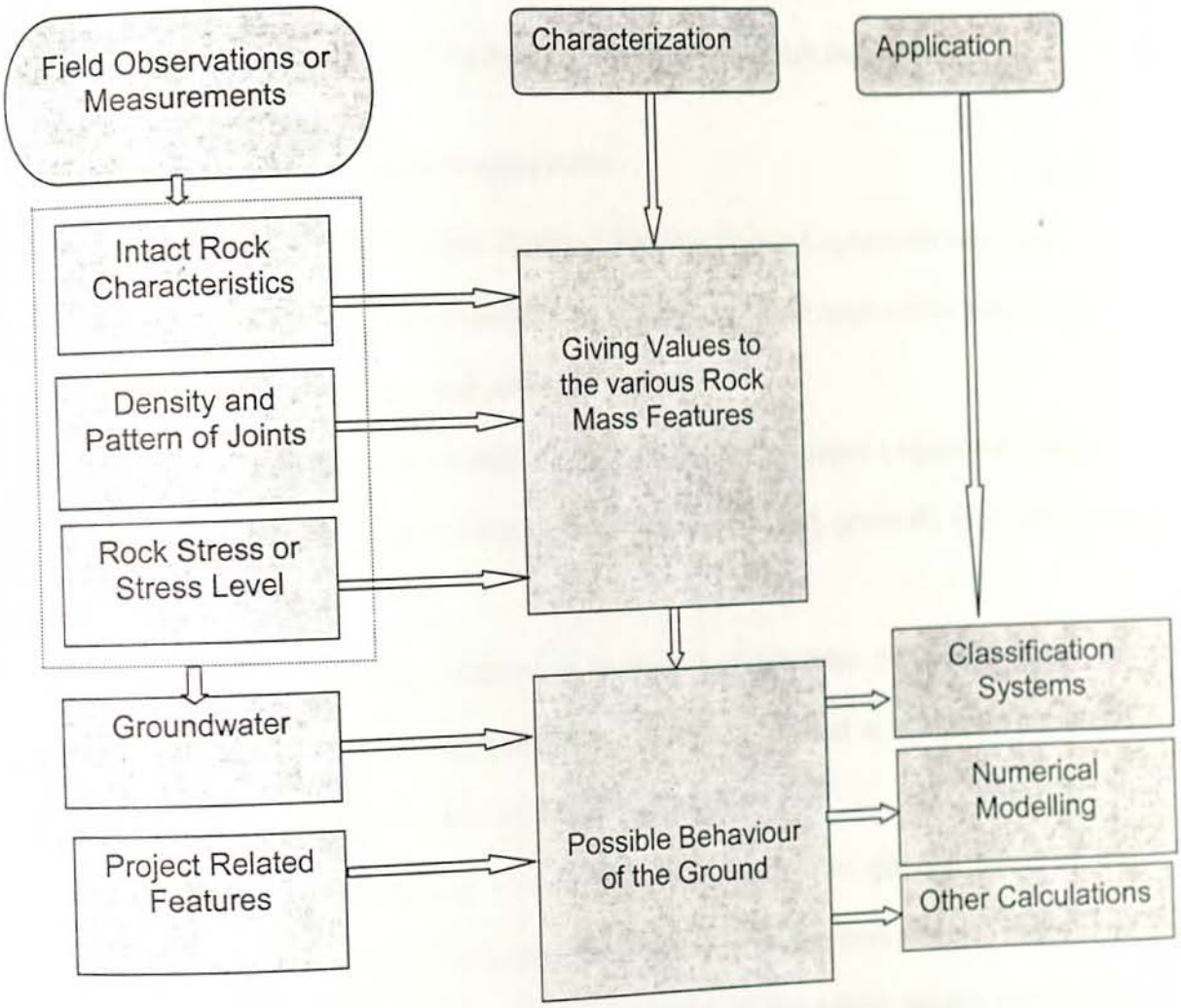

Fig 6.1 Site characterization. (Palmstrom , 2000)

In the geotechnical study of the Legadembi Underground Gold Mine, the same procedures have been followed. The geotechnical database has been compiled from the open pit feasibility study, exploration drilling data, geotechnical mapping of the underground mine ore zone, and rock testing. The structural data and excavation orientation have been analysed to assess the potential mode of failure. Based on the characterization of the underground rock mass around the ore zone the appropriate mining method and support system have been recommended.

6.3 GEOTECHNICAL DATABASE OF THE UNDERGROUND MINE

6.3.1 Geology of the underground mine

The underground excavation lies directly below the Upper Legadembi ore zone. The excavation consists of 1.34 km access tunnel, 250 m North exploration drive; 250 m ore zone drive, turning bays and generator stations.

The access tunnel portal is located in the eastern part of upper Legadembi deposit. The excavation is from east to west. It is Horseshoe shaped, generally 6 m wide, and 6 m high.

The North Exploration drive opening is located 1.15 km from the portal within the access tunnel. The general excavation trend is N330°, inclined at 40° (approximately) and 250 m long. The excavation is Horseshoe shaped.

The ore zone excavation lies 1.3 km from the portal. The general trend of the excavation is N330°. The dimension of the excavation varies from place to place. The diameter of the excavation ranges from 6 m to 9.5 m, the height ranges from 6 to 8 m. In general it is Horseshoe shaped. The layout of the underground excavation is presented in Fig 6.2.

The geology of the Legadembi underground gold deposit is the continuation of the open pit geology. The major part of the access tunnel and the North exploration drive lies within the footwall gneiss. The ore zone excavation is within the hanging wall quartz-biotite- actinolite- talc schist. The detail geology of these units has been addressed in chapter 2.

In the access tunnel for about 30 m from the portal, the footwall gneiss is highly weathered. The gneiss at places is highly fractured and banded. There are amphibole schist and amphibolites intercalated with the gneiss. The intrusive rocks range from intermediate to granitic, concordant and discordant rocks. At some places the intrusive rocks are highly sheared. Near the hanging wall there are shear zones marked by the occurrence of talc-actionolite-biotite-schists. At the contact between the hanging and the foot wall there is quartz-sercite-schist.

The ore is within quartz biotite-actinolite-talc schist. In the ore drive most of the excavation is within the quartz vein. There are places where the quartz vein is completely mined out from the walls and the host rock (quartz- biotite- actinolite-talc shist), is exposed. The roof is dominantly quartz vein and in places where the host rock is exposed it is highly silicified.

As a part of the geotechnical study, the ore zone has been mapped at 1:200 scale, covering a length of 200 m. The geological and geotechnical maps are presented from Fig. 6.3.1 to Fig. 6.3.4 The vertical geological sections of the region between the North exploration drive and the ore zone have been drawn from the exploration drill holes logging data and is presented as Fig. 6.4.

6.3.2 Geotechnical data of the access tunnel

During the excavation of the access tunnel, the project geologists have mapped and classified the rock mass using the NGI Q-system. The result shows that within the

total length of the 1.3 km access tunnel, the rock mass is very poor for 4 m stretch, poor rock for 136 m, good rock for 823.5 m, fair rock for 302 m, very good for 36 m, and extremely good for 4 m.

In the access tunnel the poor rock mass is located mainly near the portal area and in highly sheared rock mass, mostly with more than two joint sets and random fractures. The fracture openings are filled with softening clay, chlorite, talc, and carbonates. At some places the rock mass is highly weathered. The joint wall surface varies from smooth planar to smooth undulating. Close to the portal area it has been observed, that there is moderate inflow of ground water.

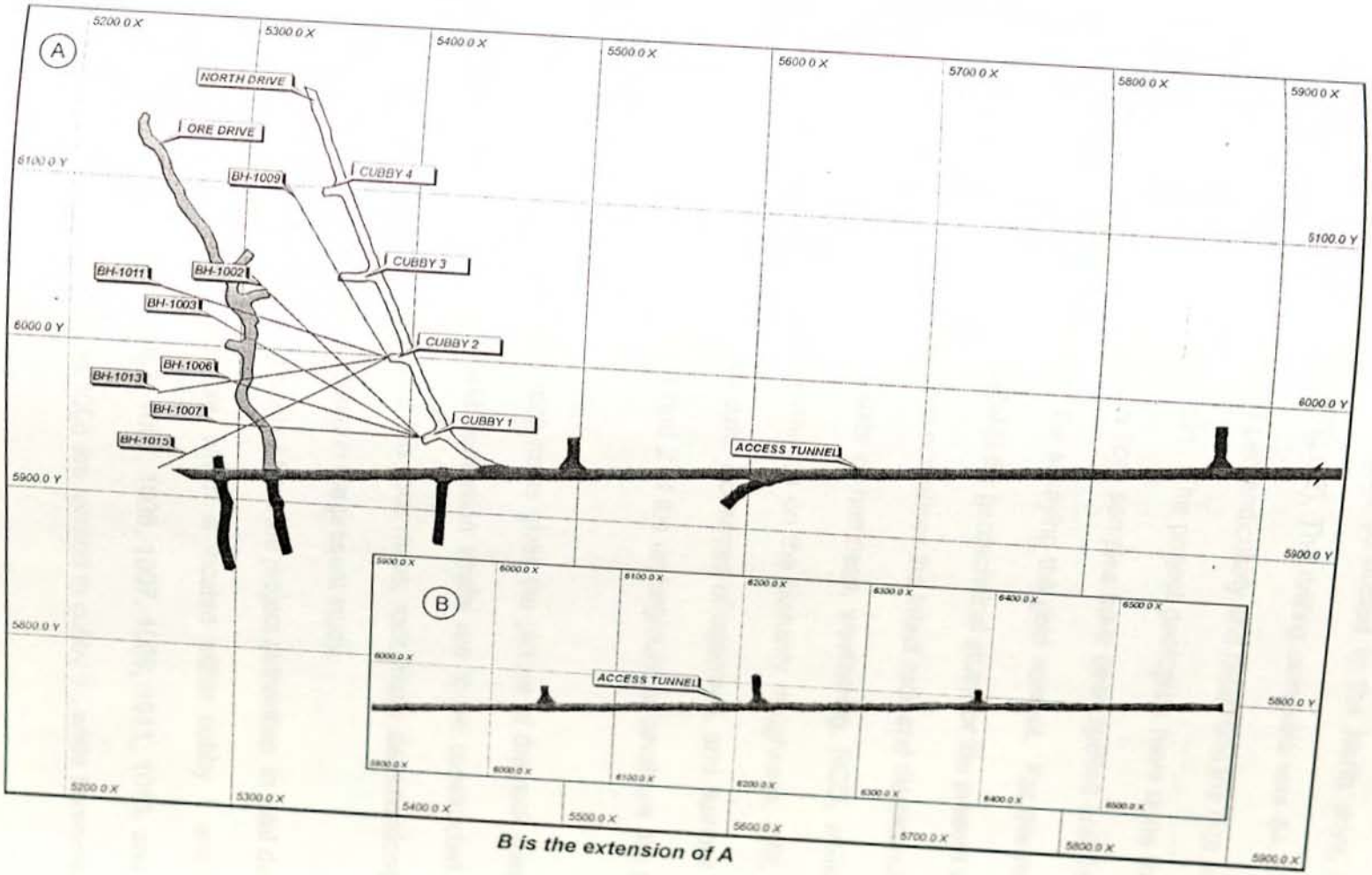

B is the extension of A

Fig.6.2 The underground excavation layout.

6.3.3 *Exploration drilling data of the shear zone*

The exploration drilling has been conducted in the North drive, in four cubbies located at 50 m intervals (Fig.6.2). The drilling core size was 54.7 mm. The prime target was to access the ore perpendicularly and determine the size and gold content of the mineralized quartz vein. The project geologists have done the geotechnical logging. After the logging the core samples have been splitted and the half samples were sent to the laboratory for assaying the gold content. For this reason the core sample were not made available for geotechnical study for the present work.

The geotechnical logging data comprises the intact rock and discontinuity conditions. The rock logging data consists of hardness, weathering, RQD, while the fracture conditions data consists information on the planarity, roughness, infill, discontinuity angles with respect to core axis, closeness of openings, and number of fractures. The drilling array in cubby 1 and 2 of the underground excavations are presented in Fig. 6.4.

The characterization of this rock mass gives the picture of the rock mass condition upon which, ramps, adits and ventilation shafts are to be constructed during the mining activity. To characterize this rock mass, rock mass classifications using the NGI Q-system have been adopted in the present study.

The logging data has been procured from the project authorities. In total data for nine boreholes were made available, which is located within cubby 1 and 2. These boreholes are BH 1000, 1002, 1003, 1006, 1007, 1009, 1011, 1013, and BH1015. Exploration boreholes 1000 to 1008 are located in cubby 1 , while boreholes 1009 to 1015 are located in cubby 2.

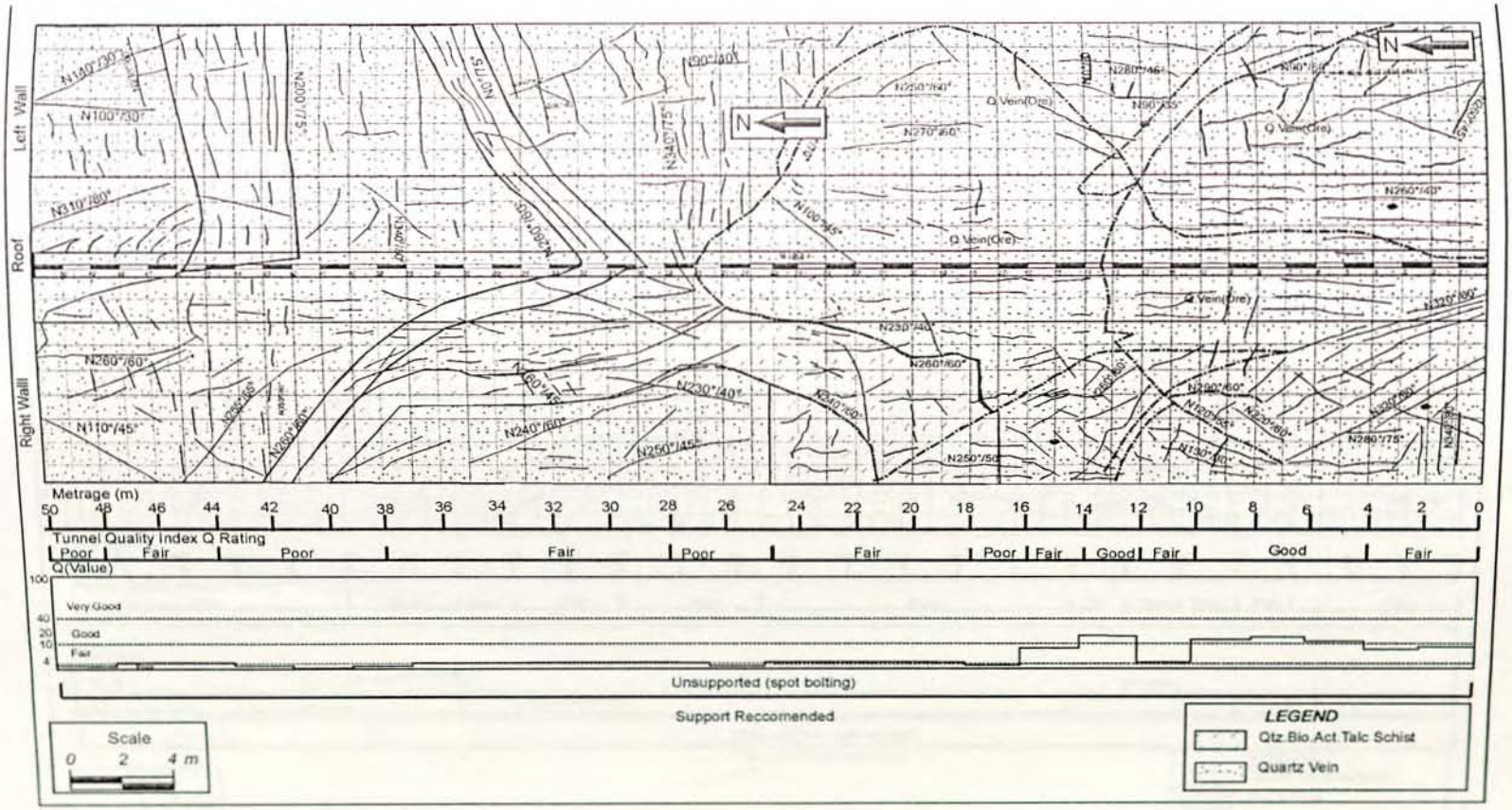

Fig.6.3.1 Geotechnical Mapping of the ore zone (0 - 50 m)

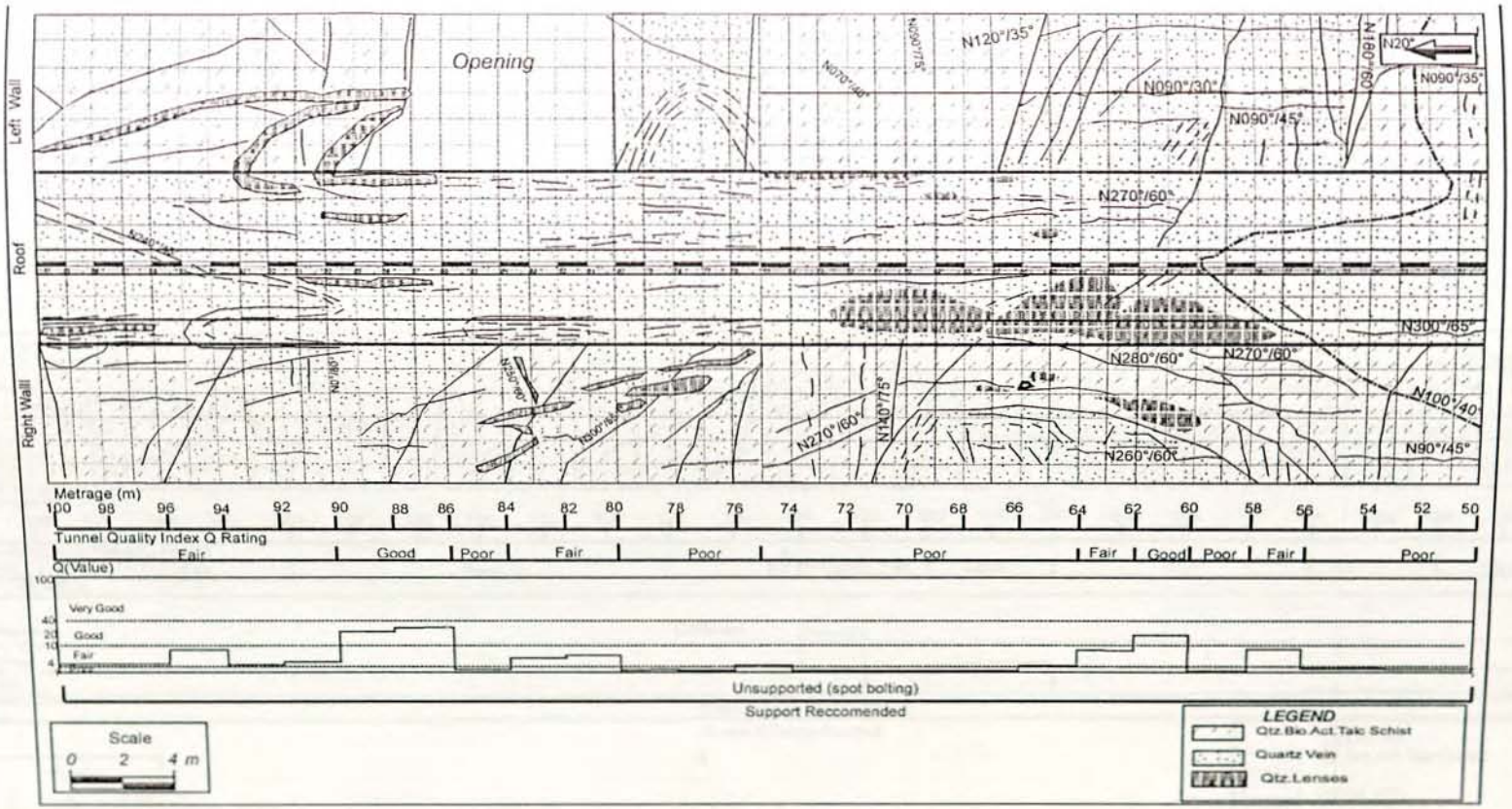

Fig.6.3.2 Geotechnical Mapping of the ore zone (50 - 100 m)

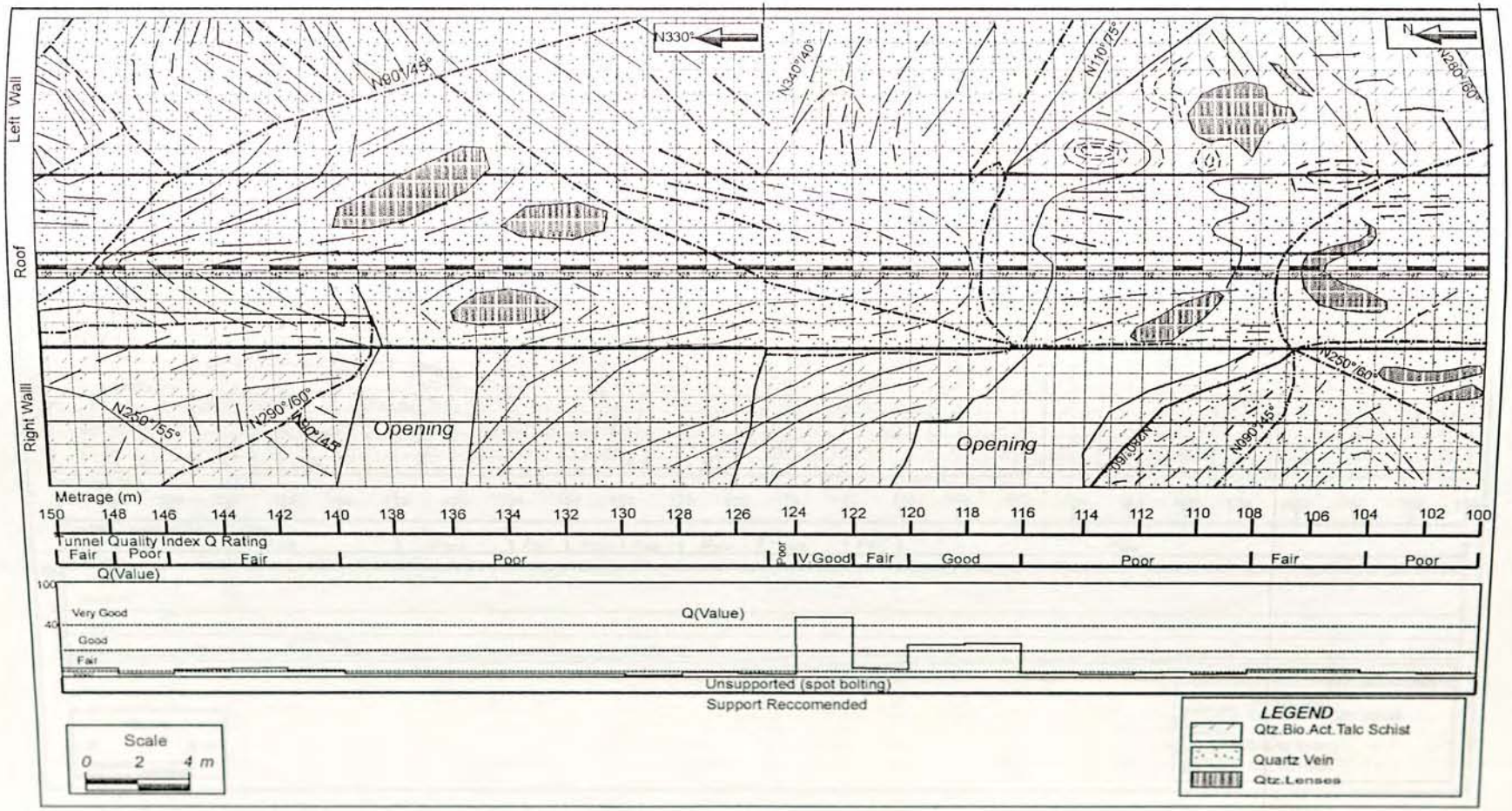

Fig.6.3.3 Geotechnical Mapping of the ore zone (100 - 150 m)

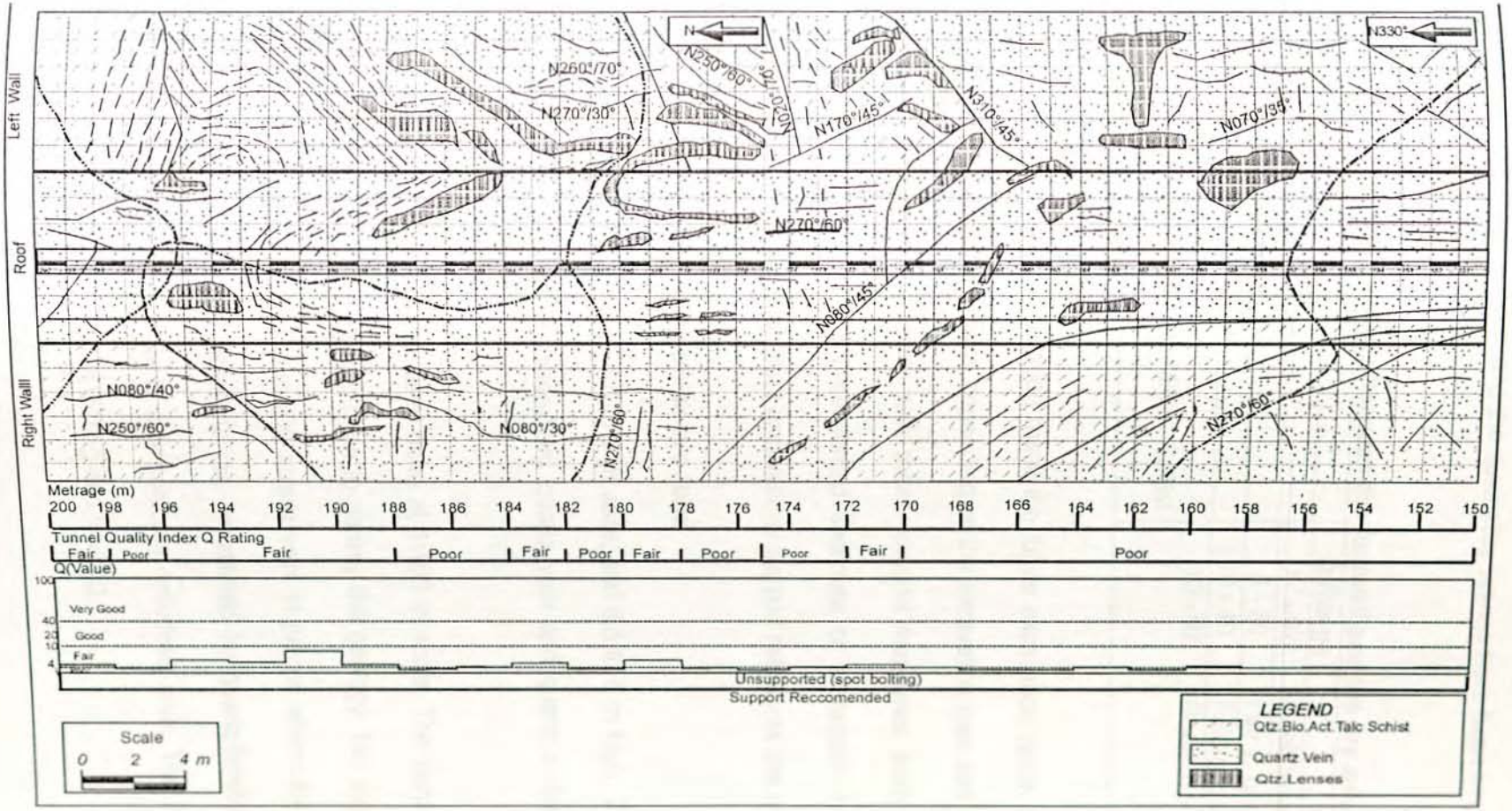

Fig.6.3.4 Geotechnical Mapping of the ore zone (150 - 200 m).

The result of the Q-system ratings on these borehole lines have been considered separately for each rock unit and the qualitative ratings have been worked out (Table 6.1).

Table 6.1 Rock mass quality between the footwall and the ore zone.

Rock Type	Q-Range	Quality
Foot wall Gneiss	17 - 62	Good to very good
Quartz-Sercite Schist	8 - 36	Fair to good
Talc-Biotitte-Actinolite Schist	8 - 40	Fair -good
Graphitic-Quartz-Mica Schist/Carbonaceous-Quartz-Mica Schist	10 - 92	Good to Very good

According to the characterization result the future excavation within this rock mass may require support measures depending on the excavation type and dimension. For permanent excavation in poor rock mass, support measures, such as systematic bolting with 40 - 100 mm unreinforced shotcrete or systematic bolting may be required. Where as for temporary excavations support measures are not required.

6.3.4 Geological mapping of the ore zone

The ore zone is 250 m long, 6.5 to 9 m wide, and 6.5 to 8 m high. The ore zone is fully excavated within the mineralized quartz vein and quartz-biotite-actinolite-talc schist rocks.

The geological mapping has been done at 1:100 m scale. The purpose of the ore zone underground mapping has been to portray the geology, the structure and the rock mass quality. The roof is mainly quartz vein. In places where the quartz vein is completely mined out the sidewalls are constituted by quartz-biotite-actinolite talc schist rocks. The ore zone is in a tectonically deformed rock. The host rocks and stringer veins shows a series of folding and faulting.

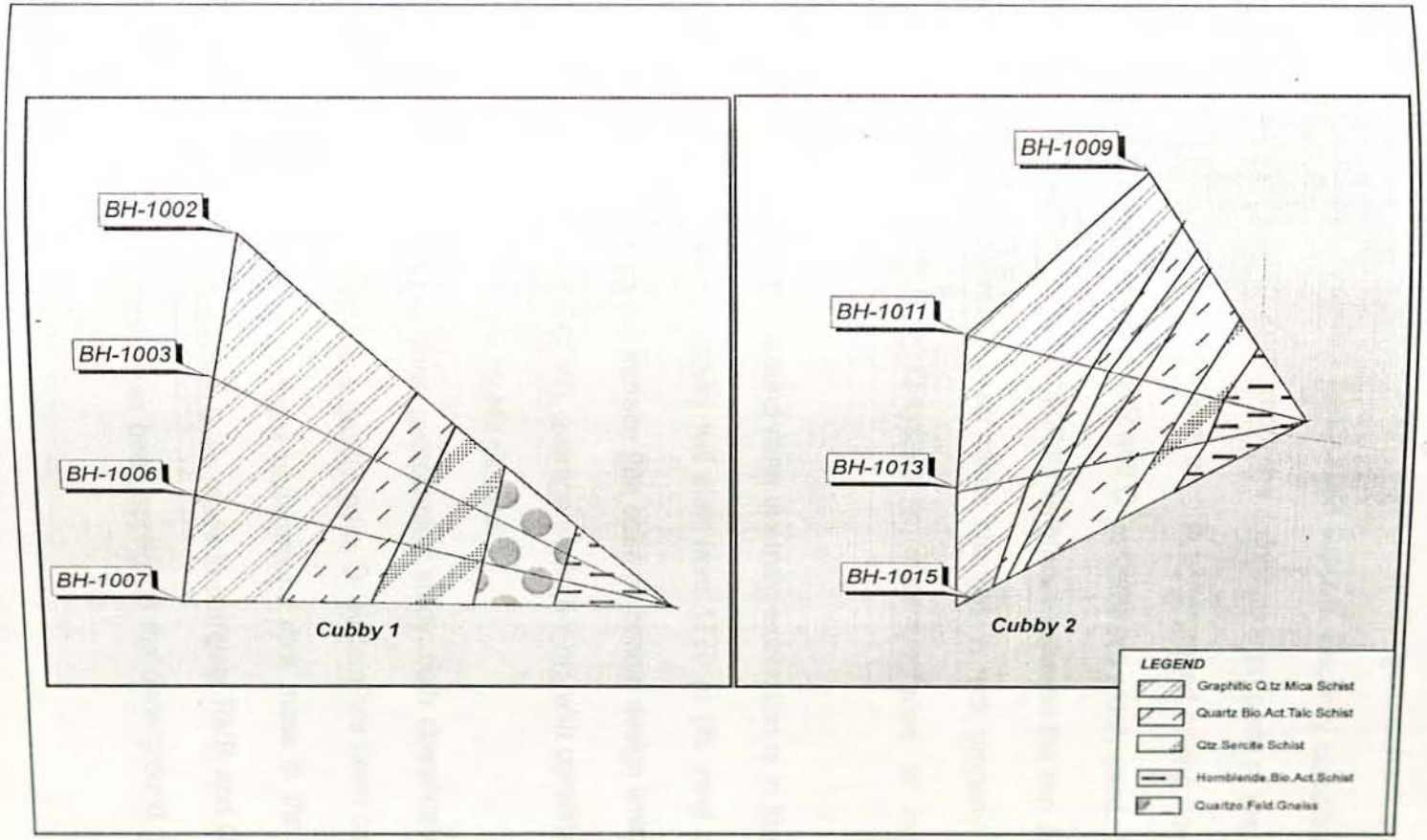

Fig.6.4 Vertical Geological sections from Cubby 1 and 2 boreholes.

6.3.5 *Rock mass classifications of the ore zone*

Rock mass classifications are tools to estimate the strength and characteristics of the rock mass. They are used to group areas of similar geomechanical characteristics, to provide guidelines to select appropriate support. Recently classification systems are being empirically used to estimate the deformation property of the rock mass. There are several classification systems used in underground mining design, however, the two classification systems, RMR and Q- systems are widely used. Both systems had their root in tunneling. The important difference between the two systems is that the Q-system is more sensitive for minor changes in rock property than RMR. The support method of the Q-system is more upgraded to include the recent developments.

In the Legadembi Underground mine the main excavation is in the ore zone and its host rock. The mining activity will start from 1770 m (its level during this study) upward to 1990 m on the surface (the open pit bottom design limit). The ore body is steeply dipping (N60° -70° W), average width (6-7 m), with consistent mineralization. The surrounding rocks are highly silicified.

In the underground ore zone geotechnical study, both classification systems have been applied. The rock mass quality index Q- system has been considered as main tool to characterize the complex underground rock mass in the ore zone. In the present study an attempt has been made to correlate RMR and Q system. For this purpose both the systems has been applied in the underground mine for length of 100 m along ore zone.

6.3.5.1 Application of the Q-system in the ore zone

The Q-classification system is expressed as a function of six independent parameters:

$$Q = \frac{RQD}{Jn} \times \frac{Jr}{Ja} \times \frac{Jw}{SRF}$$

Where RQD is rock quality designation; J_n is based on the number of joint sets; J_r is based on discontinuity roughness; J_a is based on discontinuity alteration; J_w is based on the presence of water; SRF is the Stress Reduction Factor

The rock mass index Q- parameters relation reflects block size (RQD/J_n), friction angle (J_r/J_a), and effective stress conditions (J_w/SRF).

The RQD value has been determined based on Palmstrom's (1982) volumetric count method. This method averages out the anisotropy of the RQD term and gives more representative value. It is expressed as the number of joints present in a cubic meter of rock mass and designated by J_v. RQD is calculated from the relation RQD = 115-3.3J_v. The RQD values calculated in the ore zone vary from 49% to 98.5%. The average value is 86.5%.

The joint numbers varies between 2 and 3 plus random fractures. The joint roughness varies from undulating slightly rough to irregular rough. The alteration varies from tight healed joints to softening or low friction clay filling. Dominantly the fractures are coated or filled with chlorite, talc, and calcite.

In most of the length of the ore zone the excavation is dry but there are areas with damp conditions. The ground water effect has been observed to be minor throughout the ore zone excavation. At two locations minor inflow through fault planes and exploration drill holes, have been observed.

The SRF (Stress Reduction Factor) is based on the fact that the excavation can be considered as shallow depth and the stress condition is moderate. The excavation

depth is greater than 50 m and it is a shear zone. According to Barton et al 1974, for this condition the rating value is 2.5.

Since the ore zone excavation dimension will vary with the advance of the mining activity, the ore zone excavation ESR value has been considered as 4 for temporary excavation condition. The excavation dimension dominantly varies between 6 and 9.5 m.

The rock quality index Q - classification system result shows that the rock mass quality around the ore is rated from poor to fair. The rock mass quality index rating Q-values for the 200 m (Annex-F) long ore zone excavation and the value of the equivalent dimension (D_e) has been used to determine the suggested support categories from Grimstad et al 1993. The result showed that, the underground ore zone rock mass suggested support category, with its present dimension, falls within the unsupported region.

6.3.5.2 *Applications of Geomechanics classifications (RMR)*

The RMR rock mass rating system is based on the six rock mass quality controlling parameters. These parameters are: uniaxial compressive strength of rock material; rock quality designation (RQD); spacing of discontinuities; conditions of discontinuities; groundwater conditions; and orientation of discontinuities.

Since 1973 the RMR or Geomechanics classification system has been modified several times. For the present work the RMR_{1989} version has been utilized to characterize the 100 m long ore zone excavation. The RMR_{1989} rating table is presented as Annex-A.

The result of the RMR rating shows that, out of the first 100 m stretch of the ore zone, 6 m is Poor Rock (RMR (%) 40 -21), 72 m Fair rock (RMR (%) 60 -41), and 22 m Good Rock (RMR (%) 80-61).

6.3.6 *Maximum unsupported span*

The stability of an underground excavation depends on the quality of the rock mass and the dimension of the excavation. Based on their experience and the relation between rock mass quality and unsupported excavation dimension, Barton et.al (1980) formulated empirical relation to estimate the maximum unsupported span (Hoek et al.,1995):

$$\text{Maximum Span (unsupported)} = 2\text{ESR } Q^{0.4}$$

Where ESR is the Equivalent Support Ratio and it is related with the intended use of the excavation and the degree of security, which is demanded of the support system. The estimated value of ESR for different excavation has been given by Barton et al 1974, in this work the value of ESR for the ore zone excavation is taken 4 (Barton et al., 1974). In the analysis of permanent excavation the suggested value is 1.6.

In the Legadembi underground excavation, using the Barton et.al (1980) relation, , the minimum unsupported span as estimated from the Q-system comes out to be 9 m, and the average unsupported span is 15 m Annex-F (Under ground Q-Rock mass rating data sheet).

6.3.7 *Modulus of deformation determination*

Engineering projects that require fail-safe conditions, as in mine-and tunnel-roof spans, open pit mine slopes, and highway and railroad cuts design, needs input data on the strength and rock mass deformation property.

Rock mass deformation results primarily, from the closure of discontinuities and the elastic-plastic deformation of the intact rock that comprise the rock mass. The modulus of elasticity typically is used as a measure of intact rock elastic deformation. In rock mechanics the modulus of deformation is defined as the sum of the deformation that occurs with closure of joints in the rock mass under compression

(plastic) and the deformation that occurs with continued stress application after crack closure (Johnson et al, 1988).

Determination of the modulus of deformation at site requires large-scale in-situ stress tests in which the rock mass has to be subjected for several cycles of loading and unloading. The test has to be performed in such a way that simulates both the magnitude and direction of structural loads at depth and volumes of rock appropriate for the structure. Such in situ tests require the mobilization and utilization of large equipments to the site, which is impractical for the present scale of work. Hence indirect method of estimation of the deformation characteristics of the underground rock mass has been adopted. These methods are empirical calculation from rock mass rating values, and laboratory intact rock strength tests.

6.3.7.1 Empirical estimation modulus of deformation, E_d

Since 1960 several attempts have been made to empirically relate E_d with rock mass classifications. Serafim and Pereira (1983) proposed the following relation between RMR and E_d, based on case histories:

$$E_d = 10^{(RMR-10)/40}$$

Barton et.al (1980), Barton et.al (1992), and Grimstad and Barton (1993) developed relation to estimate E_d from tunnel quality index Q:

$$E_d = 25 \log_{10} Q$$

The Legadembi Underground mine ore zone rock mass have been classified using both RMR and Tunnel Quality Index-Q. Using both rock mass classification data and the above relations, the rock mass deformation E_d, has been estimated. The results from both systems are plotted on a graph presented as Fig. 6.5.

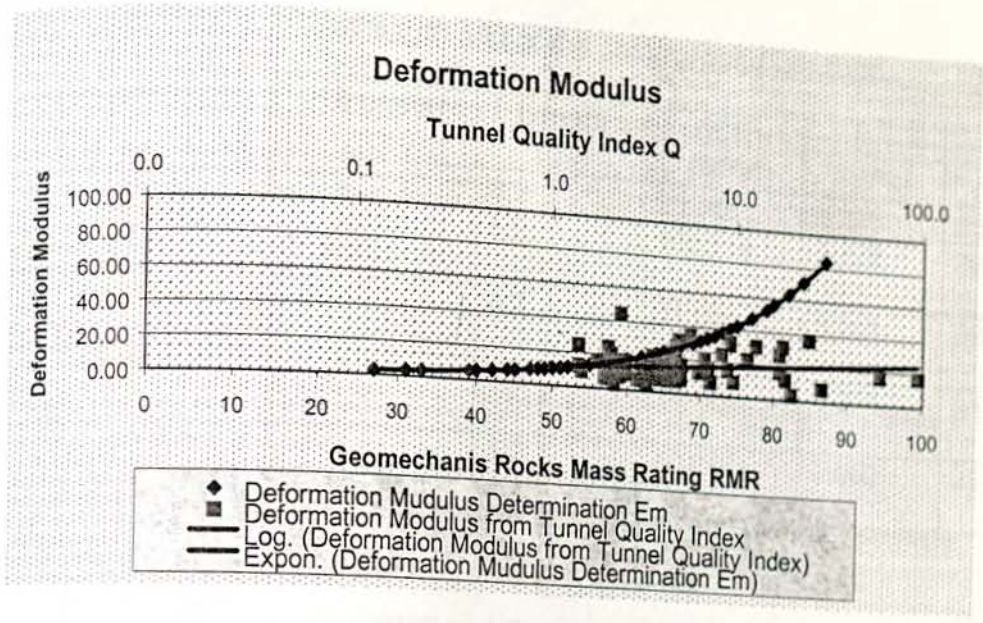

Fig 6.5 Graph of Modulus of deformation for the ore zone.

The perusual of Fig 6.5 indicates that the average value of E_d for underground ore zone excavation is 17219 Mpa.

6.3.7.2 Laboratory test for modulus of deformation

The ore zone is dominantly Quartz-Biotite-Act.Talc schist. For the underground ore zone intact rock strength test, core samples of Q-Sercite schist and Quartz-Biotite-ActinoliteTalc schist has been collected with the permission of the project authority. The core diameter of the rocks have been 41 mm and 36 mm. The core samples were from the borehole abandoned for technical reason. The boreholes drilled in the exploration drive are designed in such a way that the hole crosses the ore zone almost perpendicularly at different elevations. For this reason the orientation of the borehole was assumed to be horizontal. The uniaxial compressive strength test was conducted in the Ethiopian Construction Design Share Company, Material Testing Department Laboratory. The elastic modulus has been determined from the uniaxial compressive test, stress versus strain graph. The test data is presented in Table 6.2.

Table 6.2 Laboratory strength test of the underground ore zone.

Sample Type	Diameter (cm)	Length (cm)	UCS* (MPa)	E_t** (GPa)	γ*** (KN/m^3)
Q-Seri-Schist	4.1	8.2	95.868	5.326	25.538
Q-Bi-Act.Talc Schist	4.1	8.2	101.114	7.222	29.439
Q-Bi-Act.Talc Schist	4.1	8.2	31.506	5.251	28.077
Q-Bi-Act.Talc Schist	3.6	7.2	15.229	4.351	21.677
Q-Bi-Act.Talc Schist	3.6	7.2	40.976	2.969	22.344

*Unconfined Compressive strength; ** Elastic Modulus or Young's Modulus; *** Unit Weight

6.3.8 The correlation of RMR and Q- systems in the underground mine

Both the Q and RMR classification systems are based on a rating of three principal properties of a rock mass. These are the intact rock strength, the frictional properties of discontinuities and the geometry of intact blocks of rock defined by the discontinuities. For the Q system, the intact rock strength is only a factor in the context of the induced stress in the rock as defined by the SRF term.

In order to investigate the influence of these parameters, the approximate total range in values for RMR and Q has been adopted as a basis of comparison. Table 6.3, shows the degree by which the three principal rock mass properties influence the values of the Q and RMR classification (Miline et al., 1995).

Table 6.3 . Influence of basic rock mass properties on classification.

	Q	RMR
Basic Range in Values	**0.001 to 1000**	**8 to 100**
Strength as % of the total Range	19%	16%
Block size as a % of the Total Range	44%	54%
Discontinuity Friction as a % of the Total Range	39%	27%

Table 6.3, shows the surprising similarity between the weightings given to the three basic rock mass properties considered. Despite this, there is no basis for assuming

the two systems should be directly related. The assessment for intact rock strength and stress is significantly different in the two systems. In spite of their differences, it is common practice to use the rating from one system to estimate the rating value of the other. The following equation proposed by Bieniawski (1976) is the most popular, relation between Q and RMR:

$$RMR = 9 \ln Q + 44$$

Based on Beniawski's RMR and Q relation, different countries modified the above relation to suite the overall intact rock and discontinuity properties of their respective local condition. Choquet and Hadjigeorgiou ((Miline et al., 1995) compiled the correlation relation between RMR and Q (Table 6.4).

Table 6.4 Correlation between RMR and Q.

Correlation	Source	Comments
RMR=13.5 log Q + 43	New Zealand	Tunnels
RMR=9ln Q + 44	Diverse Origin	Tunnels
RMR=12.5 log Q + 55.2	Spain	Tunnels
RMR=5 ln Q + 60.8	S.Africa	Tunnels
RMR=43.89-9.19ln Q	Spain	Mining soft rock
RMR=10.5 ln Q + 41.8	Spain	Mining soft rock
RMR=12.11 log Q + 50.81	Canada	Mining hard rock
RMR= 8.7 ln Q + 38	Canada	Tunnels, sed. rock
RMR=10 ln Q +39	Canada	Mining hard rock

To establish the correlation between RMR and Q system an attempt has been made in the present study. For that purpose in ore zone both the systems has been applied in a zone of 100 m. The observation has been made at an interval of 2 m. The RQD parameter has been common for both classification systems and it has been determined based on the volumetric count (J_v) method. The RMR rating has been based on Bieniawski's ,1989 rock mass rating system. The result of the two-classification system has been correlated graphically (Fig.6.6), and the following correlation has been established:

$$RMR = 4.72 \ln Q + 47.8$$

The above correlation is close to the correlation developed for South African tunnels (Table 6.4). South African underground mines are one of the World's known deep underground excavations with complex stress and geological setup, therefore with all the limitations in this work, the correlation can be said sound. However, it is based on the single study, therefore it cannot be generalised. There is further scope to apply both the rating schemes in different parts of Ethiopia to establish a generalized correlation.

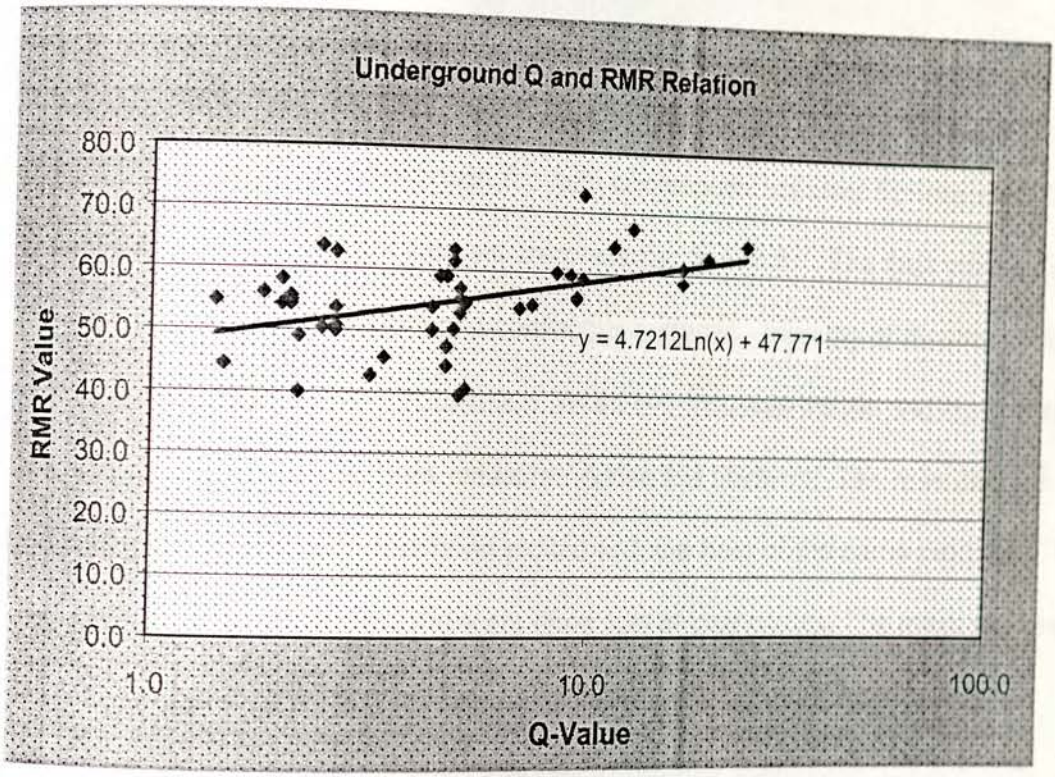

Fig 6.6 Correlation of the RMR and Q system as applied in ore zone 100 m.

6.4 STRUCTURAL DATA ANALYSIS

The presence of discontinuity planes creates anisotropy in the rock mass by dividing it into blocks. The contact between blocks can be loosened and blocks may fall or slide depending on the magnitude of the shear strength on the surface of the discontinuity planes. Hence, evaluation of the orientation of discontinuity planes with

respect to the intended excavation is an important aspect of underground excavations.

The Legadembi ore zone is structurally disturbed area. Structural geological studies conducted on the area outlined four phases of deformations (D_1-D_4), Gebreab (1992). These deformation phases have been identified to be a repeated phases of folding and faulting resulting the present folded, faulted and jointed underground ore zone rock mass.

During the underground mapping, structural data of the discontinuity planes has been collected. The discontinuity planes have been faults and joints. The total observations for joint and fault measurements have been 144. The contour analysis of joint planes has been done with the help of computer software Spheristat 2.. The resulting contour and major joint set are presented in Fig. 6.7. The fault planes have been marked by their smooth and continuous surfaces , crossing or running parallel with the roof and side of the excavation. When ever possible the dip and dip direction of these fault planes has been measured during the fieldwork. The rose diagram of the fault planes (Fig. 6.8) has been plotted with the help of the same program. The rose diagram plot shows that there are three sets of fault planes. The major fault sets are NE - SW and NW-SE trending. The third one is the E-W trending Faults.

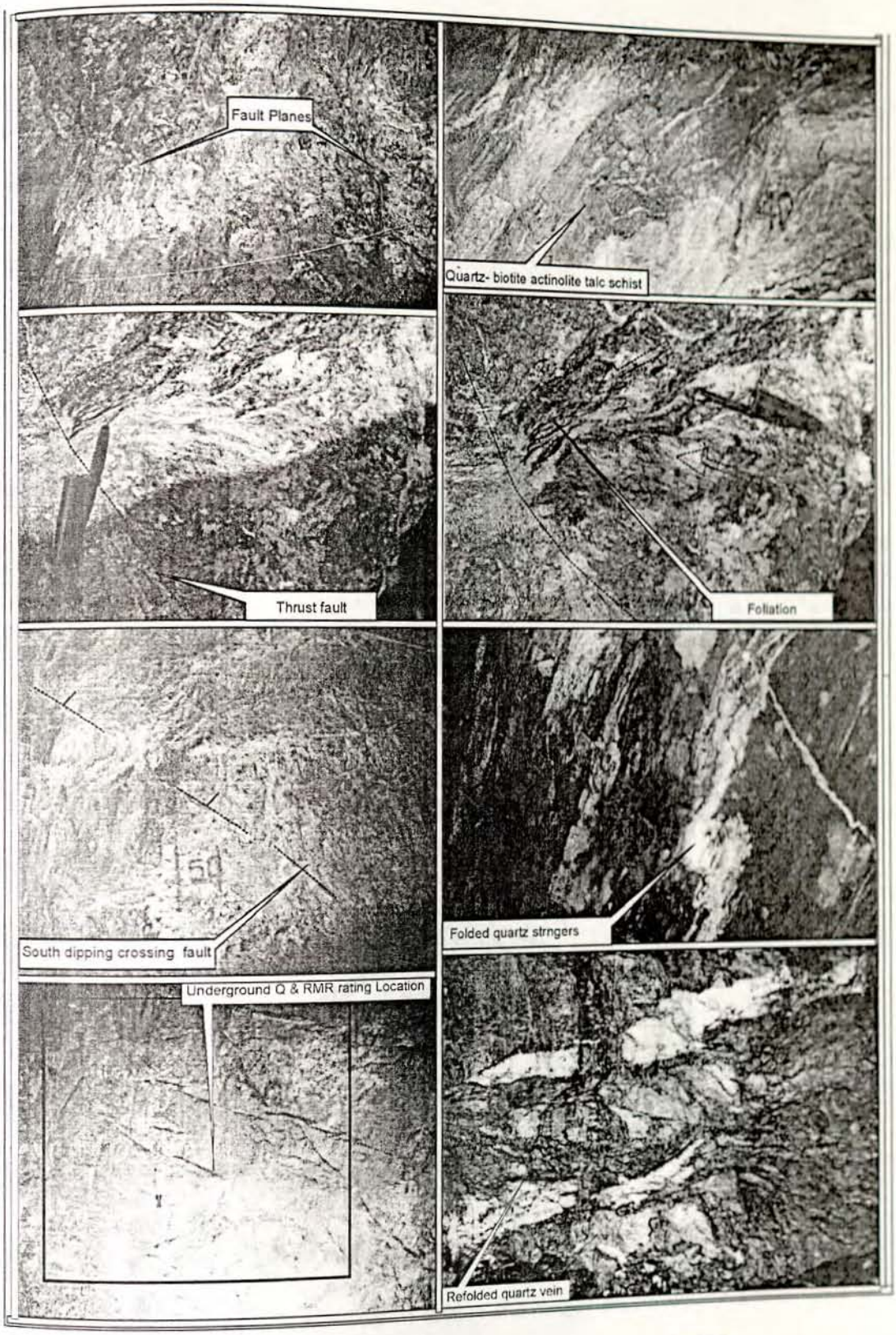

Plate 3. Underground structures.

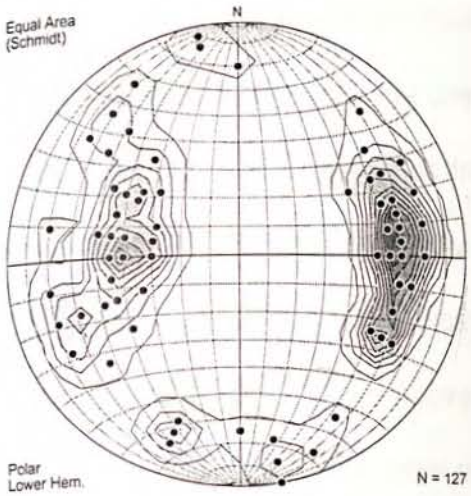

Pole density plot

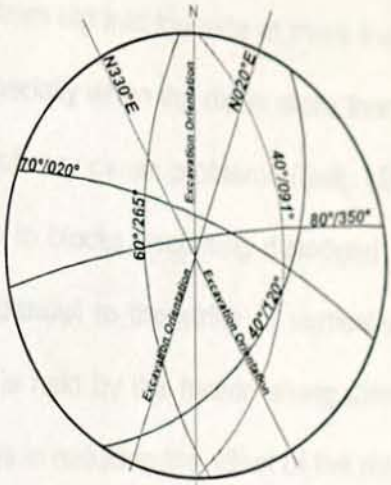

Major joint sets and ore zone excavation orientations.

Fig.6.7 Density plot and preferred orientation of discontinuity planes in ore zone.

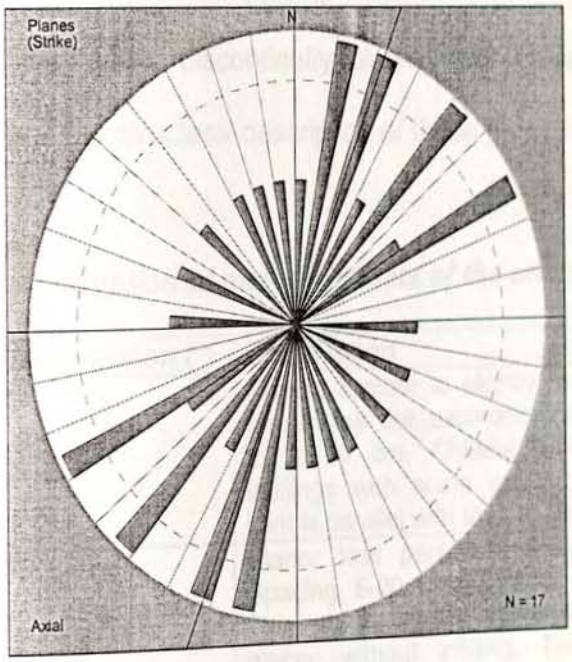

Fig.6.8 Fault planes strike rose diagram for ore zone

To determine the possible mode of failure the major discontinuity plane data has been plotted on Dips computer software. The major discontinuity planes and the excavation orientation plot is presented in Fig. 6.7.

In underground excavations when jointed strata dip into the side at more than 30° or more, the up dip side may be unstable. Especially when the dip is more than 45° the wall rock may slab and fallouts from the roof may cause problems (Bell, 1980). The presence of flat lying joints may also lead to blocks becoming dislodged from the roof. When the axis of the excavation is parallel to the strike of vertically dipping rocks, then the rock mass above the roof is held by the friction along discontinuity planes. The roughness of these planes plays in reducing the effect of the overburden stress (Bell, 1980).

In underground ore zone the excavation orientation varies from North-South with 20° to 30° deviations. The two joint sets dipping towards N265°/60° and N090°/40° are major sets. The other two joint sets dipping towards N020°/70° and N350°/70° are random sets. The two major discontinuity planes are almost parallel with the excavation orientation. The structural description of these joint planes is presented in Table 6.5.

Table 6.5 Fracture description of major joint sets of the underground ore zone.

Set	Dip (°)	Dip direction (°)	Description
Set 1	65 ± 5	265 ± 5	Planar, smooth to slightly rough. Persistent throughout the excavation length. Spacing 20 - 60 cm. Chlorite, talc, and calcite infillings with some gouge materials. The joint is parallel with the ore zone.
Set 2	40 ± 5	090 ± 10	Planar less persistent than Joint Set 1. Spacing 6-20 cm. Slightly rough surface. Talc, calcite and pyrite infillings, at some places without infilling. The joint set is parallel with the tunnel axis.
Set 3	70 ± 5	020	Planar. Considered as random. At places persistent. Spacing 20 - 60 cm. Tight, slightly rough. The strike is almost perpendicular with the tunnel axis.
Set 4	70 ± 5	350 ± 10	Planar. Considered as random. At places persistent. spacing 20 - 60 cm. Tight, slightly rough. The strike is almost perpendicular with the tunnel axis.

6.5 INSITU AND INDUCED STRESS CONDITION

In underground mining it is important to understand the stress condition of the rock mass. The rock mass has usually been subjected to numerous epochs of loading and unloading through out the geological time producing fractures and fault systems of different orientations in space, which results into interconnected blocks.

In rock mass at depth, the applied loads and spatial load distributions are unknown. The outer boundary of an underground excavation or series of excavations is often essentially infinite, so that loads initially concentrated close to the face of the excavations tend to be redistributed into the solid rock mass as the rock near the face starts to disintegrate. Excavation within a rock mass will intensify the stress difference due to inhomogeneities and discontinuities and may lead to instability and ground control problems around the excavations *(CENTEK, 1986)*.

The underground mine geological setup is complex, and the rock mass has passed through a sequence of deformation phases. In this rock mass it is expected that in-situ rock stress will vary from place to place within the rock. Computation of rock stress within a rock mass on the scale of isolated excavation is, in general impossible. However, with all this difficulty, the knowledge of the magnitudes and directions of these induced stresses is an essential part of underground excavation design.

6.5.1 In-situ stress measurements

A variety of methods have been used to determine in-situ stress in rock masses. The two most popular methods are, borehole overcoring and hydraulic fracturing. Each of these methods relies on the fact that drilling of a circular hole into the stressed rock induces stress (and strain) concentrations and associated displacements in the wall of the hole.

In borehole overcoring transducers or deformation gauges are inserted into the hole in order to determine minute changes in the dimension of the borehole, when the hole is relived from in-situ stress, by larger diameter annulus around the hole.

In hydraulic fracturing, a region of the borehole diameter will be isolated by 'packers', and the packed off interval subjected to progressively increasing radial fluid pressure, until a fracture develops in the borehole wall, propagating away from the hole driven by penetration of the pressurized fluid into the crack *(CENTEK, 1986)*.

In the case of the present study due to the lack of measuring instruments and resources, it was not possible to use both methods to determine the stress condition on site. Hence the in-situ stress determination has been based on developed empirical relations.

The vertical in-situ stress σ_v is due to the overlying rock mass weight. The overlying rock mass stress is a function of the depth and the average unit weight of the rock. It can be estimated from the relation:

$$\sigma_v = \gamma z$$

Where σ_v is the vertical stress; γ is the unit weight of the overlying rock; z is the depth below surface.

In the Legadembi Underground Mine ore zone the average unit weight of the overlying rocks is 26.8kN/m^3 (BRGM, 1991). Before the mining activity started the top of the mountain surface was at around 2200 m above mean sea level. The ore zone excavation lies at 1770 m above mean sea level. Hence because of the residual stress condition the vertical height between 2200 m and 1770 m has been considered as 430 m.

The vertical or gravitational stress σ_v can be calculated from :

$$\sigma_v = \gamma z = 26.8\text{kN/m}^3 * 430\text{m} = 5896\text{kN/m}^2 = 11.524\ \text{MPa}$$

The horizontal stress acting on an element of rock at depth z below the surface are much more difficult to estimate than the vertical stresses. The ratio of the average horizontal stress to the vertical stress is denoted by *k* such that:

$$\sigma_h = k\sigma_v = k\gamma z$$

Where σ_h is the horizontal stress. To calculate the magnitude of the horizontal stress, the ratio of the horizontal stress to the vertical stress (*k*) should be determined. There are arithmetical ways, related with the deformation property of a rock mass, to determine the value of *k*. The relation based on the Poisons ratio (ν) has been found useful to approximate the value of *k*. The magnitude of the coefficient of geostatic pressure (*k*) can be determined from $k = \frac{\nu}{(1-\nu)}$ (Hoek et al, 1995). This implies that $\sigma_h = \frac{\nu}{(1-\nu)} \times \sigma_v$. In the Legadembi underground rock mass the Poison's ratio has not been determined, hence the value of the Poisson's ratio (ν) has to be adopted from the standard table given in Selby 1993, (Table 6.6). The value of the Poisson's ratio for the underground ore zone rock mass has been considered as 0.2. Accordingly the horizontal stress in the underground ore zone has been estimated as 2.88 Mpa.

Table 6.6 Elastic properties of rocks.

Rock Type	Density T/m^3	Modulus of Elasticity (Gpa)	Shear Modulus (Gpa)	Poissons Ratio
Gabbro	3.0	55 - 90	20 - 40	0.2 - .38
Gneiss	2.7 - 2.8	55	-	.21
Schist	2.4 - 2.8	20 - 60	8 - 25	0.1 - 0.3

6.5.2 *Induced Stress Analysis*

Most underground mining excavations are irregular in shape and are frequently grouped close to other excavations. In addition ore bodies are associated with geological features, such as faults, the rock properties are seldom uniform within the

rock volume of interest (Hoek et al., 1995). There are computer based numerical methods that have been developed for obtaining the approximate value of the induced stress effected from the underground excavations. In rock mechanics, the boundary and domain method are the two numerical analysis methods of stress driven problems. In boundary method, only the boundary of the excavation is divided into elements and the interior of the rock mass is represented mathematically as an infinite continuum. Whereas in domain methods, the interior of the rock mass is divided into geometrically simple elements each with assumed properties.

Since there is no data pertaining to the stress conditions of the underground rock mass, and the softwares are also not accessible, it was not possible to approximate the magnitude and directions of the induced stresses.

6.6 STABILITY ANALYSIS OF THE UNDERGROUND ORE ZONE

In shallow depth underground excavations, in structurally affected rock mass, the most common types of failures are those involving wedges falling from the roof or sliding out of the sidewalls of the openings. Generally in mining excavation are opened in different directions and different rock mass. When the excavation of the opening creates a free face, the restraint from the surrounding rock is removed. Depending upon the relation of the fracture, the friction between blocks, the excavation size and orientation, wedges can fall from roof, or slide from the sidewalls.

Unless measures are taken to stabilize these loose wedges, the back and walls of the opening may fail.

Hoek et al. (1995) recommended steps, which are required to deal with this problem. These steps are:

1. Determination of average dip and dip direction of significant discontinuity sets in the rock mass.
2. Identification of potential wedges, which can slide or fall from the back or walls of the opening.
3. Calculation of the factor of safety of these wedges, depending upon the mode of failure.
4. Calculation of the amount of reinforcement required, to bring the factor of safety of individual wedges up to an acceptable level.

6.6.1 Identification of potential wedges

The size and shape of potential wedges in the rock mass surrounding an opening depends upon the size shape, and orientation of the opening and also upon the orientation of the major discontinuity planes.

In Legadembi Underground mine, two major consistent joint planes and two random joint planes have been identified. The excavation orientation is N330° at places north -south. Eventhough there are only two major joint sets, there is still wedge forming possibility at places where three joint sets intersect at the roof and the sidewalls. The stability of the resulting wedges has to be considered.

In underground openings in blocky hard rocks, like the Legadembi underground mine, during or some time after the opening of excavation, wedges can fail without giving sign. Wedges on a roof can fail as soon as the base of the wedge is fully exposed by excavation of the opening. For sidewall wedges, sliding of a few millimeters along one plane or the line of intersection of two planes is generally sufficient to overcome the peak strength of these surfaces. This means that the

movement along the sliding plane has to be minimized by stabilization measures (Hoek et.al, 1995).

Rock bolting is an ideal stabilizing measures in the case of wedge failure. Rock bolts generally consists of plain steel roads with a mechanical anchor at one end and faceplate at the other. They are always tensioned after installation.

In Legadembi Underground ore zone the two major and two random joint sets are:

Joint set	Dip (°)	Direction (°)	Remark
J1	60	265	Major
J2	40	090	Major
J3	70	020	Random
J4	80	350	Random

In the wedge stability analysis it is assumed that the discontinuity planes are planar and continuous and the shear strength of the discontinuity planes can be represented by angle of internal friction (ϕ) and a cohesive strength of zero. The underground rock mass is rated as fair rock (in both rock mass quality index-Q and the rock mass rating RMR systems). At places the fractures are filled with softening or low-friction mineral coatings like chlorite, talc and graphite. The angle of internal friction (ϕ) value for fair rock varies between 25° - 35° (Annex A).

To study the stability of the wedges in the underground excavation, UWEDGE computer program has been used. The software is prepared by Bhawani Singh of Indian Institute of Technology, Roorkee.

The joint set orientations, the shear strength, the excavation orientation and dimensions were feed to UWEDGE computer software.

The input parameters for UWEDGE program are: number of cases i.e. analysis for the roof, right wall and left wall; dip of the joint planes; dip direction of the joint planes; cohesion along the joint plane; angle of friction along the joint plane (degree); average seepage water pressure on joints; dip of the excavated face; dip direction of the excavated face; plunge of boundary edges; trend of boundary edges or free face; trend of bolt force (Upward=-1); span of free face or height of free face between boundary edges of walls; unit weight of rock mass (T/m^3); capacity of individual bolts; spacing of bolt in square pattern.

The program out put are: the weight of the wedge; the position of the wedge from the centerline on the roof and side walls; the factor of safety of unsupported wedge; the factor of safety of reinforced wedge; the possibility of overhanging of the wedge on opening of its base. The calculation envisaged that the discontinuity can occur any where in the rock mass. The result can also be considered as conservative since the possibility of the wedge depends on the persistence, spacing and the occurrence of wedge forming fractures within the actual rock mass.

6.6.2 Stability analysis of wedge in the ore zone

For the Legadembi underground mine ore zone orientation N330° and N360° orientation, for the roof, left wall and right wall wedge stability analysis of excavation have been made using UWEDGE computer program.

6.6.2.1 *For tunnel orientation - N330°.*

Table 6.7 General input data and values for UWEDGE stability analysis of excavation orientation N330°.

Input Parameters	Value	Input Parameters	Value
Joint set number	4	Right Wall	
		Trend	N330°
Excavation span	6.0 m	Plunge	0°
Roof trend	N330°	Excavation dip direction	N240°
Roof plunge	0°	Dip	89°
Left Wall		*Bolt Length (Swellex)	6m
Trend	N330°		
Plunge	0°	*Bolt Capacity	11T
Excavation face dip direction	N060°	Bolt Grid	2 m
Dip	89°	Seepage Water Pressure (U)	0
		Unit weight (γ)	2.68 T/m^3

*(E.Hoek et al.,1995)

Table 6.8 Joint set input data for underground excavation.

Joints set	Dip(°)	Direction(°)	Cohesion (T/m^2)	Friction,ϕ (°)
J1	60	265	0	30
J2	40	090	0	30
J3	80	350	0	30
J4	70	020	0	30

The numbers of tetrahedral wedges, which can be formed from the four joint sets in each case, are four.

Table 6.9 Wedge-forming joint sets combinations.

Joint Data	W1			W2			W3			W4		
Joint Plane	1	2	3	1	2	4	1	3	4	2	3	4
Dip (°)	60	40	80	60	40	70	60	80	70	60	80	70
Direction(°).	265	90	350	265	90	020	265	350	020	265	350	020

Table 6.10 UWEDGE software stability analysis results for N330°orientation:

Roof wedge						
Wedge	**Wt**	**Separation**	**Perpendicular Distance from apex.**	**Failure Mode**	***FOS.U**	****FOS.S**
W1	3 T	J3	0.58 m	Fall	0.0	7.29
W2	3 T	J4	0.59 m	Fall	0.0	6.6
W3	65 T	J1 & J4	6.47 m	Fall	0.1	3.12
W4	74 T	J2	7.8 m	Fall	0.61	15.26

Left wall wedge				
Wedge	**Separation**	**Failure Mode**	***FOS.U**	****FOS.S**
W1	J1	slide	0.85	7.82
W2	J4 & J1	slide	0.69	9.00
W3	J1	slide	0.77	12.09
W4	J2	Fall	0.77	12.90

Right wall wedge				
W1	J1	Slide	0.33	0.95
W2	J2 & J4	Slide	0.33	2.5
W3	J4	Slide	0.39	5.4
W4		Stable		

*FOS.U= Factor of safety of Unsupported Wedge; **FOS.S= Factor of safety of Supported wedge

In the analysis the FOS of the roof wedges , W_1, W_2 and W_3 are zero. Which implies that when their bases are exposed, unsupported wedges will immediately fall,. In the right wall W_1, the supported FOS is less than 1.5. This implies that for the N330° the right wall will need additional support than that considered in the analysis. For the left wall and the roof wedges, the support measure considered in the analysis will be enough.

6.6.2.2 For tunnel orientation - N360 °.

Table 6.11 General input data and values for UWEDGE stability analysis of excavation orientation N360°.

Parameter	Value
Joint set number	4
Excavation span	6.0 m
Roof trend	N360°
Roof plunge	0°
Left wall trend	N330°
Left wall plunge	0°
Excavation face dip direction	N90°
Excavation dip	0°
Right wall trend	N360°
Right wall plunge	0°
Right wall dip direction	N270°
Right wall dip	0°
Bolt length *	6m
Bolt capacity (Swellex, mechanically anchored bolt) *	11T
Bolt grid	2m
Seepage water pressure (U)	0
Unit weight γ	2.68 T/m^3

Joins set	Dip(°)	Direction(°)	Cohesion	Friction, ϕ (°)
J1	60	265	0	30
J2	40	090	0	30
J3	80	350	0	30
J4	70	020	0	30

(Hoek et al., 1995)

Table 6.12 UWEDGE software stability analysis result of 360° orientation.

Roof wedge						
Wedge	Wt	Separation	Perpendicular Distance form apex	Failure Mode	*FOS.U	**FOS.S
W1	630 T	J3	3.37 m	Fall	0.0	1.24
W2	585 T	J4	3.29 m	Fall	0.0	1.18
W3	49 T	J1 & J4	6.47 m	Fall	0.1	3.88
W4	65 T	J2	7.44 m	Fall	0.77	27.92

Left wall wedge				
Wedge	Separation	Failure Mode	*FOS.U	**FOS.S
W1	J1	slide	0.85	2.56
W2	J1 & J4	slide	0.09	3.6
W3	J1	slide	0.77	4.84
W4	J2	slide	0.77	2.77
Right wall wedge				
W1	J2 & J3	slide	0.33	0.32
W2	J2 & J4	slide	0.33	1.00
W3	J1 & J3	slide	0.39	2.10
W4		stable		

**FOS.U= Factor of safety of Unsupported Wedge; **FOS.S= Factor of safety of Supported wedge*

The roof wedges W1, W2, and W3 will immediately fall when their base is exposed. The supported wedge FOS of W1 and W2 are less than 1.5. The result indicates that for the roof wedges W1 and W2 additional support will be required. The right wall W1 and W2 supported FOS is less than 1.5. For these wedges additional wedges will be required.

6.7 MINING

In hard rock underground mining the mining system has to be effective in assuring the safety of persons and equipment, and minimizing dilution of the ore due to failure of the surrounding rock mass. Underground mining systems are very diverse and further divided into subsystems based on the: type and location of development; direction of stopping, relative to the ore body; stage and method of support of the stopping areas; organization and shape of the stopping face; methods of breaking

and haulage of ore in stopping. The basic classification systems and their subdivision have been summarized from Agoshkov et al., (1988), and presented in Table 6.9.

Table 6.13 Mining systems.

System	Description	Group	Group descriptions
I	Open stope systems	1	Underhand systems
		2	Overhand system
		3	Longwall systems
		4	Room-and-Pillar systems
		5	Sublevel stoping systems
		6	Room-and-level systems
II	Shrinkage Systems	1	Systems with blasting from shrinkage stopes
		2	Systems with breaking from special workings
		3	Systems with breaking by deep holes
III	Supported stope system	1	Systems with reinforced stulls and square set
		2	Systems with stone and composite support
IV	Cut and fill systems	1	Horizontal slicing system with filling
		2	Inclined slicing system with filling
		3	Overhand system with filling
		4	Descending slicing systems filling
		5	Longwall systems with filling
		6	Systems with support and filling
V	Rock Caving systems	1	Slicing and caving systems
		2	Sheild systems
		3	Pillar systems with roof caving
VI	Ore and rock caving systems	1	Sublevel caving systems
		2	Level self caving systems
		3	Level forced caving systems
VII	Combined system	1	Combined room open slope systems
		2	Combined room shrinkage systems
		3	Combined room stoping and filling systems

The shape of the deposit has much more effect on the mining method because it usually changes more abruptly. Apart from the shape of the deposit its contact with the country rock is also important, weather it has clearly defined or indefinite boundaries.

The angle of dip and the thickness of the deposit also have a considerable effect on the choice of the mining method. According to their angle of dip, deposits are divided

up from the point of mining method into gently sloping (up to 25°), inclined (25°-45°), and steep deposits (45°-90°), (Agoshkov et al., 1988).

According to their thickness, ore deposits are divided into five groups: very thin from 0.6 to 0.8 m, thin from 0.7 to 2 m, medium thick 2-5 m, thick from 5 to 20 m, and extremely thick more than 20 m (Agoshkov et al., 1988).

In metal mining the mine take is divided into horizons, which have a vertical interval between 25-30 m and 80-100 m.

The upper Legadembi underground ore zone has been considered as having consistent gold grade with average width of 5.5 m and 225 m length. Based on the Agoshkov (1988), the ore body can be classified as steeply dipping moderately thick lense.

The Legadembi Underground ore is mainly the quartz vein, hosted within quartz biotite- actinolite-talc schist. In the underground ore zone excavation the roof is constituted dominantly by quartz vein. The mineralized quartz vein can be considered as strong rock with uniaxial compressive strength of 100-200 Mpa (Sellby 1993). On the other hand, the host rock constituting the sidewalls can be classified as weak rock with uniaxial compressive strength of 20-50 Mpa (when unsilicified), (Sellby 1993) .

In the structural analysis it has been addressed that, the ore zone contains faults and joints which strike parallel and dip angle > 45°. These planes are considered as unfavorable for the stability of the excavations. The UWEDGE analysis has showed that there is a possibility of sliding failure where wedge-forming fracture occurs.

The Legadembi underground ore zone rock mass can be safely excavated for 15 m span with temporary support systems of spot bolting. However during the actual mining operations the height of the span may increase to 25-30 m, this in turn will

affect the deformation property of the rock around the ore body. The stability of the rock mass of the hanging wall and further back into the footwall should be main concern. These with the increase of the excavation dimension the long-term stability of the working depend in maintaining the sidewalls from sliding or caving.

Cut and fill mining method comprise a system where the space created because of the removal of the ore, will be filled by rock from surface works or mill tailings. The filling is used to prevent the caving or subsidence of the surface. This system allows mining a deposit with a fault and jointing in a branching ore body. Both regular and reinforced supports of various types can be applied during opening the stop. The cut and fill systems ensure a high degree of mineral extraction, labor safety under difficult geological conditions. The most significant disadvantages are high cost of the filling material in transporting and placement.

The detail advantages and disadvantages of the other mining systems may not be addressed well in this work because of limitations, but with its high operational cost the cut and fill mining system is more safe for the long term stability and safety of persons equipment and machineries in a rock mass condition of the Legadembi Underground ore zone excavation.

CHAPTER VII

CONCLUSION AND RECOMMENDATIONS

The Legadembi Gold Mine is located in southern Ethiopia in Adola area. The Adola area Precambrian rocks are grouped into Awata, Mormora and Adola Group. The Awata and Mormora Group rocks are dominantly repeatedly folded and sheared gneissic rocks intercalated with schits and intruded by pre to syntectonic granitic rocks. The Mormora Group rocks surround the Adola Group rocks. The Adola Group rocks are dominantly metavolcano- sedimentry rocks with patches of mafic-ultramafic rocks intruded by syn to post tectonic intermediate to granite rocks. The gneissic rocks are Late Proterozoic age, metamorphosed in granulite to upper amphibolite facies, and they are the oldest rock in the region. The metavolcano-sedimentary rocks are the younger basement rocks, and metamorphosed in greenschist to lower amphibolite facies.

The Adola Precambrian metavolcano-sedimentary rocks and the associated mafic-ultramafic rocks occur in two N-S striking zones, separated by gneissic terrain, the Kenticha and Megado belts. The Legadambi gold deposit is located in Megado zone. The main lithotypes and their distributions from east to west are: quartzo-feldspathic, quartz-biotite and amphibole gneisses in the east; quartz biotite actinolite-talc-schist and graphite-quartz mica schist rocks, in the central; and amphibolite and gabbro intrusives at the western part. The auriferous quartz veins are hosted in metavolcano-sedimentary units (mainly in quartz-biotite-actinolite talc and graphite-quartz-mica schists) and mafic-ultramafic sheared rocks. The contact between the gneiss and the schist rock units are marked by a horizontal transcurrent shear thrusts, with transverse or oblique brittle structures.

The Legadembi gold deposit ore bodies are separated by the oblique faults trending ENE-WSW and at present it has been regrouped into, Upper and Central Legadembi. The ore bodies are structurally controlled and plunge towards North at low angle.

The geotechnical study conducted during the feasibility study stage and the present work indicated that the footwall gneiss rocks are strong, with uniaxial compressive strength of 200-300 Mpa. The hanging wall rocks strength varies from strong to weak rocks. In the hanging wall rock units the graphitic quartz mica schist is a strong rock with uniaxial compressive strength of 50 -140 Mpa. The quartz biotite actinolite talc schist rock's strength varies from weak to strong. When it is silicified, its uniaxial compressive strength is 50-100 Mpa, and falls in strong rock group. Otherwise, it's uniaxial compressive strength is 20-50 Mpa and falls within weak rock. The talc-actinolite-tremolite rocks are located at the contact between the footwall and the hanging wall. The uniaxial compressive strength of this rock is 15-40 Mpa and it falls within the weak rock group.

The ground water flow, at the open pit and underground excavations has been found not to be in amount, which can create water pressure that can cause stability problem. On the other hand both from the feasibility and the present study, the chemical analysis of the water samples from underground workings has showed high amount of sulphates and chlorides, which makes the ground water highly corrosive with corrosivity ratio up to 8.

The open pit average RMR rating has showed that the rock mass falls within the FAIR rock mass class (RMR= 60-41). According to the Beniawiski's RMR, the shear strength parameters, ϕ and c, values ranges 25°-35° and 200-300 kpa, respectively.

The slope stability analysis around the open pit has been carried out based on 7 slope sections. From the kinematic check analysis, with the slope geometry and the

954 structural measurements analysis, 6 plain mode of failures, 8-wedge mode of failure and one circular mode of failure has been identified. The Factor of safety analysis for these critical cases showed that slope section SL3 and SL4A are not stable for possible worst condition defined by dynamic moderately saturated condition. Based on the rock mass conditions of these slopes, safe slope design for FOS = 1.3 and 1.2 have been worked out by varying the height and slope angle. The slope design for moderately saturated dynamic conditions indicated that, the western slope hard rock sections will be stable at FOS 1.3, with 35° to 40° overall slope angle and 50°-60° bench slope face, 20 m bench height and 6 m berm width. The Eastern slope has been found to be stable for existing and possible worst conditions.

Geotechnical study conducted for underground mine was focused to characterize the ore zone rock mass from 1770 m to 1990 m above sea level. The present ore drive level (1770 m) is the starting level of the underground mine and 1990 m is the ultimate level. To characterize the rock mass around the ore zone, geotechnical and structural data from previous work and the present work have been collected and analyzed. In the ore zone excavations two major and two random joints have been identified from the structural data analysis. The ore zone excavation is almost parallel to the two major discontinuity planes. The wedge forming possibility in the ore zone excavation has been considered and analyzed with UWEDGE computer software. The results indicate that there is four wedge forming combinations of the discontinuity planes. From the analysis it has been found that most of the wedges can be stabilized with 11 T capacities and 6 m long rock bolts. However, from the analysis it has been found that there are heavy wedges present, which may require additional supports, like shotcreeting. The ore zone excavation is considered as a temporary excavation with ESR (Equivalent Support Ratio) value of 4. Using the ESR value and

the excavation dimension ratio, versus the Q rating value, on the Q - support graph, the ore zone excavation doesn't need permanent support. However, for safety purpose spot bolting is required in wedge forming and susceptible sliding wall places. The maximum excavation span has been empirically calculated from the relation developed by Barton et al 1980. Accordingly the minimum and maximum excavation span has been estimated to be 9m and 15 m respectively.

When permanent development excavations (ESR=1.6), such as hauling ramps, are to be excavated within the rock mass between the footwall and the ore zone, the excavation may require permanent support of categories 4 and 3 of estimated Q-support graph. Category 4 is systematic bolting with 40-100 mm unreinforced shotcrete and category 3 is systematic bolting.

During the mining activity the excavation height may increase considerably (20-30 m). The increase in the excavation dimension will alter the stress condition around the ore zone rock mass. The stress conditions around the underground rock mass could have been approximated with finite element analysis. Because of the lack of measured values of the magnitude and directions of principal stresses, rock mass deformation properties and the limitation in acquiring computer programs, which facilitates this analysis, the ore zone deformation behavior could not be determined.

The long-term stability of the open pit and underground mining excavations depends on the mining system, which is going to be implemented. From the underground mining systems, the cut and fill mining system has high operational cost but it has been found that it provides more safety for the rock mass condition. Hence, cut and fill mining system is considered to be the best suitable mining method for the

Legadembi underground works . However, unless the deformation property of the ore zone rock mass is determined properly, other mining systems may not be justified.

The ground water corrosive action can affect bolts both in the access tunnel and the future excavations. Hence, support measures should be protected from corrosion by grouting with the right cement or at least should be galvanized.

To monitor the movement of the underground mine rock mass, deformation-measuring instruments such as extensometers, should be installed in the access tunnel and the future hauling ramps.

In the underground mining work, as the mining progresses upward to the surface there will be a reduction in the normal stress across discontinuity planes, this may result in the reduction of shear strength, which practically resists the down ward movement of blocks of rock mass. Hence, in the future mining activity the occurrence of discontinuity planes and the ground reaction with the excavation should be closely studied and the proper support measures should be immediately adopted.

For the Legadembi underground mine, the following stabilization method should be adopted to prevent the wedge failures (Hoek et.al, 1995):

1. For roof wedges the total force, should be applied by the reinforcement, should be sufficient to support the full dead weight of the wedge, plus an allowance for errors and poor quality support installation. The total tension applied to the rock bolts or cables should be 1.3 to 1.5 x W, giving factor of safety of 1.3 to 1.5.

2. When the wedge is clearly identifiable, some attempt should be made to distribute the support elements uniformly about the wedge center. This will prevent any rotations, which can reduce the factor of safety.

3. In selecting the rock bolts to be used, attention must be paid to the length and location of these bolts. For grouted cable bolts, the length through the wedge and the length in the rock behind the wedge should both be sufficient to ensure that adequate anchorage is made available. When mechanically anchored bolts with faceplates are used, the lengths should be sufficient to ensure that enough rock is available to distribute the loads from these attachments.

4. In the case of sidewall wedges, the bolts can be placed in such a way that the shear strength of the sliding surface is increased. More bolts have to be driven to cross the sliding plane than across the separation planes. Where possible, these bolts or cables should be inclined so that the angle θ between the bolt and the sliding plane is between 15° and 30°, since this inclination will induce the highest shear resistance along the sliding surface.

During the mining activity, to be saved from unprecedented problems, the engineering geologist and the mining engineer should work closely together.

REFERENCES

Arlid Palmstrom, Doug Miline, and Warren Peck , (2000). The reliability of rock mass classification used in underground excavation and support., *International workshop at GeoEng2000 (Internet File).*

Ashanti Gold Fields, (1996). Development Proposal (Bid Document for Legadembi Gold Mine Privatisation). *Mineral Operations Department.*

Astrup.J.(1948). Exploration with drilling of alluvial gold in Mengist Valley. *Unpub., Ethiopian Mineral Resources Development Corporation (EMRDC).*

Astrup J. (1950). Report on prospecting result of Awata River valley, Adola Goldfield. *Unpub., Ethiopian Mineral Resources Development Corporation (EMRDC).*

Ayalew T., Bellk., Moore J.M., & Parrishi R.R., 1990. U.Pub & Rb-Sr geochronology of the western Ethiopian shield. *Geol. Soc.Am.Bull. 102:109-1316.*

Ayelew and Gichiles S., 1990. Preliminary U-Pb ages from Southern Ethiopia. *African Geology , France. Extended Abstracts: 127-130.*

BRGM, (Bureau de Recherches Géologiues et Miniéres) (1991). Environmental Impact and Safety Feasibility Study of Upper and Central Legadembi (Unpublished). *Ministry of Mines.*

BRGM (1991). Geotechnical Feasibility Study of Upper and Central Legadembi (Unpublished). *Ministry of Mines.*

Chater A.M. (1971). The Geology of the Megado Region of Southern Ethiopia. *Ph.D thesis, Leeds University, Leeds (unpublished).*

Centeck Publishers (1986). Fundamentals of Rock Joints. Proceedings of the International Symposium on Fundamentals of Rock Joints/Björkliden/15-20 September 1985. *Luleå University of Technology, Sweden.*

Centeck Publishers (1985). Large Scale Underground Mining. Proceedings of the International Symposium on Large Scale Underground Mining/Luleå/ 6-7November. *Luleå University of Technology, Sweden.*

Centeck Publishers 1986. Rock Stress and Rock Stress Measurements. Proceedings of the International Symposium on Rock Stress and Rock Stress Measurments/Stockholm/1-3 September 1986. *Luleå University of Technology, Sweden.*

D.Miline, J Hajigeorgiou, and R.Pakalnis, (1988). Rock Mass Characterization for Underground Hard Rock Mines. *Internet File.*

Demissie, S.Marchuk, Yu.Evdakimov V. (1987). Summary of the geology and mineral potential of the Adola area. Unpub., *Ethiopian Mineral Resources Development Corporation (EMRDC).*

Dewit M.J. & S. Chewaka., (1981). Plate tectonic and Metalogenesis: Some Guide Lines to Ethiopiaan Mineral deposits of Ethiopia and Origin of its mineral Deposits. *Ministry of Mines.*

EMRDC (1990). Annual Report. *Public Relation & Training Service of EMRDC.*

EMRDC (1995). Legadembi Gold Mine, Background Operational Information. *EMRDC (Unpub).*

Evert Hoek & John Bray (1977). Rock Slope Engineering. The institution of Mining and Metallurgy, London. *The Institution of Mining and Metallergy London.*

E.Hoek, P.K.Kaiser, W.F.Bawden (1995). Support of Underground Excavations in Hard Rock. *A.A Blkema/Rotterdam/Bookfield.*

Fekadu Kebede and Laike M. Asfaw (1996). Seismic Hazard Assessment For Ethiopia and the Neighbouring countries. *SINET: Ethiopia. J. Sci., 19(1): 15-50.*

F. G. Bell (1980). Engineering Geology and Geotechnics. *Butterworth and Co Ltd.*

Gilboy C.F. (1970). The Geology of the Gariboro Region of Southern Ethiopia. *Ph.D. thesis, Leeds University.*

G. Popov. (1971). The working of Mineral Deposits. *Mir Publishers Moscow.*

G.M. Mahadevaswamy (2002). Hydrogeologic Appraisal (using convensional and remote sensing methodology) of Lokapavani Microwater Shed, Mandya District, Karnataka. *Ph.D thesis, University of Mysore.*

Kazmin V. (1971). Precambrian of Ethiopia. *Nature 230. 176-177.*

Kazmin V. (1972). The Geology of Ethiopia. *Minstry of Mines, Addis Ababa.*

Kazmin V. et al. (1973). Geological Map of Ethiopia (1:2000,000), 1st edition. *Geological Survey of Ethiopia Addis Ababa.*

Kazmin V. (1975). The Precambrian of Ethiopia and some aspects of the Geology of the Mozambique Belt. *Bulletin of Geophysical Observatory Addis Ababa 15: 22-43, Addis Ababa.*

Kazmin V et al. (1978). The Ethiopian basement: Stratigraphy and possible manner of evolution.

Lee W.Abrahmson, Thomas S.Lee, Sunil Sharma, Glenn M.Boyce (1996). Slope Stability and Stabilization Methods. *John Wiley & Sons, Inc.*

Laike Mariam Asfaw (1986). Catalogue of Ethiopian earthquakes, Earthquake Parameters, Strain Release and Seismic Risk. In: proceedings of the SAREC-ESTC conference *On Research Development and Current Research Activities in Ethiopia, pp. 252-279.*

M.Agoshkov, S.Borisov, V.Boyarsky (1988). Mining of Ores and Non-Metallic Minerals. *Mirr Publishers Moscow.*

M.J Sellby (1993). Hillslope Materials and Processes. *Oxford University Press. Oxford New York.*

Wolday Gebreab (1992). The geological evolution of the Adola Precambrian greenstone belt, Southern Ethiopia. *Jur. of African Earth Sciences, Vol 14. No. 4 pp. 457-469.*

Worash Getaneh (1994). Sulfide Mineralization in the Legadembi Primary Gold Dposit. M.Sc. *Thesis, School of Graduate studies, A.A.U., Addis Ababa.*

Woldehaimanot B.(1995). Structural Geology and Geochemistry of the Neoproterozoic Adobha and Adola Belts. *Ph.D thesis.*

Hailu Worku and Yifa K. (1992). The tectonic evolution of the Precambrian metamorphic rocks of the Adola belt (southern Ethiopia). *Journal of Earth Sciences 14: 37-55.*

Hailu Worku (1996). Gedynamic development of the Belt (southern Ethiopia) in the Neopreterozoic and its control on gold mineralization. *Ph.D thesis Technical University of Berlin.*

Sanjeev Sharma, Tarun Raghuvanshi , Atul Sahai (1999). An engineering Geological Appraisal of the Lakhwar Dam, Grahwal Himalaya, India. *Engineering Geology,53 (1999) 381-398, Elsevier.*

Sharma S., Raguvanishi T.K.and.Anbalagan R (1995). Technical Note, Plain Failure Analysis of Rock Slopes. *Geotechnical and Geological Engineering , 13, 105-111.*

Robert B.Johnson, Jerome V.Degar (1988). Principles of Engineering Geology. *John Wiley & Sons.*

ANNEX-A: Open pit RMR Rating data.

Annex A- Open pit average RMR Rating Data																
Section line	Location	Average UCS	Average Jv	Average RQD	Average RQD Rating	Average spacing	Average condition of discontinuities	Average groundwater condition	Rating adjustment range	Average RMR	Lithology	Average Cohesion kg/cm2	Average Angle of Internal Friction (°)	AverageCohesion kg/cm2	Angle of Internal Friction (degree)	Section Line Average RMR
SL1	L1	12	7	91.9	20	10.13	29.00	15	-50 - 0	61.13	Quartz vein/ore	3.05	35.56	2.83	33	57
	L2	12	12	75.4	17	11.67	26.67	15	-50 - 0	74.00	Quartz vein/ore	3.70	42.00			
	L3	12	14	68.8	13	11.25	23.69	15	-50 - 0	53.75	Quartz Vein/ Ore	2.69	31.88			
	L4	7	11	78.7	17	9.40	18.00	15	-50 - 0	56.40	Quartz Vein with Biotite Actinolite Talc Schist/ Ore	2.82	33.20			
	L5	7	7	91.9	20	9.50	18.75	15	-50 - 0	55.25	Quartz Vein with Biotite Actinolite Talc Schist/ Ore	2.76	32.63			
	L6	7	11	78.7	17	9.25	15.00	15	-50 - 0	42.63	Quartz Vein with Graphitic Mica Schist/ Ore					
	L7	7	7	91.9	20	10.00	21.67	15	-50 - 0	53.67	Quartz Vein with Graphitic Mica Schist/ Ore	2.68	31.83			
SL2	L8	7	6	95.2	20	10.00	23.00	15	-50 - 0	54.60	Quartz Vein with Graphitic Mica Schist/ Ore	2.73	32.30	2.45	30	49
	L9	7	10	82	7	8.67	15.00	15	-50 - 0	46.00	Quartz Vein with Graphitic Mica Schist/ Ore	2.30	28.00			
	L10	7	7	91.9	20	10.00	13.00	15	-50 - 0	53.00	Quartz Vein with Graphitic Mica Schist/ Ore	2.65	31.50			
	L11	7	12	75.4	15	8.86	22.86	15	-50 - 0	45.86	Quartz Vein with Graphitic Mica Schist/ Ore	2.29	27.93			
	L12	7	18	55.6	13	8.09	16.82	15	-50 - 0	49.00	Graphite Mica Schist with quartz and talc schist	2.45	29.50			
	L13	7	11	78.7	7	8.40	23.00	15	-50 - 0	60.40	Graphite Mica Schist with quartz and talc schist	3.02	35.20			
	L14	7	13	72.1	17	10.20	18.00	15	-50 - 0	47.20	Graphite Mica Schist with quartz and talc schist	2.36	28.60			
	L15	7	12	75.4	17	8.67	23.33	15	-50 - 0	29.33	Graphite Mica Schist with quartz and talc schist	1.47	19.67			
	L16	7	5	98.5	20	10.00	20.00	15	-50 - 0	47.00	Graphite Mica Schist with quartz and talc schist	2.35	28.50			
	L17	7	8	88.6	7	9.00	23.75	15	-50 - 0	59.25	Graphite Mica Schist with quartz and talc schist	2.96	34.63			
	L18	7	10	82	17	8.75	26.88	15	-50 - 0	55.88	Graphite Mica Schist with quartz and talc schist	2.79	32.94			
	L19	7	11	78.7	17	8.86	19.29	15	-50 - 0	45.71	Graphite Mica Schist with quartz and talc schist	2.29	27.86			
	L20	7	11	78.7	17	9.20	14.00	10	-50 - 0	47.20	Graphite Mica Schist with quartz and talc schist	2.36	28.60			
SL3	L21	7	7	91.9	20	9.75	20.00	15	-50 - 0	46.75	Graphite Mica Schist with quartz and talc schist	2.34	28.38	2.29	28	46

Annex A- Open pit average RMR Rating Data

	L22	7	10	82	17	8.67	22.50	10	-50 - 0	56.83	Graphite Mica Schist with quartz and talc schist					
	L23	7	7	91.9	20	8.86	22.86	10	-50 - 0	54.43	Graphite Mica Schist with quartz and talc schist	2.72	32.21			
	L24	7	7	91.9	20	9.20	20.50	10	-50 - 0	21.70	Graphite Mica Schist with quartz and talc schist	1.09	15.85			
	L25	7	16	62.2	13	8.38	23.85	15	-50 - 0	51.85	Graphite Mica Schist with quartz and talc schist	2.59	30.92			
	L26	7	7	91.9	20	9.71	16.43	10	-50 - 0	48.86	Graphite Mica Schist with quartz and talc schist	2.44	29.43			
	L27	4	11	78.7	17	8.22	20.56	10	-50 - 0	43.11	Biotite Actinolite Talc schist with quartz veins	2.16	26.56			
	L28	4	8	88.6	17	9.00	19.58	15	-50 - 0	47.92	Biotite Actinolite Talc schist with quartz veins					
	L29	4	8	88.6	17	9.50	20.00	15	-50 - 0	46.75	Biotite Actinolite Talc schist with quartz veins	2.34	28.38			
SL4	L30	4	10	82	17	8.29	14.29	15	-50 - 0	37.14	Biotite Actinolite Talc schist with quartz veins	1.86	23.57	2.15	27	43
	L31	4	11	78.7	17	8.57	14.29	15	-50 - 0	44.57	Biotite Actinolite Talc schist with quartz veins	2.23	27.29			
	L32	4	15	65.5	13	8.67	11.67	15	-50 - 0	46.78	Biotite Actinolite Talc schist with quartz veins	2.34	28.39			
SL5	L33	4	7	91.9	20	9.75	25.63	4	-50 - 0	50.88	Biotite Actinolite Talc schist with quartz veins	2.54	30.44	2.42	29	48
	L34	4	8	88.6	17	9.20	22.00	15	-50 - 0	47.20	Biotite Actinolite Talc schist with quartz veins	2.36	28.60			
SL6	L40	12	15	65.5	13	7.60	20.00	15	-50 - 0	57.60	Quartzo Feldspatic Gneiss	2.88	33.80	2.48	30	50
	L41	12	10	82	17	9.00	21.25	15	-50 - 0	55.50	Amphibolite	2.78	32.75			
	L42	12	10	68.8	13	8.00	26.67	15	-50 - 0	58.00	Amphibolite	34.00	34.00			
	L43	12	14	68.8	13	10.00	28.75	15	-50 - 0	53.25	Quartzo Feldspatic Gneiss	2.66	31.63			
	L44	12	10	82	17	8.80	14.00	15	-50 - 0	36.80	Quartzo Feldspatic Gneiss	1.84	23.40			
	L45	12	13	72.1	17	8.75	19.38	15	-50 - 0	47.13	Quartzo Feldspatic Gneiss	2.36	28.56			
	L46	12	9	85.3	17	8.80	17.00	15	-50 - 0	44.80	Amphibolite	2.24	27.40			
	L47	12	12	75.4	17	9.20	13.00	15	-50 - 0	26.20	Quartzo Feldspatic Gneiss	1.31	18.10			
	L48	12	13	72.1	17	8.67	20.00	15	-50 - 0	64.33	Quartzo Feldspatic Gneiss	37.17	37.17			
	L49	12	6	95.2	20	9.67	20.00	15	-50 - 0	51.67	Quartzo Feldspatic Gneiss	2.58	30.83			
	L50	7	15	65.5	13	8.70	27.00	15	-50 - 0	55.70	Biotite Schist	2.79	32.85			
	L51	12	14	68.8	13	8.38	21.25	15	-50 - 0	26.00	Quartzo Feldspatic Gneiss	1.30	18.00			

Annex A- Open pit average RMR Rating Data																
	L52	12	11	78.7	17	8.29	18.57	15	-50 - 0	49.43	Quartzo Feldspatic Gneiss	2.47	13.67			
	L53	12	12	75.4	17	9.14	21.43	15	-50 - 0	60.29	Quartzo Feldspatic Gneiss	3.01	35.14			
SL7	L35	12	7	91.9	20	10.00	29.29	10	-50 - 0	52.71	Amphibole Gneiss	2.64	31.36	2.55	30	51
	L36	4	8	88.6	17	9.50	30.00	15	-50 - 0	50.50	Actinolite Tremolite Talc Schist with quartz vein	2.53	30.25			
	L37	4	7	91.9	20	8.20	22.00	15	-50 - 0	39.20	Actinolite Tremolite Talc Schist with quartz vein	1.96	24.60			
	L38	4	10	82	17	7.43	28.57	15	-50 - 0	57.71	Actinolite Tremolite Talc Schist with quartz vein	2.89	12.65			

ANNEX -B: Q rating data for underground mine ore zone excavation.

ANNEX-B Tunnel Quality Index - Q Rock Mass Rating of the underground ore Zone

Location		RQD		Joint Number	Joint Roughness	Joint Alteration	Joint Water Condition	Stress Reduction Factor	RQD/Jn	Jr/Ja	Jw/SRF	Q	Excavation		ESR	De	Deformation Modulus (Em) in Gpa	Maximiu Unsupported Span
From (m)	To (m)	Jv	RQD										Diameter	Height				
0	2	6	95.2	6	1.5	1	1	2.5	15.9	1.5	0.40	9.5	6.5	6	4	1.6	24.47	19.70
2	4	10	82	6	1.5	1	1	2.5	13.7	1.5	0.40	8.2	6.5	6	4	1.6	22.85	18.56
4	6	9	85.3	6	2	1	1	2.5	14.2	2.0	0.40	11.4	6.5	6	4	1.6	26.40	21.16
6	8	9	85.3	6	3	1	1	2.5	14.2	3.0	0.40	17.1	6.5	6	4	1.6	30.80	24.88
8	10	6	95.2	6	2	1	1	2.5	15.9	2.0	0.40	12.7	6.5	6	4	1.6	27.59	22.11
10	12	7	91.9	6	3	4	1	2.5	15.3	0.8	0.40	4.6	6.5				16.56	14.72
12	14	9	85.3	6	3	1	1	2.5	14.2	3.0	0.4	17.1	6.5	6	4	1.6	30.80	24.88
14	16	7	91.9	3	3	4	1	2.5	30.6	0.8	0.4	9.2	6.5	6	4	1.6	24.08	19.43
16	18	11	78.7	6	1.5	4	1	2.5	13.1	0.4	0.4	2.0	6.5	6	4	1.6	7.35	10.49
18	20	7	91.9	6	3	4	1	2.5	15.3	0.8	0.4	4.6	6.5	6	4	1.6	16.56	14.72
20	22	5	98.5	3	1.5	4	1	2.5	32.8	0.4	0.4	4.9	6.5	6	4	1.6	17.31	15.14
22	24	6	95.2	6	3	4	1	2.5	15.9	0.8	0.4	4.8	6.5	6	4	1.6	16.94	14.93
24	26	10	82	6	3	4	1	2.5	13.7	0.8	0.4	4.1	6.5	6	4	1.6	15.32	14.07
26	28	5	98.5	6	1.5	4	1	2.5	16.4	0.4	0.4	2.5	6.5	6	4	1.6	9.78	11.47
28	30	6	95.2	6	3	4	1	2.5	15.9	0.8	0.4	4.8	6.5	6	4	1.6	16.94	14.93
30	32	6	95.2	6	3	4	1	2.5	15.9	0.8	0.4	4.8	7	6	4	1.6	16.94	14.93
32	34	6	95.2	6	3	4	1	2.5	15.9	0.8	0.4	4.8	7	6	4	1.6	16.94	14.93

ANNEX-B Tunnel Quality Index - Q Rock Mass Rating of the underground ore Zone

Location		RQD		Joint Number	Joint Roughness	Joint Alteration	Joint Water Condition	Stress Reduction Factor	RQD/Jn	Jr/Ja	Jw/SRF	Q	Excavation		ESR	De	Deformation Modulus (Em) in Gpa	Maximu Unsupported Span
From (m)	To (m)	Jv	RQD										Diameter	Height				
34	36	6	95.2	6	3	4	1	2.5	15.9	0.8	0.4	4.8	7	6	4	1.8	16.94	14.93
36	38	5	98.5	6	3	4	1	2.5	16.4	0.8	0.4	4.9	7	6	4	1.8	17.31	15.14
38	40	5	98.5	6	1.5	4	1	2.5	16.4	0.4	0.4	2.5	7	6	4	1.8	9.78	11.47
40	42	9	85.3	9	1.5	4	1	2.5	9.5	0.4	0.4	1.4	7	6	4	1.8	3.82	9.21
42	44	6	95.2	9	3	4	1	2.5	10.6	0.8	0.4	3.2	7	6	4	1.8	12.54	12.70
44	46	8	88.6	6	3	4	1	2.5	14.8	0.8	0.4	4.4	7	6	4	1.8	16.16	14.51
46	48	6	95.2	6	3	4	1	2.5	15.9	0.8	0.4	4.8	7	6	4	1.8	16.94	14.93
48	50	5	98.5	6	1.5	4	1	2.5	16.4	0.4	0.4	2.5	6.25	6	4	1.6	9.78	11.47
50	52	5	98.5	6	1.5	4	1	2.5	16.4	0.4	0.4	2.5	6.25	6	4	1.6	9.78	11.47
52	54	7	91.9	6	1.5	4	1	2.5	15.3	0.4	0.4	2.3	6.25	6	4	1.6	9.03	11.16
54	56	7	91.9	6	1.5	4	1	2.5	15.3	0.4	0.4	2.3	6.25	6	4	1.6	9.03	11.16
56	58	6	95.2	6	3	2	1	2.5	15.9	1.5	0.4	9.5	6.25	6	4	1.6	24.47	19.70
58	60	10	82	9	1.5	4	1	2.5	9.1	0.4	0.4	1.4	6.25	6	4	1.6	3.39	9.06
60	62	5	98.5	6	3	1	1	2.5	16.4	3.0	0.4	19.7	6.25	6	4	1.6	32.36	26.36
62	64	7	91.9	6	1.5	1	1	2.5	15.3	1.5	0.4	9.2	6.25	6	4	1.6	24.08	19.43
64	66	7	91.9	6	1.5	2	1	2.5	15.3	0.8	0.4	4.6	6.25	6	4	1.6	16.56	14.72
66	68	12	75.4	6	1.5	4	1	2.5	12.6	0.4	0.4	1.9	6.25	6	4	1.6	6.88	10.31
68	70	11	78.7	6	1.5	4	1	2.5	13.1	0.4	0.4	2.0	6.25	6	4	1.6	7.35	10.49
70	72	12	75.4	6	1.5	4	1	2.5	12.6	0.4	0.4	1.9	6.25	6	4	1.6	6.88	10.31
72	74	11	78.7	6	1.5	4	1	2.5	13.1	0.4	0.4	2.0	6	7	4	1.5	7.35	10.49
74	76	9	85.3	6	3	4	1	2.5	14.2	0.8	0.4	4.3	6	7	4	1.5	15.75	14.29
76	78	14	68.8	6	1.5	4	1	2.5	11.5	0.4	0.4	1.7	6	7	4	1.5	5.89	9.94
78	80	10	82	6	1.5	4	1	2.5	13.7	0.4	0.4	2.1	6	7	4	1.5	7.79	10.66
80	82	6	95.2	4	3	4	1	2.5	23.8	0.8	0.4	7.1	6	7	4	1.5	21.34	17.56
82	84	8	88.6	4	3	4	1	2.5	22.2	0.8	0.4	6.6	6	7	4	1.5	20.56	17.06
84	86	10	82	6	1.5	4	1	2.5	13.7	0.4	0.4	2.1	6	7	4	1.5	7.79	10.66
86	88	13	72.1	3	3	1	1	2.5	24.0	3.0	0.4	28.8	6	7	4	1.5	36.50	30.70
88	90	5	98.5	3	3	4	2.5	2.5	32.8	0.8	1	24.6	7	7	4	1.8	34.78	28.82
90	92	8	88.6	6	1.5	4	2.5	2.5	14.8	0.4	1	5.5	7	7	4	1.8	18.58	15.86
92	94	10	82	6	3	4	1	2.5	13.7	0.8	0.4	4.1	7	7	4	1.8	15.32	14.07
94	96	8	88.6	3	3	4	1	2.5	29.5	0.8	0.4	8.9	7	7	4	1.8	23.69	19.15

ANNEX-B Tunnel Quality Index - Q Rock Mass Rating of the underground ore Zone

Location		RQD		Joint Number	Joint Roughness	Joint Alteration	Joint Water Condition	Stress Reduction Factor	RQD/Jn	Jr/Ja	Jw/SRF	Q	Excavation		ESR	De	Deformation Modulus (Em) in Gpa	Maximiu Unsupported Span
From (m)	To (m)	Jv	RQD										Diameter	Height				
96	98	8	88.6	6	3	4	1	2.5	14.8	0.8	0.4	4.4	7	7	4	1.8	16.16	14.51
98	100	8	88.6	6	3	4	1	2.5	14.8	0.8	0.4	4.4	7	7	4	1.8	16.16	14.51
100	102	8	88.6	6	2	4	1	2.5	14.8	0.5	0.4	3.0	7	7	4	1.8	11.76	12.34
102	104	12	75.4	6	3	4	1	2.5	12.6	0.8	0.4	3.8	7	7	4	1.8	14.41	13.60
104	106	7	91.9	6	3	4	1	2.5	15.3	0.8	0.4	4.6	7	7	4	1.8	16.56	14.72
106	108	8	88.6	6	3	4	1	2.5	14.8	0.8	0.4	4.4	7	7	4	1.8	16.16	14.51
108	110	20	49	6	3	4	1	2.5	8.2	0.8	0.4	2.5	7	7	4	1.8	9.73	11.45
110	112	19	52.3	4	3	4	1	2.5	13.1	0.8	0.4	3.9	7	7	4	1.8	14.84	13.82
112	114	8	88.6	6	1.5	4	1	2.5	14.8	0.4	0.4	2.2	7	7	4	1.8	8.63	11.00
114	116	10	82	4	1.5	4	1	2.5	20.5	0.4	0.4	3.1	9.5	8	4	2.4	12.20	12.54
Pillar (0)	2	7	91.9	6	3	1	1	2.5	15.3	3.0	0.4	18.4	9.5	8	4	2.4	31.61	25.63
2	4	8	88.6	6	3	1	1	2.5	14.8	3.0	0.4	17.7	9.5	8	4	2.4	31.21	25.26
4	6	6	95.2	6	3	4	1	2.5	15.9	0.8	0.4	4.8	9.5	8	4	2.4	16.94	14.93
122	124	5	98.5	2	3	1	1	2.5	49.3	3.0	0.4	59.1	6	8	4	1.5	44.29	40.90
124	126	7	91.9	6	1.5	4	1	2.5	15.3	0.4	0.4	2.3	6	8	4	1.5	9.03	11.16
126	128	9	85.3	4	1.5	4	1	2.5	21.3	0.4	0.4	3.2	6	8	4	1.5	12.62	12.74
128	130	10	82	9	1.5	4	1	2.5	9.1	0.4	0.4	1.4	6	8	4	1.5	3.39	9.06
130	132	9	85.3	6	1.5	4	1	2.5	14.2	0.4	0.4	2.1	6	8	4	1.5	8.22	10.83
132	134	9	85.3	6	1.5	4	1	2.5	14.2	0.4	0.4	2.1	6	8	4	1.5	8.22	10.83
134	136	11	78.7	6	1.5	4	1	2.5	13.1	0.4	0.4	2.0	6	8	4	1.5	7.35	10.49
136	138	9	85.3	6	1.5	4	1	2.5	14.2	0.4	0.4	2.1	6	8	4	1.5	8.22	10.83
138	140	8	88.6	6	1.5	4	1	2.5	14.8	0.4	0.4	2.2	6	8	4	1.5	8.63	11.00
140	142	10	82	6	3	4	1	2.5	13.7	0.8	0.4	4.1	6	8	4	1.5	15.32	14.07
142	144	7	91.9	6	3	4	1	2.5	15.3	0.8	0.4	4.6	6	8	4	1.5	16.56	14.72
144	146	8	88.6	6	3	4	1	2.5	14.8	0.8	0.4	4.4	6	8	4	1.5	16.16	14.51
146	148	9	85.3	6	1.5	4	1	2.5	14.2	0.4	0.4	2.1	6	8	4	1.5	8.22	10.83
148	150	7	91.9	6	3	4	1	2.5	15.3	0.8	0.4	4.6	6	8	4	1.5	16.56	14.72
150	152	10	82	6	1.5	4	1	2.5	13.7	0.4	0.4	2.1	6	8	4	1.5	7.79	10.66
152	154	8	88.6	6	1.5	4	1	2.5	14.8	0.4	0.4	2.2	6	8	4	1.5	8.63	11.00
154	156	7	91.9	6	1.5	4	1	2.5	15.3	0.4	0.4	2.3	6	8	4	1.5	9.03	11.16
156	158	8	88.6	6	1.5	4	1	2.5	14.8	0.4	0.4	2.2	6	8	4	1.5	8.63	11.00

ANNEX-B Tunnel Quality Index - Q Rock Mass Rating of the underground ore Zone

Location		RQD		Joint Number	Joint Roughness	Joint Alteration	Joint Water Condition	Stress Reduction Factor	RQD/Jn	Jr/Ja	Jw/SRF	Q	Excavation		ESR	De	Deformation Modulus (Em) in Gpa	Maximu Unsupported Span
From (m)	To (m)	Jv	RQD										Diameter	Height				
158	160	14	68.8	6	3	4	1	2.5	11.5	0.8	0.4	3.4	7	8	4	1.8	13.41	13.11
160	162	10	82	6	1.5	4	1	2.5	13.7	0.4	0.4	2.1	7	8	4	1.8	7.79	10.66
162	164	11	78.7	6	3	4	1	2.5	13.1	0.8	0.4	3.9	7	8	4	1.8	14.87	13.84
164	166	12	75.4	6	1.5	4	1	2.5	12.6	0.4	0.4	1.9	7	8	4	1.8	6.88	10.31
166	168	12	75.4	6	1.5	4	1	2.5	12.6	0.4	0.4	1.9	7	8	4	1.8	6.88	10.31
168	170	9	85.3	9	3	4	1	2.5	9.5	0.8	0.4	2.8	7	8	4	1.8	11.35	12.15
170	172	7	91.9	6	3	4	1	2.5	15.3	0.8	0.4	4.6	7	8	4	1.8	16.56	14.72
172	174	12	75.4	6	3	4	1	2.5	12.6	0.8	0.4	3.8	7	8	4	1.8	14.41	13.60
174	176	10	82	6	1.5	4	1	2.5	13.7	0.4	0.4	2.1	7	8	4	1.8	7.79	10.66
176	178	12	75.4	6	3	4	1	2.5	12.6	0.8	0.4	3.8	7	8	4	1.8	14.41	13.60
178	180	7	91.9	4	3	4	1	2.5	23.0	0.8	0.4	6.9	7	8	4	1.8	20.96	17.32
180	182	14	68.8	6	3	4	1	2.5	11.5	0.8	0.4	3.4	7	8	4	1.8	13.41	13.11
182	184	10	82	4	3	4	1	2.5	20.5	0.8	0.4	6.2	7	8	4	1.8	19.72	16.54
184	186	10	82	6	3	4	1	2.5	13.7	0.8	0.4	4.1	7	8	4	1.8	15.32	14.07
186	188	8	88.6	6	1.5	4	1	2.5	14.8	0.4	0.4	2.2	7	8	4	1.8	8.63	11.00
188	190	5	98.5	3	1.5	4	1	2.5	32.8	0.4	0.4	4.9	7	8	4	1.8	17.31	15.14
190	192	8	88.6	3	3	4	1	2.5	29.5	0.75	0.4	8.9	7	8	4	1.8	23.69	19.15
192	194	10	82	4.00	3.00	4	1.0	2.5	20.5	0.75	0.40	6.2	7	8	4	1.8	19.72	16.54
194	196	7	91.9	4	3	4	1	2.5	23.0	0.75	0.4	6.9	7	8	4	1.8	20.96	17.32
196	198	9	85.3	9	3	4	1	2.5	9.5	0.75	0.4	2.8	7	8	4	1.8	11.35	12.15
198	200	5	98.5	3	1.5	4	1	2.5	32.8	0.375	0.4	4.9	7	8	4	1.8	17.31	15.14

ANNEX -C: Underground RMR rating data.

Annex C. RMR data for underground mine orezone excavation (0 - 100 m).

Location		Average UCS	Average JV	Average RQD	Average RQD rating	Average discontinuity spacing	Average condtions of discontinuities	Average groundwater condtions	Rating adjustment range	Average RMR	Lithology	Average cohesion kg/ cm2	Averag angle of internal friction (°)	Average Deformation Modulus (Ed) in Gpa
From	To													
0	2	12	6	95	20	9.00	21.67	15	-12 - 0	73	Q.vein	3.64	41.42	44.62
2	4	12	10	82	17	9.00	9.50	15	-12 - 0	60	Q.vein	3.00	35.00	20.77
4	6	12	9	85	17	8.63	18.13	15	-12 - 0	64	Q.vein	3.22	37.19	27.00
6	8	12	9	85	17	8.80	14.00	15	-12 - 0	59	Q.vein	2.93	34.30	23.40
8	10	12	6	95	20	28.44	20.00	15	-12 - 0	68	Q.vein	3.38	38.75	29.92
10	12	12	7	92	20	9.33	15.83	15	-12 - 0	63	Q.vein	3.17	36.67	27.70
12	14	12	9	85	17	8.20	16.00	15	-12 - 0	61	Q.vein	3.05	35.50	22.84
14	16	12	7	92	20	7.80	10.00	15	-12 - 0	56	Q.vein	2.78	32.80	13.97
16	18	12	11	79	17	8.00	10.00	15	-12 - 0	54	Q.vein	2.71	32.07	13.36
18	20	4	7	92	20	8.00	15.00	15	-12 - 0	50	Quartz Biotite Actinolite Talc schist	2.52	30.20	11.49
20	22	4	5	99	20	8.67	10.00	10	-12	41	Quartz Biotite Actinolite Talc schist	2.03	25.33	5.85
22	24	4	6	95	20	7.67	10.00	6	-12 - 0	40	Quartz Biotite Actinolite Talc schist	1.98	24.83	5.96
24	26	4	10	82	17	7.40	10.00	15	-12 - 0	50	Quartz Biotite Actinolite Talc schist	2.51	30.10	11.15
26	28	12	5	99	20	8.40	10.00	11	-12 - (-5)	51	Q.vein	2.54	30.40	10.90
28	30	12	6	95	20	8.00	10.00	15	-12 - 0	57	Q.vein	2.85	33.50	15.83
30	32	12	6	95	20	8.00	10.00	15	-12 - (-5)	55	Q.vein	2.77	32.67	13.85
32	34	12	6	95	20	8.00	10.00	15	-12	53	Q.vein	2.65	31.50	11.89
34	36	12	6	95	20	8.00	10.00	15	-12	53	Q.vein	2.65	31.50	11.89
36	38	4	5	99	20	8.50	17.50	15	-12 - (-5)	55	Quartz Biotite Actinolite Talc schist	2.51	30.10	11.15

Annex C. RMR data for underground mine orezone excavation (0 - 100 m).

Location		Average UCS	Average JV	Average RQD	Average RQD rating	Average discontinuity spacing	Average conditions of discontinuities	Average groundwater condtions	Rating adjustment range	Average RMR	Lithology	Average cohesion kg/ cm2	Averag angle of internal friction (°)	Average Deformation Modulus (Ed) in Gpa
From	To													
38	40	4	5	99	20	9.33	20.00	15	-12 - 0	63	Quartz Biotite Actinolite Talc schist	3.13	36.33	21.59
40	42	4	9	85	17	8.33	10.00	15	-12 - 0	44	Quartz Biotite Actinolite Talc schist	2.22	27.17	7.48
42	44	4	6	95	20	8.67	10.00	15	-12	46	Quartz Biotite Actinolite Talc schist	2.28	27.83	7.80
44	46	12	8	89	17	8.00	13.00	15	-12 - 0	59	Q.vein	2.95	34.50	19.97
46	48	12	6	95	20	8.00	10.00	15	-12	53	Q.vein	2.65	31.50	11.89
48	50	4	5	99	20	8.00	15.00	15	-12	50	Quartz Biotite Actinolite Talc schist	2.50	30.00	11.55
50	52	4	5	99	20	8.67	10.00	15	-12 - 0	54	Quartz Biotite Actinolite Talc schist	2.68	31.83	13.08
52	54	4	7	92	20	9.33	10.00	15	-12 - 0	50	Quartz Biotite Actinolite Talc schist	2.52	30.17	10.90
54	56	4	7	92	20	9.33	23.33	15	-12 - 0	64	Quartz Biotite Actinolite Talc schist	3.18	36.83	28.41
56	58	12	6	95	20	8.00	10.00	15	-12 - 0	59	Q.vein	2.95	34.50	17.80
58	60	12	10	82	17	8.00	10.00	15	-12 - 0	55	Q.vein	2.74	32.38	13.73
60	62	12	10	99	20	8.67	16.67	15	-12 - (-5)	63	Q.vein	3.13	36.33	22.90
62	64	12	7	92	20	8.67	10.00	15	-12 - (-5)	56	Q.vein	2.80	33.00	14.57
64	66	12	7	92	20	9.50	14.00	15	-12 - (-5)	61	Q.vein	3.07	35.70	23.24
66	68	12	12	75	17	8.67	10.00	15	-12 - (-5)	54	Q.vein	2.71	32.08	12.99
68	70	12	11	79	17	8.67	10.00	15	-12 - 0	55	Q.vein	2.73	32.33	14.13
70	72	4	12	75	17	8.67	20.00	15	-12 - 0	58	Quartz Biotite Actinolite Talc schist	2.91	34.08	21.06

Annex C. RMR data for underground mine orezone excavation (0 - 100 m).

Location		Average UCS	Average JV	Average RQD	Average RQD rating	Average discontinuity spacing	Average condtions of discontinuities	Average groundwater condtions	Rating adjustment range	Average RMR	Lithology	Average cohesion kg/ cm2	Averag angle of internal friction (°)	Average Deformation Modulus (Ed) in Gpa
From	To													
72	74	4	11	79	17	8.00	22.00	15	-12 - (-5)	55		2.77	32.70	16.48
74	76	4	9	85	17	8.00	26.67	15	-12	59	Quartz Biotite Actinolite Talc schist	2.95	34.50	18.08
76	78	12	14	69	17	8.50	13.75	15	-12 - (-5)	56	Q.vein	2.80	33.00	17.45
78	80	4	10	82	17	6.00	10.00	15	-12	40	Quartz Biotite Actinolite Talc schist	2.00	25.00	5.64
80	82	4	6	95	20	8.80	16.00	15	-12 - (-5)	55	Quartz Biotite Actinolite Talc schist	2.73	32.30	16.44
82	84	12	8	89	17	8.00	10.00	15	-12 - 0	54		2.70	32.00	13.32
84	86	4	10	82	17	9.50	20.00	4	-12 - 0	49	Quartz Biotite Actinolite Talc schist	2.45	29.50	11.22
86	88	4	13	72	13	8.00	13.75	4	-12 - 0	36	Quartz Biotite Actinolite Talc schist	1.78	22.75	5.02
88	90	12	5	99	20	9.20	18.00	15	-12 - (-5)	65	Q.vein	3.25	37.50	32.66
90	92	12	8	89	17	9.33	30.00	15	-12 - (-5)	76	Q.vein	3.80	43.00	45.29
92	94	12	10	82	17	8.50	10.00	15	-12 - (-5)	54	Q.vein	2.70	32.00	12.94
94	96	12	8	89	17	8.40	13.00	15	-12 - 0	60	Q.vein	2.98	34.80	19.32
96	98	4	8	89	17	8.50	15.00	15	-12	48	Quartz Biotite Actinolite Talc schist	2.38	28.75	9.91
98	100	4	8	89	17	8.00	10.00	15	-12 - 0	44	Quartz Biotite Actinolite Talc schist	2.22	27.20	7.57
100	102	4	8	89	17	8.67	10.00	15	-12	43	Quartz Biotite Actinolite Talc schist	2.13	26.33	6.57

The thesis is my original work and has not been presented for a degree in any other university.

Name: Yonas Bekele

Signature: Yonas B.

Date of Submission: _____.

The thesis has been submitted for examination with my approval as a university advisor.

Dr. Tenalem Ayenew

Tarun Raghuvanshi

Dr. Tarun Kumar Raghuvanshi